

## Durham Research Online

---

### Deposited in DRO:

15 September 2014

### Version of attached file:

Published Version

### Peer-review status of attached file:

Peer-reviewed

### Citation for published item:

Larter, R.D. and Anderson, J.B. and Graham, A.G.C. and Gohl, K. and Hillenbrand, C.-D. and Jakobsson, M. and Johnson, J.S. and Kuhn, G. and Nitsche, F.O. and Smith, J.A. and Witus, A.E. and Bentley, M.J. and Dowdeswell, J.A. and Ehrmann, W. and Klages, J.P. and Lindow, J. and Ó Cofaigh, C. and Spiegel, C. (2014) 'Reconstruction of changes in the Amundsen Sea and Bellingshausen Sea sector of the West Antarctic Ice Sheet since the Last Glacial Maximum.', *Quaternary science reviews.*, 100 . pp. 55-86.

### Further information on publisher's website:

<http://dx.doi.org/10.1016/j.quascirev.2013.10.016>

### Publisher's copyright statement:

© 2014 The Authors. Published by Elsevier Ltd. This is an open access article under the CC BY license (<http://creativecommons.org/licenses/by/3.0/>).

### Additional information:

## Use policy

---

The full-text may be used and/or reproduced, and given to third parties in any format or medium, without prior permission or charge, for personal research or study, educational, or not-for-profit purposes provided that:

- a full bibliographic reference is made to the original source
- a [link](#) is made to the metadata record in DRO
- the full-text is not changed in any way

The full-text must not be sold in any format or medium without the formal permission of the copyright holders.

Please consult the [full DRO policy](#) for further details.



## Invited review

# Reconstruction of changes in the Amundsen Sea and Bellingshausen Sea sector of the West Antarctic Ice Sheet since the Last Glacial Maximum<sup>☆</sup>



Robert D. Larter<sup>a,\*</sup>, John B. Anderson<sup>b</sup>, Alastair G.C. Graham<sup>a,c</sup>, Karsten Gohl<sup>d</sup>, Claus-Dieter Hillenbrand<sup>a</sup>, Martin Jakobsson<sup>e</sup>, Joanne S. Johnson<sup>a</sup>, Gerhard Kuhn<sup>d</sup>, Frank O. Nitsche<sup>f</sup>, James A. Smith<sup>a</sup>, Alexandra E. Witus<sup>b</sup>, Michael J. Bentley<sup>g</sup>, Julian A. Dowdeswell<sup>h</sup>, Werner Ehrmann<sup>i</sup>, Johann P. Klages<sup>d</sup>, Julia Lindow<sup>j</sup>, Colm Ó Cofaigh<sup>g</sup>, Cornelia Spiegel<sup>j</sup>

<sup>a</sup> British Antarctic Survey, High Cross, Madingley Road, Cambridge CB3 0ET, UK

<sup>b</sup> Department of Earth Sciences, Rice University, 6100 Main Street, Houston, TX 77005, USA

<sup>c</sup> College of Life and Environmental Sciences, University of Exeter, Exeter EX4 4RJ, UK

<sup>d</sup> Alfred Wegener Institute, Helmholtz-Centre for Polar and Marine Research, Am Alten Hafen 26, D-27568 Bremerhaven, Germany

<sup>e</sup> Department of Geological Sciences, Stockholm University, 106 91 Stockholm, Sweden

<sup>f</sup> Lamont-Doherty Earth Observatory of Columbia University, Palisades, NY, USA

<sup>g</sup> Department of Geography, Durham University, South Road, Durham DH1 3LE, UK

<sup>h</sup> Scott Polar Research Institute, University of Cambridge, Cambridge CB2 1ER, UK

<sup>i</sup> Institute of Geophysics and Geology, University of Leipzig, Talstraße 35, D-04103 Leipzig, Germany

<sup>j</sup> Department of Geosciences, University of Bremen, Bremen, Germany

## ARTICLE INFO

## Article history:

Received 28 March 2013

Received in revised form

4 October 2013

Accepted 15 October 2013

Available online 12 November 2013

## Keywords:

Ice sheet

Last Glacial Maximum

Holocene

Ice stream

Grounding line

Radiocarbon

Cosmogenic isotope

Surface exposure age

Multibeam swath bathymetry

Sediment

Glacimarine

Diamicton

Continental shelf

Circumpolar deep water

Subglacial meltwater

Sea level

## ABSTRACT

Marine and terrestrial geological and marine geophysical data that constrain deglaciation since the Last Glacial Maximum (LGM) of the sector of the West Antarctic Ice Sheet (WAIS) draining into the Amundsen Sea and Bellingshausen Sea have been collated and used as the basis for a set of time-slice reconstructions. The drainage basins in these sectors constitute a little more than one-quarter of the area of the WAIS, but account for about one-third of its surface accumulation. Their mass balance is becoming increasingly negative, and therefore they account for an even larger fraction of current WAIS discharge. If all of the ice in these sectors of the WAIS were discharged to the ocean, global sea level would rise by ca 2 m.

There is compelling evidence that grounding lines of palaeo-ice streams were at, or close to, the continental shelf edge along the Amundsen Sea and Bellingshausen Sea margins during the last glacial period. However, the few cosmogenic surface exposure ages and ice core data available from the interior of West Antarctica indicate that ice surface elevations there have changed little since the LGM. In the few areas from which cosmogenic surface exposure ages have been determined near the margin of the ice sheet, they generally suggest that there has been a gradual decrease in ice surface elevation since pre-Holocene times. Radiocarbon dates from glacimarine and the earliest seasonally open marine sediments in continental shelf cores that have been interpreted as providing approximate ages for post-LGM grounding-line retreat indicate different trajectories of palaeo-ice stream recession in the Amundsen Sea and Bellingshausen Sea embayments. The areas were probably subject to similar oceanic, atmospheric and eustatic forcing, in which case the differences are probably largely a consequence of how topographic and geological factors have affected ice flow, and of topographic influences on snow accumulation and warm water inflow across the continental shelf.

Pauses in ice retreat are recorded where there are “bottle necks” in cross-shelf troughs in both embayments. The highest retreat rates presently constrained by radiocarbon dates from sediment cores are found where the grounding line retreated across deep basins on the inner shelf in the Amundsen Sea, which is consistent with the marine ice sheet instability hypothesis. Deglacial ages from the Amundsen

<sup>☆</sup> This is an open access article under the CC BY license (<http://creativecommons.org/licenses/by/3.0/>).

\* Corresponding author.

E-mail addresses: [rdla@bas.ac.uk](mailto:rdla@bas.ac.uk), [rdlarter@gmail.com](mailto:rdlarter@gmail.com) (R.D. Larter).

Sea Embayment (ASE) and Eltanin Bay (southern Bellingshausen Sea) indicate that the ice sheet had already retreated close to its modern limits by early Holocene time, which suggests that the rapid ice thinning, flow acceleration, and grounding line retreat observed in this sector over recent decades are unusual in the context of the past 10,000 years.

© 2014 The Authors. Published by Elsevier Ltd. All rights reserved.

## 1. Introduction

### 1.1. Recent ice sheet change

Over recent decades, rapid changes have occurred in the sector of the West Antarctic Ice Sheet draining into the Amundsen and Bellingshausen seas (Fig. 1). These changes include thinning of ice shelves and thinning, flow velocity acceleration and grounding line retreat of ice streams feeding into them (Rignot, 1998, 2008; Pritchard et al., 2009, 2012; Scott et al., 2009; Wingham et al., 2009; Bingham et al., 2012). Ice shelves and ice streams in the ASE have exhibited the highest rates of change. These ice streams

include Pine Island Glacier (PIG) and Thwaites Glacier, which are the outlets from large drainage basins in the centre of the WAIS with a combined area of 417,000 km<sup>2</sup> (basin “GH”; Rignot et al., 2008). This amounts to about 60% of the area of the entire Amundsen-Bellingshausen sector as defined in Fig. 1 (ca 700,000 km<sup>2</sup>).

Modern snow accumulation rates in the sector are, on average, more than twice those in the drainage basins of the Siple Coast ice streams that flow into the Ross Ice Shelf (Arthern et al., 2006). Consequently, although the Amundsen-Bellingshausen sector comprises just a little more than a quarter of the area of the WAIS, it collects about one-third of the total accumulation. If the ice sheet

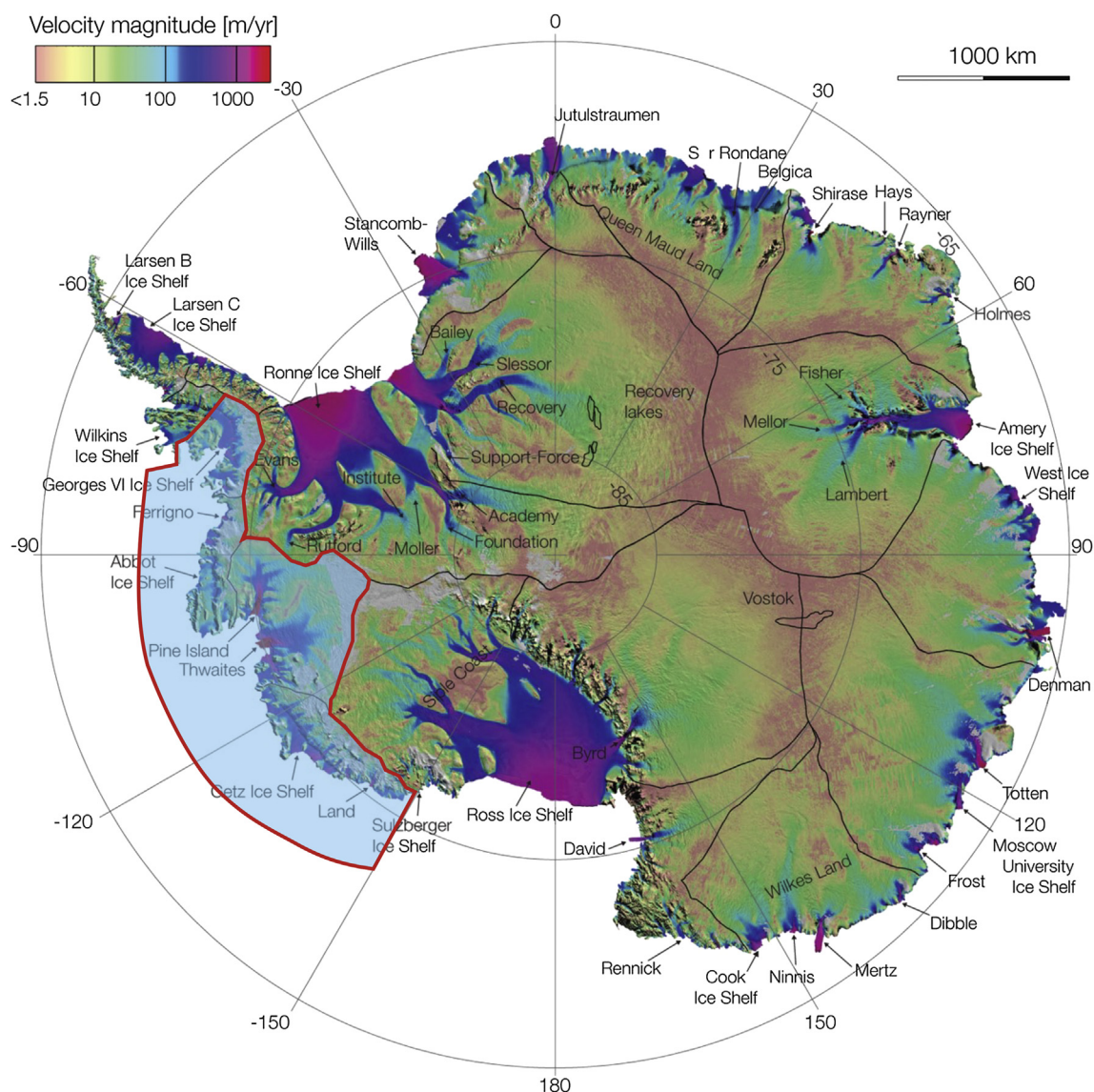


**Fig. 1.** Amundsen-Bellingshausen sector limits (red outline with semi-transparent blue fill) overlaid on map of Antarctic ice flow velocities and ice divides (black lines) from Rignot et al. (2011).

was in balance, this would imply that the sector also accounted for one-third of the total ice discharge. However, mass loss from the sector has increased over recent decades, such that by 2006 basin “GH” contributed  $37 \pm 2\%$  of the entire outflow from the WAIS ( $261 \pm 4 \text{ Gt yr}^{-1}$  out of a total of  $700 \pm 23 \text{ Gt yr}^{-1}$  according to Rignot et al., 2008). Since 2006 the rate of mass loss has continued to increase (Shepherd et al., 2012).

The accelerating changes to ice shelves and glaciers in the ASE over recent decades have focused renewed attention on concerns that climate change could eventually cause a rapid deglaciation, or “collapse”, of a large part of the WAIS (Mercer, 1978; Hughes, 1981; Bindshadler, 1998; Oppenheimer, 1998; Vaughan, 2008; Joughin and Alley, 2011). The total potential contribution to global sea level rise from the WAIS is 4.3 m, whereas the potential contribution from ice in the WAIS grounded below sea level, and therefore widely considered to be most vulnerable, is 3.4 m (Bamber et al., 2009b; Fretwell et al., 2013). The Pine Island and Thwaites drainage basins alone contain enough ice to raise sea level by 1.1 m (Rignot et al., 2002; Holt et al., 2006; Vaughan et al., 2006), and the total potential contribution from the whole Amundsen-Bellinghshausen sector may be as much as 2 m. Future rapid dynamical changes in ice flow were identified as the largest uncertainty in projections of sea level rise in the Fourth Assessment Report of the Intergovernmental Panel on Climate Change, and it was stated in the report that the recently-observed accelerations in West Antarctic ice streams were an important factor underlying this uncertainty (Solomon et al., 2007).

Even before the above-described changes in ASE ice shelves and glaciers were known, Hughes (1981) had suggested a chain of events whereby reduction of ice shelf buttressing in Pine Island Bay (PIB) could cause flow acceleration of PIG and Thwaites Glacier, drawing down ice from their drainage basins, and ultimately leading to disintegration of the WAIS. This hypothesis developed from the realisation that the two ice streams drain large basins in the centre of the WAIS and are not buttressed by a confined and pinned ice shelf. Hughes (1981) encapsulated the hypothesis by coining the memorable description of the region as “The weak underbelly of the West Antarctic Ice Sheet”.

## 1.2. The need for long-term records of change

Recent rates of change in the Amundsen-Bellinghshausen sector are undoubtedly too fast to be a simple continuation of a progressive deglaciation that started shortly after the LGM (23–19 cal ka BP). For example, grounding line retreat at a rate of  $>1 \text{ km/yr}$ , as measured on PIG (Rignot, 1998, 2008), would have resulted in deglaciation of the entire continental shelf within 500 years. Without considering records spanning thousands of years, however, there can be no certainty that the recent changes are not the latest phase of a step-wise retreat resulting from internal ice dynamic processes or variations in forcing parameters, or a combination of both. There is a growing consensus that the recent changes have been driven by increased inflow of relatively warm Circumpolar Deep Water (CDW) across the continental shelf, which has increased basal melting of ice shelves (Jacobs et al., 1996, 2011; Shepherd et al., 2004; Arneborg et al., 2012; Pritchard et al., 2012). However, historical observations do not provide any indication of when the inflow started to increase, and leave open the question of whether or not there have been previous periods since the LGM when similar inflow has driven phases of rapid retreat. Moreover, whereas some aspects of ice sheet response to external forcing occur within decades, other aspects of their response take centuries to millennia (e.g. conduction of surface temperature and advection of accumulated snow to the bed; changes in surface configuration resulting from shifting accumulation patterns; Bamber et al., 2007;

Bentley, 2010). Therefore, it is important to consider long-term records of change in order to fully test and calibrate ice sheet models, and improve confidence in their skill to predict future ice sheet contributions to sea-level rise. Records of ice sheet change spanning millennia are also important for modelling the glacial isostatic adjustment of the lithosphere, which is essential for calculating recent ice mass changes from satellite-measured changes in the Earth's gravity field (Ivins and James, 2005; King et al., 2012; Lee et al., 2012; Whitehouse et al., 2012).

The amount of data available to constrain ice sheet change in the Amundsen-Bellinghshausen sector over the past 25 ka has increased greatly since the start of this century. In this review we use the available data to inform a set of reconstructions depicting changes in the ice sheet in 5 ka steps. On the basis of the synthesis we also highlight significant data gaps and suggest some priorities for future research.

## 1.3. Sector definition

The divides between ice drainage sectors, which are now mostly well-defined from satellite remote sensing data (Bamber et al., 2009a), provide a practical basis for defining sector boundaries for ice sheet reconstruction studies. For the purposes of this review, we have used ice divides to define most of the Amundsen-Bellinghshausen sector boundary (Fig. 1). At the western limit of the sector we extended the boundary with the Ross Sea sector northwards across the narrow continental shelf from where it meets the coast. At the eastern boundary of the sector, there must have been a palaeo-divide extending from Palmer Land across George VI Sound and Alexander Island, as marine geological and geophysical data provide compelling evidence that palaeo-ice streams flowed out of each end of George VI Sound (Ó Cofaigh et al., 2005a, 2005b; Hillenbrand et al., 2010a; Kilfeather et al., 2011; Bentley et al., 2011). The deglacial history of the northern arm of George VI Sound suggests that this divide must have been located on the southern part of Alexander Island (Bentley et al., 2005, 2011; Smith et al., 2007), although its position is not precisely constrained. We have tentatively drawn the palaeo-divide along the length of Latady Island and then northwards across the continental shelf (Fig. 1).

## 1.4. Geological factors that may influence ice dynamics

Following earlier development at the active Pacific margin of Gondwana, West Antarctica has been affected by several phases of rifting since mid-Cretaceous time, possibly continuing until as recently as the Middle Miocene (Cande et al., 2000; Siddoway et al., 2005; Granot et al., 2010). As a consequence, most of the continental crust in the Amundsen-Bellinghshausen sector is relatively thin and dissected by rift basins (Gohl et al., 2007, 2013a; Jordan et al., 2010; Bingham et al., 2012; Gohl, 2012). Gohl (2012) and Gohl et al. (2013a) postulated that tectonic lineaments inherited from continental breakup and rift basins have influenced the major ice-flow paths of the Amundsen Sea shelf. Bingham et al. (2012) proposed that intersections of rift basins with the ice sheet margin have steered palaeo-ice streams paths across the shelf, and that many of the cross shelf troughs eroded by the ice streams now channel inflow of CDW to the grounding line. The parts of the grounding line in such troughs are likely to be particularly vulnerable to retreat due to reverse gradients on the ice bed leading back to the deepest parts of the basins, and possibly also elevated geothermal heat flow as a legacy of the Neogene rifting (Bingham et al., 2012).

Tomographic inversions of earthquake seismic data show that much of West Antarctica overlies a region of relatively warm upper



mantle centred beneath Marie Byrd Land (Danesi and Morelli, 2000; Shapiro and Ritzwoller, 2004). The warm mantle is probably associated with elevated geothermal heat flow (Shapiro and Ritzwoller, 2004), but there are no published heat flow measurements to confirm this. The region is volcanically active, and eruptions since mid-Oligocene time have constructed 18 large volcanoes in Marie Byrd Land with exposed volumes up to 1800 km<sup>3</sup> (LeMasurier et al., 1990). Although volcanic edifices beyond Marie Byrd Land are smaller, the alkaline volcanic province they are part of extends across the entire Amundsen-Bellingshausen sector and along the Antarctic Peninsula (Hole and LeMasurier, 1994; Finn et al., 2005). Of the large volcanoes in Marie Byrd Land, Mount Berlin and Mount Takahe are known to have erupted since the LGM (Wilch et al., 1999). A volcano in the Hudson Mountains, north of PIG, erupted only ca 2200 year ago (Corr and Vaughan, 2008). There may have been other eruptions in the sector since the LGM that are yet to be detected. In addition to local effects around the eruption sites and a temporary, more widespread effect of tephra deposition on ice surface albedo, eruptions could have affected ice dynamics by supplying meltwater to the ice sheet bed.

## 2. Methods

### 2.1. Marine survey data

Echo sounding data collected over many decades and multi-beam swath bathymetry data collected during the past two decades have been collated to produce regional bathymetric grids for the Amundsen Sea (Nitsche et al., 2007, 2013) and Bellingshausen Sea (Graham et al., 2011). These grids have recently been incorporated into Bedmap2 (Fretwell et al., 2013), which we have used to produce the regional basemaps for this review.

We have used more detailed, local grids generated from multi-beam swath bathymetry data to map areas in which streamlined bedforms occur and the positions of features such as grounding zone wedges (GZWs) that represent past limits of grounded ice extent. Multibeam data have been collected on the continental shelf in the sector on numerous research cruises of RVIB *Nathaniel B. Palmer*, RV *Polarstern*, RRS *James Clark Ross* and IB *Oden*. The extent of individual surveys is described in subsequent sections. Most data were collected using Kongsberg multibeam systems (EM120/EM122) that transmit at ca 12 kHz. Surveys before 2002 on RVIB *Nathaniel B. Palmer* were conducted using a Seabeam 2112 system, which also transmits at 12 kHz, whereas Hydrosweep DS-1 and DS-2 systems that transmit at 15 kHz were used on RV *Polarstern*. These systems are all capable of surveying swaths with a width more than three times the water depth and collecting data with vertical precision better than a metre at the depths on the continental shelf. The spatial accuracy of the data, referenced to ship positions determined using GPS, is better than a few metres.

Acoustic sub-bottom profiler data were also collected during most multibeam swath bathymetry surveys, and on many other cruises, using systems that transmit signals in the range 1.5–5 kHz. These data provide information about the physical nature of the upper few metres, or sometimes several tens of metres, of seabed sediments, which is helpful in interpreting geomorphic features observed in multibeam data (e.g. Graham et al., 2010; Klages et al., 2013) and also valuable for selecting sediment core sites. On many parts of the continental shelf, hemipelagic sediments deposited since glacial retreat in seasonally open water conditions have an acoustically-laminated character on sub-bottom profiles. Such sediments are often observed to overlie less well-laminated or acoustically-transparent units, which sediment cores typically reveal as being deglacial transitional sediments or low-shear-

strength diamictos (e.g. Dowdeswell et al., 2004; Ó Cofaigh et al., 2005b). On some parts of the continental shelf these latter types of sediments occur with little or no cover of acoustically-laminated sediments, whereas in other areas any acoustic stratigraphy that was once present has been disrupted as a result of ploughing by iceberg keels. In still other areas bedrock or high-shear-strength diamictos, which sub-bottom profiler signals cannot penetrate, occur with little or no glacial marine sediment cover.

Seismic reflection profiles acquired using airgun sources have been collected on the continental shelf during several research cruises on RV *Polarstern*, RRS *James Clark Ross* and RVIB *Nathaniel B. Palmer* over the past two decades. Airgun sources generate signals with frequencies that range from less than 10 Hz to a few hundred Hz, and these penetrate much further into the subsurface than the higher frequencies transmitted by acoustic sub-bottom profiling systems. The primary aim in collecting such data has usually been to study geological structure and patterns of sediment erosion and deposition over millions of years. However, airgun seismic data also provide a means of examining the thickness and internal stratigraphy of sedimentary units deposited during the last glacial cycle that are too thick, too coarse grained or too compacted for acoustic sub-bottom profiler signals to penetrate (e.g. high shear strength diamictos, GZWs and meltwater channel infills).

### 2.2. Continental shelf sediment cores

Sediment cores have been collected on the Amundsen-Bellingshausen sector continental shelf on many research cruises using a range of different coring devices, including gravity corers, piston corers, kasten corers, vibrocorers and box corers. Supplementary Table 1 lists all cores collected on the continental shelf that recovered more than 1 m of sediment. Cores that recovered <1 m of sediment, but from which radiocarbon dates have been obtained are also included in Supplementary Table 1.

Shelf sediment cores have typically recovered a succession of facies in which diamictos are overlain by gravelly and sandy muds, which are in turn overlain by a layer of predominantly terrigenous mud bearing scarce diatoms, foraminifera and ice-rafted debris (IRD) that varies in thickness from a few centimetres to a few metres. This succession of facies has been widely interpreted as recording grounding line retreat (Wellner et al., 2001; Hillenbrand et al., 2005, 2010a, 2013; Smith et al., 2009, 2011; Kirshner et al., 2012; Klages et al., 2013). Some diamictos have been interpreted as having been deposited in a proximal glacial marine setting (e.g. ones containing scarce microfossils or some stratification), whereas others have been interpreted as having formed subglacially (Wellner et al., 2001; Hillenbrand et al., 2005; Smith et al., 2011; Kirshner et al., 2012). Within diamictos interpreted as having a subglacial origin, particularly in cores from cross-shelf troughs, a downward transition is often observed from low shear strength diamicton ("soft till"; usually < 25 kPa) to diamicton with higher shear strength ("stiff till"; Wellner et al., 2001; Ó Cofaigh et al., 2007; Hillenbrand et al., 2005, 2010a; Smith et al., 2009, 2011; Kirshner et al., 2012; Klages et al., 2013). The soft tills probably formed as dilated sediment layers like those observed beneath some modern ice streams (Alley et al., 1987; Tulaczyk et al., 1998; Kamb, 2001; Dowdeswell et al., 2004; Smith and Murray, 2009; Smith et al., 2013). The uppermost mud facies is generally considered to have been deposited in a setting distal from the grounding line in seasonally open water conditions (Wellner et al., 2001; Hillenbrand et al., 2005; Kirshner et al., 2012).

Locally, cores have recovered a variety of other facies types that are significant for reconstructing processes and the progress of deglaciation. A few examples are: (1) in deep inner shelf basins in

the western ASE, a diatom ooze layer was deposited soon after ice had retreated from the area (Hillenbrand et al., 2010b; Smith et al., 2011); (2) in the mid-shelf part of Pine Island Trough, a homogenous mud unit that contains very little IRD has been interpreted as a sub-ice shelf facies (Kirshner et al., 2012); (3) in the axis of a seabed channel in PIB, a unit comprising well-sorted sands and gravels has been interpreted as having been deposited from subglacial meltwater (Lowe and Anderson, 2003).

### 2.3. Dating of core samples

Supplementary Table 2 lists 207 published accelerator mass spectrometry (AMS)  $^{14}\text{C}$  dates obtained on samples from sediment cores collected in this sector. These comprise 41 dates on sea-floor surface (or near-surface) samples and 166 dates on samples taken down core. One of the surface dates and three of the down-core dates are previously unpublished.

It is widely accepted that calcareous microfossils provide the most reliable AMS  $^{14}\text{C}$  dates from marine sediments, but the scarcity of such microfossils in many Antarctic sediment cores has driven researchers to attempt to date other carbon-bearing materials (Andrews et al., 1999; Heroy and Anderson, 2007; Rosenheim et al., 2008). Where present, other carbonate materials (e.g. bryozoans or shell fragments) have been dated, but in many cores these are also lacking and the only carbon available is in organic matter from bulk sediment samples. Acid-insoluble organic matter (AIOM) is mainly derived from diatomaceous organic matter, and its dating has been widely applied to provide age models for sediment cores recovered from the Antarctic shelf (e.g. Licht et al., 1996, 1998; Andrews et al., 1999; Domack et al., 1999; Ó Cofaigh et al., 2005a; Pudsey et al., 2006; Hillenbrand et al., 2010a, 2010b).

AMS  $^{14}\text{C}$  dates on AIOM, however, are often biased by fossil carbon derived from glacial erosion of the Antarctic continent and by reworking of unconsolidated sediments. Such contamination by fossil carbon can be demonstrated in sea-floor surface sediments by paired AMS  $^{14}\text{C}$  dating of AIOM and foraminifera (where foraminifera are present) or comparison of  $^{14}\text{C}$  dates on AIOM to  $^{210}\text{Pb}$  profiles (e.g. Hillenbrand et al., 2010a, 2010b). Circumstantial evidence of such contamination is also provided by the fact that dates on AIOM in surface sediments vary by up to several thousand years between different regions of the Antarctic shelf and even between different core sites in the same region (e.g. Andrews et al., 1999; Pudsey et al., 2006).

Even for cores where several down-core AMS  $^{14}\text{C}$  dates on AIOM yield ages in correct stratigraphic order, a sharp increase in reported ages with depth within deglacial transitional sediments (typically sandy gravelly muds) is often observed. This sharp increase has been referred to as a “dog leg”, and interpreted as the result of a down-core increase in fossil carbon contamination within the transitional unit, implying that the dates from its lower part are unreliable (Pudsey et al., 2006; Heroy and Anderson, 2007). While such a rapid increase in AMS  $^{14}\text{C}$  ages with depth could result from much slower sedimentation rates in the deglacial unit than in the overlying sediments, glaciomarine sedimentation models (e.g. Powell, 1984) generally imply that relatively high sedimentation rates are expected in this unit, and therefore the “dog-leg” is unlikely to result from a down-core change in sedimentation rate.

The occurrence of old surface ages combined with potential variability in the amount of fossil carbon contamination down core complicates the reliability of age models derived from AMS  $^{14}\text{C}$  dating of AIOM for Antarctic post-LGM sedimentary sequences. Usually, down-core AIOM ages are corrected by subtracting the core-top age (e.g. Andrews et al., 1999; Domack et al., 1999; Mosola and Anderson, 2006; Pudsey et al., 2006). This approach assumes that (1) the core top represents modern sedimentation, and (2) the

contribution of reworked fossil carbon from the hinterland remained constant through time. The first assumption can be validated by deploying coring devices that are capable of recovering undisturbed sediment samples from the modern seabed surface (e.g. box and multiple corers), paired  $^{14}\text{C}$  dating of the AIOM and calcareous microorganisms (if present) and application of  $^{210}\text{Pb}$  dating in addition to AIOM  $^{14}\text{C}$  dating (e.g. Harden et al., 1992; Andrews et al., 1999; Domack et al., 2001, 2005; Pudsey et al., 2006). The validity of the second assumption might be tested by paired  $^{14}\text{C}$  down-core dating of both AIOM and calcareous material, if the latter is present in any cores in a study area (e.g. Licht et al., 1998; Domack et al., 2001; Licht and Andrews, 2002; Rosenheim et al., 2008).

In Supplementary Table 2, most dates on AIOM have been corrected by subtracting a core-top age from the same or a nearby core. A few dates on AIOM from sediment cores in the Bellingshausen Sea have been corrected by subtracting the difference between paired core-top ages on AIOM and foraminifera. In each case the correction procedure is explained in the “Comments” column in Supplementary Table 2. Age calibrations to convert  $^{14}\text{C}$  years to calendar years were carried out using the CALIB Radiocarbon Calibration Program version 6.1.0. We used the Marine09 calibration dataset (Reimer et al., 2009) and a marine reservoir effect correction of  $1300 \pm 70$  years (Berkman and Forman, 1996) for consistency with age calibrations in other sector reviews in this volume, although the range of ages from the 14 calcareous core-top samples listed in Supplementary Table 2 is somewhat greater than the quoted uncertainty. Ages quoted in subsequent sections are calibrated ages unless stated otherwise.

The oldest AMS  $^{14}\text{C}$  age in each core that was considered as providing a reliable constraint on deglaciation by the authors who originally published it is shown in bold type in Supplementary Table 2. Older ages that occur in some cores are either on diamicton or from transitional deglacial sediments in which the age may be significantly biased by fossil carbon (i.e. part of a “dog leg” in down-core age progression). It is important to bear in mind that the ages shown in bold type in Supplementary Table 2 are *minimum* ages for grounding line retreat. In contrast, ages obtained on diamicton recovered at the base of some cores are likely to represent maximum ages for the preceding ice advance, since the dated material was probably derived from previously deposited shelf sediments that were incorporated into the diamicton (Hillenbrand et al., 2010a).

Relative palaeomagnetic intensity measurements have been used to provide additional constraints on age of deglaciation for a small number of cores recovered in the western ASE (Hillenbrand et al., 2010b).

### 2.4. Onshore survey data

Airborne and oversnow radio echo sounding data and oversnow seismic soundings collected over many decades have recently been collated into Bedmap2 (Fretwell et al., 2013). The PIG and Thwaites Glacier drainage basins are covered by systematic airborne surveys with 15–30 km line spacing (Holt et al., 2006; Vaughan et al., 2006), but in some other parts of the sector sounding data remain very sparse (Fretwell et al., 2013).

### 2.5. Terrestrial exposure age data

Published terrestrial data on the timing of deglaciation of this sector is limited to  $^{10}\text{Be}$  and  $^{26}\text{Al}$  surface exposure ages. Some published ages are also available from locations outside, but close to, the margins of the sector, for example from the Ford Ranges of Marie Byrd Land, Mount Waesche in the interior of West Antarctica,

and Two Step Cliffs in eastern Alexander Island, so we have included those in addition. These ages are shown in [Supplementary Table 3](#), with data used to calculate the  $^{10}\text{Be}$  and  $^{26}\text{Al}$  ages in [Supplementary Table 4](#). All  $^{10}\text{Be}$  and  $^{26}\text{Al}$  concentrations reported are blank-corrected. We have recalculated the published  $^{10}\text{Be}$  and  $^{26}\text{Al}$  ages in order to make them comparable across the sector. This was achieved by incorporating the published information about each sample into version 2.2 of the CRONUS-Earth online exposure age calculator ([Balco et al., 2008](#)). We applied the erosion rate that the original authors assumed (zero in all cases), quartz density of  $2.7 \text{ g cm}^{-3}$  for each sample, and used the Antarctic pressure flag ('ant') for the input file. We took  $^{10}\text{Be}$  and  $^{26}\text{Al}$  concentrations, sample thicknesses, and shielding corrections from the original papers.

We have chosen to report all the  $^{10}\text{Be}$  and  $^{26}\text{Al}$  exposure ages in reference to the global production rates ([Balco et al., 2008](#); CRONUS v.2.2), since these are currently the most widely used. Since the calibration sites on which this  $^{10}\text{Be}$  production rate is based are in the Northern Hemisphere,  $^{10}\text{Be}$  exposure ages from sites in Antarctica have to be calculated by extrapolating production rates from the Northern Hemisphere to the Southern Hemisphere using one of five published scaling schemes ('St': [Lal, 1991](#); [Stone, 2000](#); 'De': [Desilets et al., 2006](#); 'Du': [Dunai, 2001](#); 'Li': [Lifton et al., 2005](#); 'Lm': [Lal, 1991](#); [Stone, 2000](#); [Nishiizumi et al., 1989](#)). Here we report exposure ages based on the most commonly-used scaling scheme, 'St'. We did not apply a geomagnetic correction. The  $^3\text{He}$  and  $^{36}\text{Cl}$  ages from Mt Waesche ([Ackert et al., 1999](#)) reported here have not been recalculated.

## 2.6. Ice core constraints on past ice surface elevation

Past ice surface elevations can be estimated from total gas content in ice cores, as this is a function of past atmospheric pressure (elevation of the site) and, to a lesser extent, palaeo-temperature ([Raynaud and Lebel, 1979](#); [Martinierie et al., 1992](#)). The latter variable can be constrained by parameters measured on the ice cores themselves, such as oxygen and hydrogen isotope ratios. The WAIS Divide ice core site at  $79^\circ 28' \text{ S}$ ,  $112^\circ 05' \text{ W}$  ([Fig. 2](#)), where drilling started in 2005 and has recently been completed (austral summer 2012–2013; <http://www.waisdivide.unh.edu/>; [WAIS Divide Project Members, 2013](#)), is the only location from which a deep ice core has been recovered in the Amundsen–Bellingshausen sector, but no palaeo-elevation estimates based on it have yet been published. Results from the Byrd Station ice core, (drilled at  $80^\circ 01' \text{ S}$ ,  $119^\circ 31' \text{ W}$  in the Ross Sea sector of the WAIS; [Fig. 2](#)), however, provide valuable constraints on changes in ice surface elevation since the LGM in the interior of the WAIS (see [Section 3.2](#) for details).

## 3. Datasets

### 3.1. Amundsen Sea marine studies

#### 3.1.1. Geophysical surveys and geomorphological studies

The first marine geoscientific investigations on the Amundsen Sea continental shelf ([Fig. 2](#)) were carried out on the "Deep Freeze" cruises on the USCGC *Glacier* in 1981 and 1985 ([Anderson and Myers, 1981](#); [Kellogg and Kellogg, 1987a, 1987b](#)). Echo sounding data and sub-bottom profiles collected with a sparker system on the 1985 cruise revealed deep troughs on the inner shelf in the eastern part of the ASE, which [Kellogg and Kellogg \(1987a\)](#) suggested represent paths of palaeo-ice streams.

The first systematic echo sounding survey on the ASE shelf was carried out during the 'South Pacific Rim International Tectonic Expedition' (SPRITE) aboard RV *Polar Sea* in 1992. This provided a

preliminary bathymetric map of a cross-shelf trough extending from inner PIB to the mid-shelf ([SPRITE Group and Boyer, 1992](#)), which we refer to as Pine Island Trough (PIT; [Fig. 3](#)). In 1994, single beam echo-sounding data from the outer shelf in the eastern ASE and from the outer and middle shelf in the western ASE were collected during expedition ANT-XI/3 with RV *Polarstern* ([Miller and Grobe, 1996](#)). The first multichannel seismic profile extending onto the shelf in the region was also collected in the eastern ASE during the same expedition ([Nitsche, 1998](#); [Nitsche et al., 1997, 2000](#); [Gohl et al., 2013b](#)).

The first multibeam swath bathymetry data from the ASE were collected on RVIB *Nathaniel B. Palmer* Cruise NBP9902 in 1999 ([Anderson et al., 2001](#); [Wellner et al., 2001](#); [Lowe and Anderson, 2002, 2003](#)). A single-channel seismic reflection profile extending along PIT from the inner shelf to the shelf edge was collected on the same cruise ([Lowe and Anderson, 2002, 2003](#); [Jakobsson et al., 2012](#); [Gohl et al., 2013b](#)). Using these data, [Lowe and Anderson \(2002, 2003\)](#) identified a set of geomorphic zones along PIT, from glacially-scoured crystalline basement on the inner shelf, through glacially lineated surfaces over sedimentary strata and a large GZW on the middle shelf, to a pervasively iceberg-furrowed surface on the outer shelf. [Wellner et al. \(2001\)](#) and [Lowe and Anderson \(2002, 2003\)](#) also presented multibeam swath bathymetry data that revealed evidence of an extensive subglacial meltwater drainage network having been active in PIB.

Subglacial bedforms revealed by sparse swath bathymetry data covering parts of the seabed directly offshore from the easternmost Getz Ice Shelf were presented by [Wellner et al. \(2001\)](#) and led these authors and [Anderson et al. \(2001\)](#) to the conclusion that another palaeo-ice stream trough is present in this part of the ASE, which we refer to as Dotson-Getz Trough (DGT; [Fig. 3](#)). Sparse swath bathymetry data collected still farther west, in Wrigley Gulf, were interpreted by [Anderson et al. \(2001\)](#) as evidence of another palaeo-ice stream trough, which we refer to as Wrigley Gulf Trough (WGT; [Fig. 2](#)). Seismic reflection data collected on the same cruise revealed a significant geological boundary running across the ASE, between acoustic basement underlying the inner shelf and sedimentary strata underlying middle and outer shelf areas ([Wellner et al., 2001, 2006](#); [Lowe and Anderson, 2002](#)). [Wellner et al. \(2001, 2006\)](#) observed that this boundary coincided with a change in the types of bedforms observed in multibeam swath bathymetry data and suggested that it had exerted a significant influence on past ice dynamics.

Early in 2000, further multibeam swath bathymetry data were collected on RVIB *Nathaniel B. Palmer* Cruise NBP0001. The most significant addition to swath bathymetry coverage during this cruise was over the former subglacial meltwater drainage network in PIB ([Nitsche et al., 2013](#)).

[Evans et al. \(2006\)](#) presented multibeam swath bathymetry showing elongated bedforms near the shelf edge in a trough that branches off from PIT in a northwestward direction, and which we refer to as Pine Island Trough West (PITW). The authors interpreted these bedforms as having formed at the base of a fast flowing ice stream ([Fig. 4](#)). These data were collected on RRS *James Clark Ross* Cruise JR84 in 2003. Acoustic sub-bottom profiler data collected on the same cruise did not reveal any discernible post-glacial sediment layer overlying the bedforms, and [Evans et al. \(2006\)](#) interpreted this as evidence that the WAIS grounding line had advanced to the shelf edge during the last glaciation.

Co-ordinated cruises on RRS *James Clark Ross* (JR141) and RV *Polarstern* (ANT-XXIII/4) early in 2006 collected extensive multibeam bathymetry, sub-bottom profiler and seismic reflection data off the Dotson and eastern Getz ice shelves in the western part of the ASE ([Larter et al., 2007](#); [Gohl, 2007](#); [Weigelt et al., 2009, 2012](#)). The multibeam data revealed a varied assemblage of landforms,



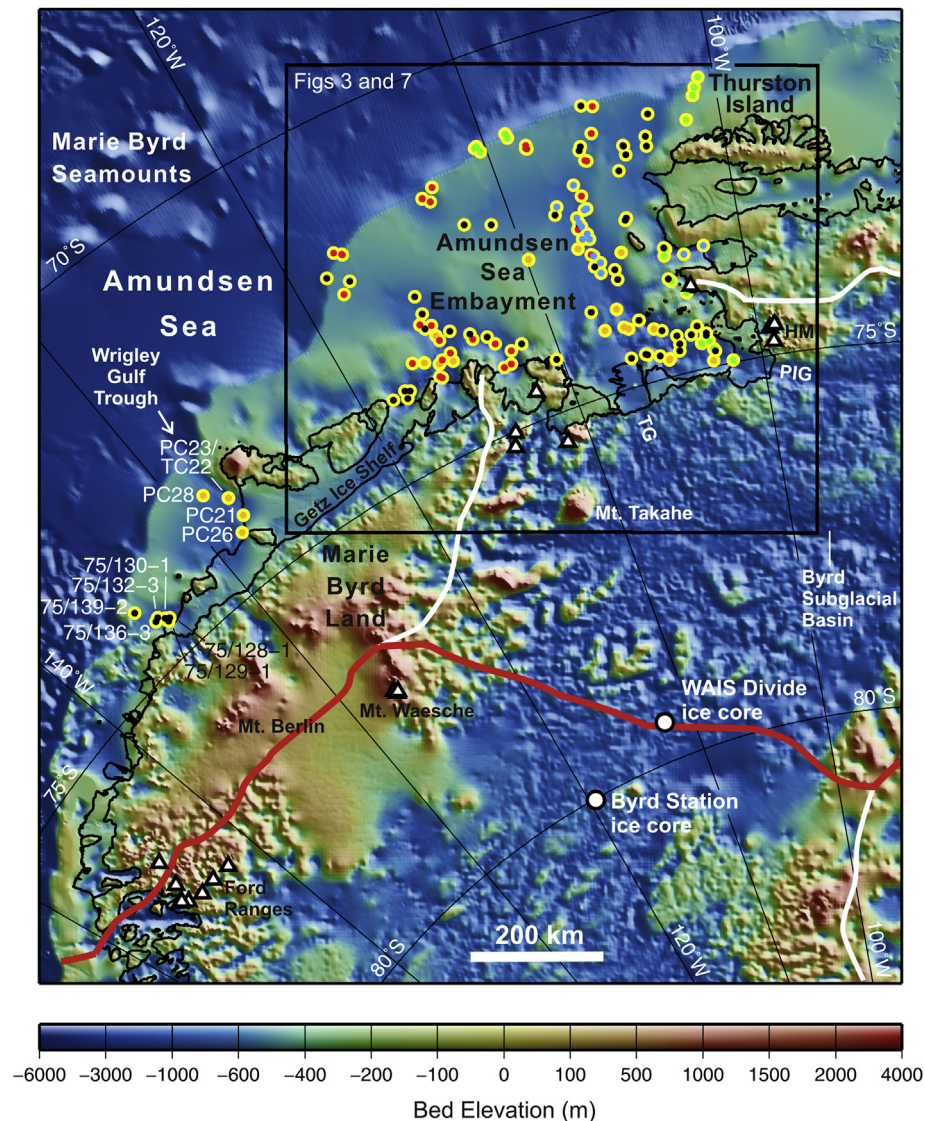


**Fig. 2.** Map of the Amundsen Sea region showing continental shelf sediment core sites (yellow circles), cosmogenic surface exposure age sample locations (white-filled triangles) and deep ice core sites (white-filled circles), overlaid on Bedmap2 ice sheet bed and bathymetry (Fretwell et al., 2013), which is displayed with shaded-relief illumination from the upper right. Sediment core sites are shown for cores that recovered more than 1 m of sediment and for shorter cores from which AMS  $^{14}\text{C}$  dates have been obtained. Core site symbol fill colour indicates ship the core was collected on: green – USCGC *Glacier*; orange – RVIB *Nathaniel B. Palmer*; red – RRS *James Clark Ross*; black – RV *Polarstern*; blue – IB *Oden*. Thick red line marks sector limit, along the main ice divide between the Amundsen Sea and the Ross Sea. Thick white lines mark other major ice divides. Black rectangle outlines area shown in greater detail in Figs. 3 and 7. Core sites outside the area shown in Figs. 3 and 7 are labelled with the core ID. PIG – Pine Island Glacier; TG – Thwaites Glacier; HM – Hudson Mountains.

some of which were indicative of formerly extensive fast ice flow in three glacially-eroded troughs that merge into the DGT (Fig. 3), even though acoustic basement is exposed at the sea floor across most of the inner shelf (Graham et al., 2009; Larter et al., 2009). This implies that the onset of fast flow was not fixed at the geological boundary identified by Wellner et al. (2001) throughout past glacial periods. Graham et al. (2009) interpreted multibeam data together with acoustic sub-bottom profiles and seismic profiles from the DGT and its tributaries, and argued that the varied assemblage of landforms observed over the inner shelf represents a multi-temporal record of past ice flow, not simply a “snapshot” of conditions immediately prior to the last deglaciation. The absence of any morphological features on bathymetric profiles along the outer shelf part of the DGT that could potentially represent a limit of grounding line advance during the LGM was interpreted by Larter et al. (2009) as evidence that the last advance reached the shelf edge.

Multibeam data over the innermost part of one of the troughs in front of the eastern Getz Ice Shelf revealed evidence of an extensive channel network interpreted as having been eroded by subglacial meltwater, similar to the one previously described in PIB (Graham et al., 2009; Larter et al., 2009). During the JR141 and ANT-XXIII/4 research cruises, additional acoustic and seismic profiles were also collected from outer continental shelf and slope of the ASE (Gohl, 2007; Gohl et al., 2007; Larter et al., 2007). RV *Polarstern* also reached inner PIB, and multichannel seismic profiles collected in PIB and along a corridor near the eastern coast of the ASE were interpreted as indicating differences in rate of glacial retreat and basal meltwater activity between these two areas (Uenzelmann-Neben et al., 2007).

Nitsche et al. (2007) compiled all of the single beam and multibeam echo sounding data available up to 2007, producing a continuous gridded regional bathymetry map of the Amundsen Sea that provided the first accurate representation of the continental



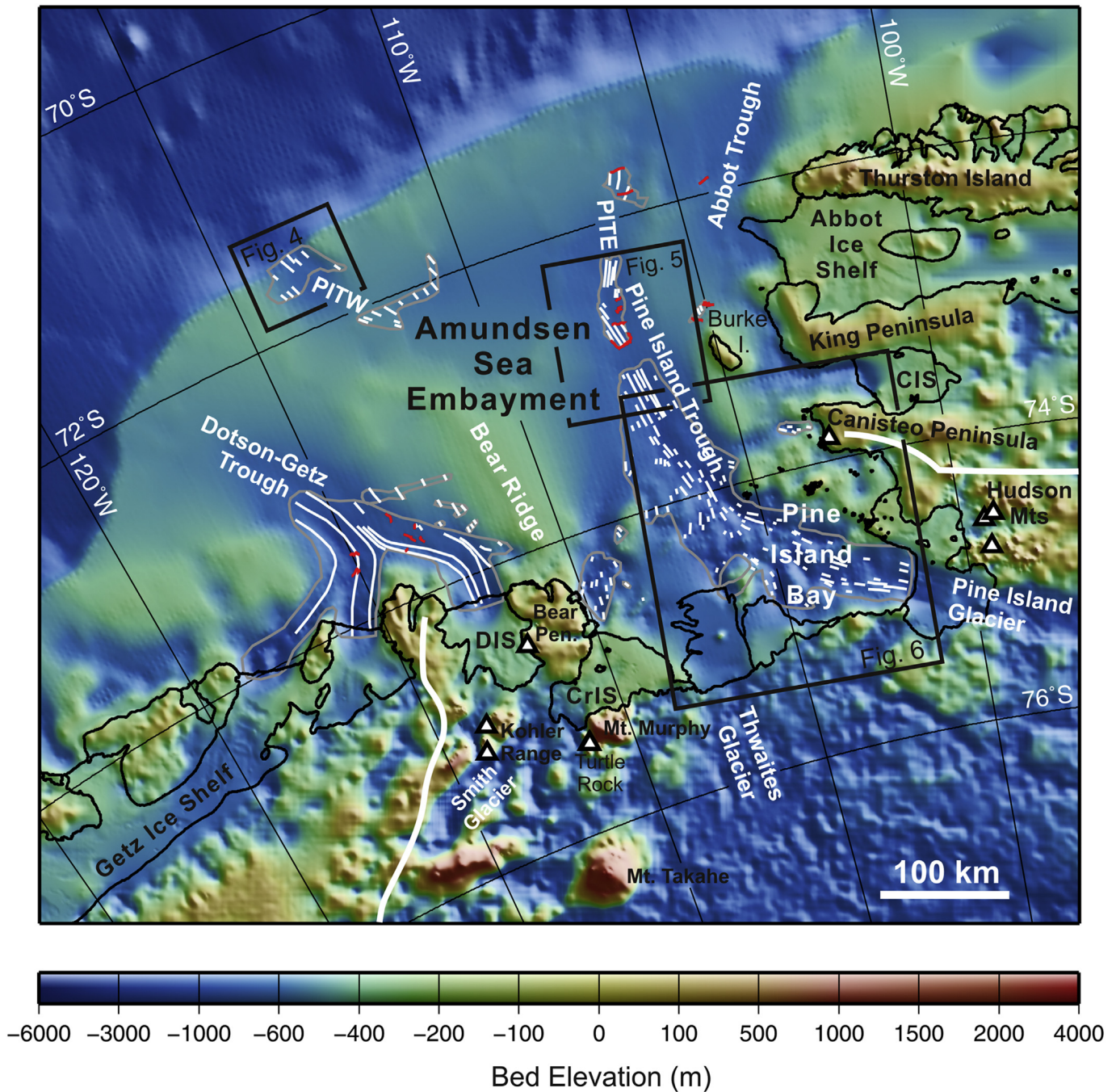


**Fig. 3.** Map of the Amundsen Sea Embayment showing main geomorphological features on the continental shelf and cosmogenic surface exposure age sample locations onshore, overlaid on Bedmap2 ice sheet bed and bathymetry (Fretwell et al., 2013), which is displayed with shaded-relief illumination from the upper right. Grey outlines mark areas in which bedforms indicative of past ice flow direction are observed in multibeam swath bathymetry data. Thin white lines indicate flow alignment. Red lines mark the crests of grounding zone wedges and moraines that represent past grounding line positions. Thick white lines mark major ice divides. Black rectangles outline areas shown in greater detail in Figs. 4–6. CIS – Cosgrove Ice Shelf; CrIS – Crosson Ice Shelf; DIS – Dotson Ice Shelf; PITE – Pine Island Trough East; PITW – Pine Island Trough West.

slope and major cross shelf troughs (Figs. 2 and 3). In addition to PIT, PITW, DGT and WGT, the data also showed additional troughs that extend seawards from other ice shelf fronts along the eastern

ASE coast (e.g. a trough extending NNE-wards from the Abbot Ice Shelf, which is referred to as 'Abbot Trough' by Hochmuth and Gohl, 2013; Gohl et al., 2013b), the Crosson Ice Shelf and various sections



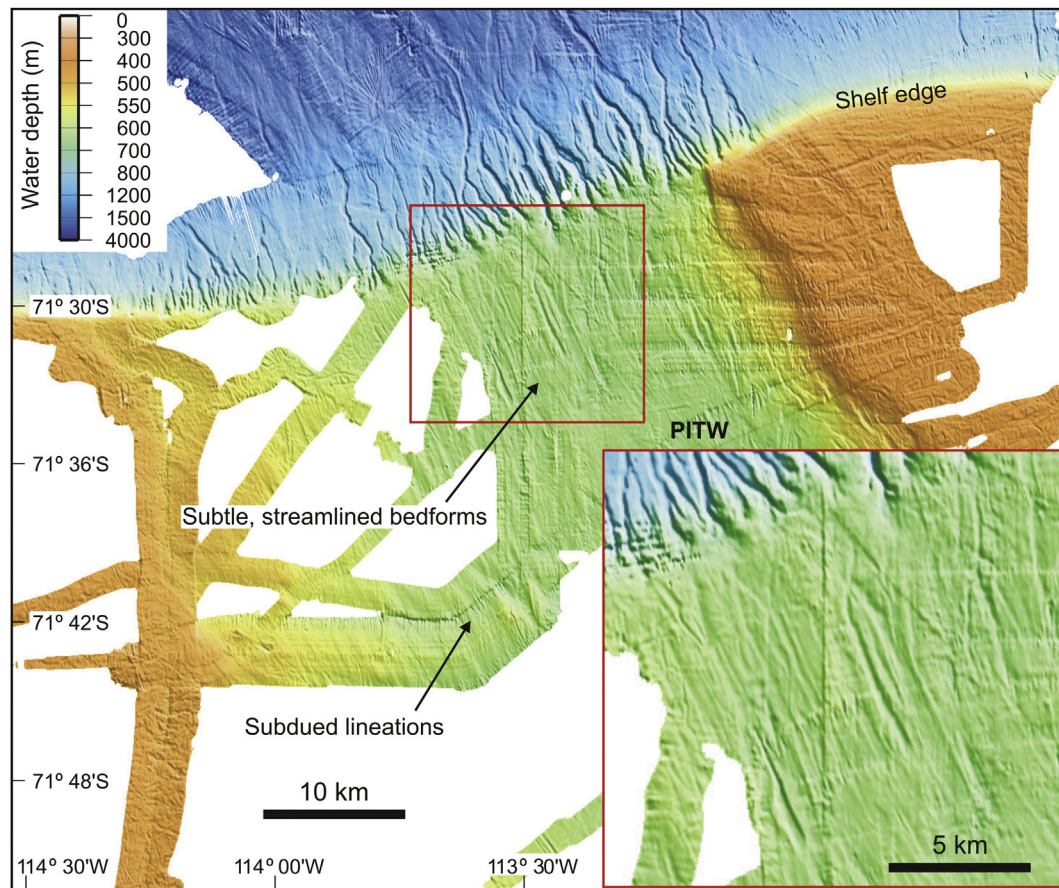


**Fig. 4.** Multibeam swath bathymetry data from the outer part of Pine Island Trough West showing streamlined bedforms. Data shown were collected on RRS *James Clark Ross* cruises JR84 and JR141, RVIB *Nathaniel B. Palmer* cruises NBP0001 and NBP0702, and RV *Polarstern* cruise ANT-XXIII/4. The grid was generated using a near neighbour algorithm, has a cell size of 50 m and is displayed with shaded-relief illumination from 65° (modified from [Graham et al., 2010](#)).

of the Getz Ice Shelf (e.g. a small glacial trough extending north-westwards from the westernmost Getz Ice Shelf). A possible tectonic basement control for the locations of the main palaeo-ice stream troughs in the ASE has recently been suggested by [Gohl \(2012\)](#). One multibeam swath bathymetry dataset included in the compilation by [Nitsche et al. \(2007\)](#) that has not been mentioned above was collected early in 2007 on RVIB *Nathaniel B. Palmer* cruise NBP0702. The additional multibeam data collected on that cruise improved definition of the continental shelf break and augmented previous coverage of inner shelf areas, including PIB ([Nitsche et al., 2007](#)).

Guided by the [Nitsche et al. \(2007\)](#) bathymetry map, multibeam swath bathymetry data were collected in a continuous corridor from the continental shelf edge along the axis of the eastern branch of PIT (PITE; [Fig. 3](#)) and the main trunk of the trough to PIB on RRS *James Clark Ross* Cruise JR179 early in 2008. Two overlapping swaths were collected along most of this corridor and in places the coverage also overlapped with data collected on previous cruises (NBP9902, NBP0001, JR141 and ANT-XXIII/4). Streamlined landforms observed along this corridor confirmed that it represented a flow-line of former ice motion, at least to within 68 km of the shelf edge ([Graham et al., 2010](#)). The presence of other streamlined landforms along PITW ([Fig. 4](#)), as previously reported by [Evans et al. \(2006\)](#), was interpreted by [Graham et al. \(2010\)](#) as evidence of palaeo-ice stream flow switching on the outer shelf. [Graham et al. \(2010\)](#) also described five sediment bodies that they interpreted as GZWs, two of which are in the axis of PITE, whereas the other three are located in a “bottle neck” in PIT, just landward of where it

divides into its two outer shelf branches ([Figs. 3 and 5](#)). The most landward of these GZWs was the one previously identified by [Lowe and Anderson \(2002\)](#). The existence of multiple GZWs implies that the retreat history of the ice stream was punctuated by pauses in landward migration of the grounding line and minor re-advances ([Graham et al., 2010](#)).

Bathymetry data collected early in 2009 beneath the ice shelf that extends from the grounding line of PIG, using the Autosub3 autonomous underwater vehicle (AUV), revealed a transverse ridge ([Jenkins et al., 2010](#)). Bedforms imaged on the crest of the ridge using the multibeam echo sounding system on the AUV were interpreted by [Jenkins et al. \(2010\)](#) as evidence that it was a former grounding line, and the smooth surface on the seaward slope was interpreted as having formed by deposition of sediment scoured from the crest. [Jenkins et al. \(2010\)](#) also interpreted a bump in the ice surface seen in a 1973 Landsat image as an ice rumple caused by contact between the ice and the highest point of the ridge. By 2005 the grounding line was more than 30 km upstream of that point ([Vaughan et al., 2006](#)), but combining the AUV observations with grounding line retreat and ice shelf thinning rates measured since the mid-1990s ([Rignot, 1998, 2008; Wingham et al., 2009](#)) implies that these rates must have been slower over the preceding 20 years. Inversion of airborne gravimetry data collected by the NASA Ice-bridge project provided additional constraints on the geometry of the ridge and the sub-ice-shelf cavity on its upstream side ([Studinger et al., 2010](#)). The inversion, however, predicts a shallower ridge than observed in the AUV data, which implies that the ridge consists mainly of dense bedrock rather than being a GZW

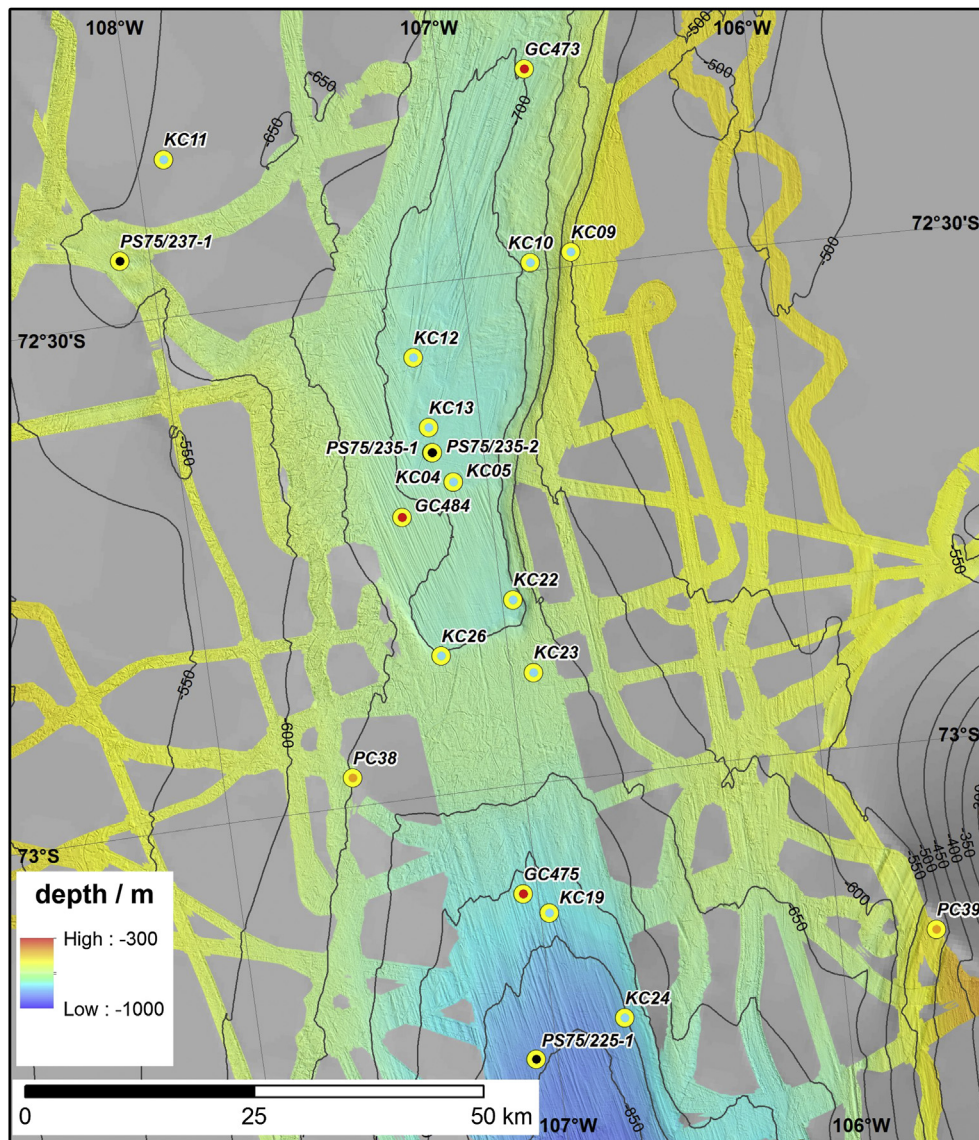


**Fig. 5.** Map of the mid-shelf part of Pine Island Trough showing shelf sediment core sites overlaid on multibeam swath bathymetry (Lowe and Anderson, 2002; Graham et al., 2010; Jakobsson et al., 2011, 2012). Bathymetry contours from a regional compilation (Nitsche et al., 2007) are shown at 50 m intervals and highlight the “bottle neck” in this part of Pine Island trough. Sediment core sites are shown and labelled with the core ID for cores that recovered more than 1 m of sediment and for shorter cores from which AMS  $^{14}\text{C}$  dates have been obtained. Core site symbol fill colour indicates ship the core was collected on, as in Fig. 2.

built by deposition of glacial sediments. By modelling the gravimetry data, however, Muto et al. (2013) estimated a sediment thickness of  $479 \pm 143$  m beneath the crest of the ridge, and their model shows that the bathymetric crest is offset about 8 km up-stream from the crest of a buried bedrock ridge. Inversion of airborne gravimetry data over the ice shelf that extends seaward from Thwaites Glacier (Fig. 3) also revealed a submarine ridge that undulates between 300 and 700 m below sea level and has an average relief of 700 m (Tinto and Bell, 2011).

Autosub3 was deployed from RVIB *Nathaniel B. Palmer* during Cruise NBP0901 to collect the sub-ice shelf data described above. At the time of the AUV missions, PIB was unusually clear of sea ice, and this allowed almost complete swath bathymetry coverage of inner PIB to be achieved using the hull-mounted multibeam echo sounding system. These data showed that the former subglacial meltwater drainage network identified by Lowe and Anderson (2002, 2003) was more extensive than previously realised, and received substantial subglacial meltwater inflow from the east as well as from the Pine Island and Thwaites glaciers (Fig. 6; Nitsche

et al., 2013). The swath bathymetry data also revealed a zone of relatively smooth topography directly in front of Pine Island ice shelf, which was shown to be the surface of 300 m-thick sedimentary deposits by multichannel seismic profiles collected on RV *Polarstern* a year later (Nitsche et al., 2013).

Early in 2010, a second successive austral summer with unusually sparse sea ice cover on the Amundsen Sea continental shelf allowed systematic multibeam swath bathymetry survey over the mid-shelf part of PIT on IB *Oden* (OSO0910; Jakobsson et al., 2011, 2012) and acquisition of an extensive network of multichannel seismic lines on RV *Polarstern* (ANT-XXVI/3; Gohl, 2010; Gohl et al., 2013b).

Using the multibeam bathymetry data collected over the mid-shelf part of PIT on OSO0910 (Fig. 5), Jakobsson et al. (2011, 2012) were able to map the full extent of the GZWs and associated bedforms previously identified by Lowe and Anderson (2002) and Graham et al. (2010). Jakobsson et al. (2011) identified unusual 1–2 m-high “corrugation ridges” associated with and transverse to curvilinear-linear furrows in the axis of PIT, seaward of the mid-



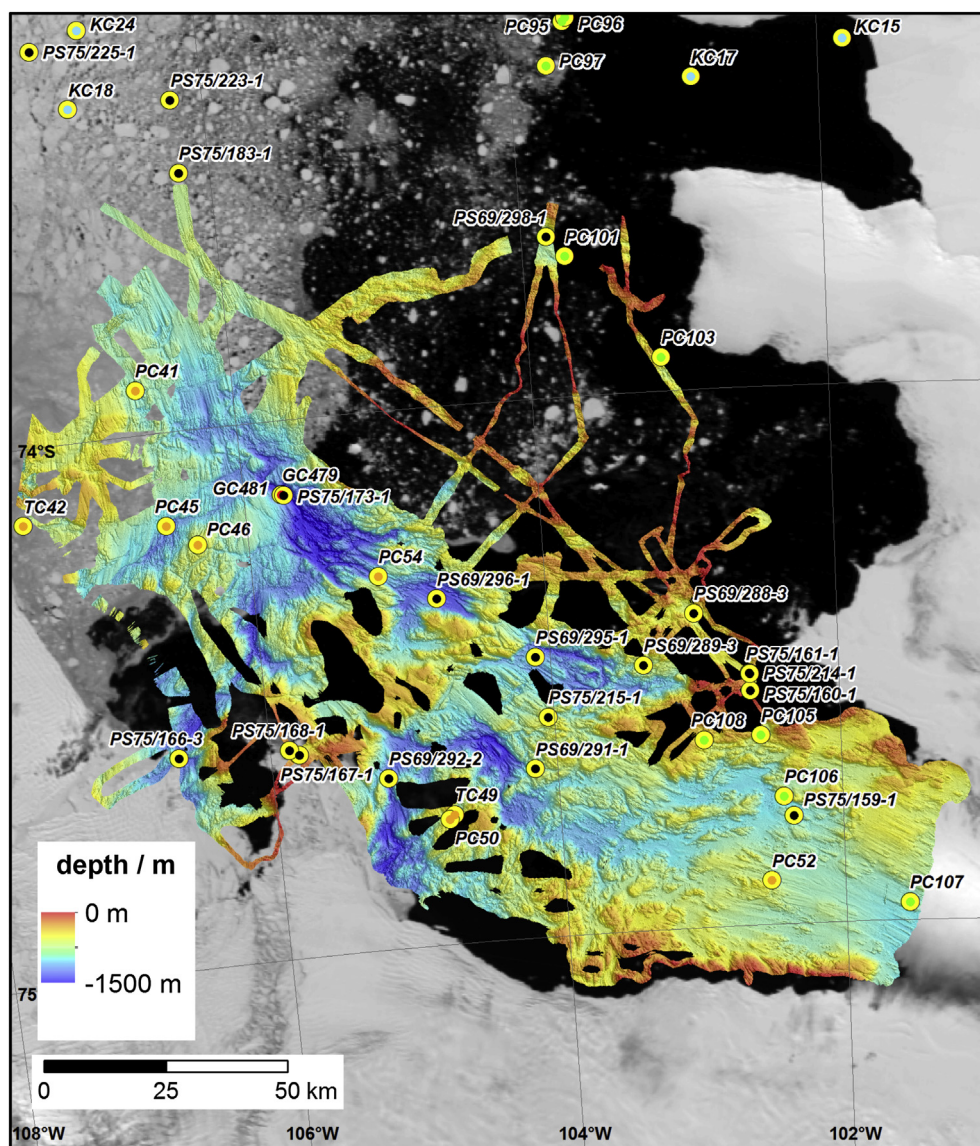


**Fig. 6.** Map of Pine Island Bay showing shelf sediment core sites overlaid on multibeam swath bathymetry (Nitsche et al., 2013). Sediment core sites are shown and labelled with the core ID for cores that recovered more than 1 m of sediment and for shorter cores from which AMS  $^{14}\text{C}$  dates have been obtained. Core site symbol fill colour indicates ship the core was collected on, as in Fig. 2. In most cases, where a box core or giant box core from which only a surface sample has been dated is co-located (within 50 m) with another core, only the other core is labelled (see co-ordinates in Supplementary Table 1 to identify co-located cores).

shelf GZWs, and interpreted these as having been generated by tidal motion of icebergs resulting from ice shelf collapse and calving directly at the grounding line. The area in which the corrugation ridges occur is seaward of, and at greater water depth than the mid-shelf GZWs, implying that the hypothesized ice shelf break-up must have occurred before formation of the GZWs. Jakobsson et al. (2012) interpreted palaeo-ice stream flow as having switched from PITW to PITE at an early stage during the last deglaciation, and estimated the length of time required for the largest GZW to develop as between 600 and 2000 years, assuming that sediment flux rates at the bed of the palaeo-ice stream were between 500 and  $1650 \text{ m}^3 \text{ a}^{-1} \text{ m}^{-1}$ .

Klages et al. (2013) presented multibeam swath bathymetry data, acoustic sub-bottom profiles, a multichannel seismic profile, and results of analyses of two sediment cores collected on a bank to the east of PIT and north of Burke Island on ANT-XXVI/3 (Fig. 3). The authors interpreted the unusual assemblage of bedforms revealed by the multibeam data as indicating that the bank supported an inter-ice stream ridge during the LGM, and recording two still-

stands or minor re-advances of the grounding line during the last deglaciation.

### 3.1.2. Sediment core studies and geochronological data

The first sediment cores from the Amundsen Sea continental shelf were collected on the “Deep Freeze” cruises on the USCGC *Glacier* in 1981 and 1985 (Fig. 7; Anderson and Myers, 1981; Kellogg and Kellogg, 1987a, 1987b). On the 1981 cruise, three piston cores on the outer shelf recovered glacial deposits, and five piston cores on the continental slope recovered a variety of glacial marine sediments and mass flow deposits, such as debris flows and turbidites (Anderson and Myers, 1981; Dowdeswell et al., 2006; Kirshner et al., 2012). AMS  $^{14}\text{C}$  dating was carried out recently on foraminifera in samples from one of the shelf cores (Kirshner et al., 2012).

Kellogg and Kellogg (1987a, 1987b) reported results from micropalaeontological and sedimentological examination of 20 sediment cores collected on the continental shelf during the Deep Freeze 85 cruise, and inferred from the widespread occurrence of



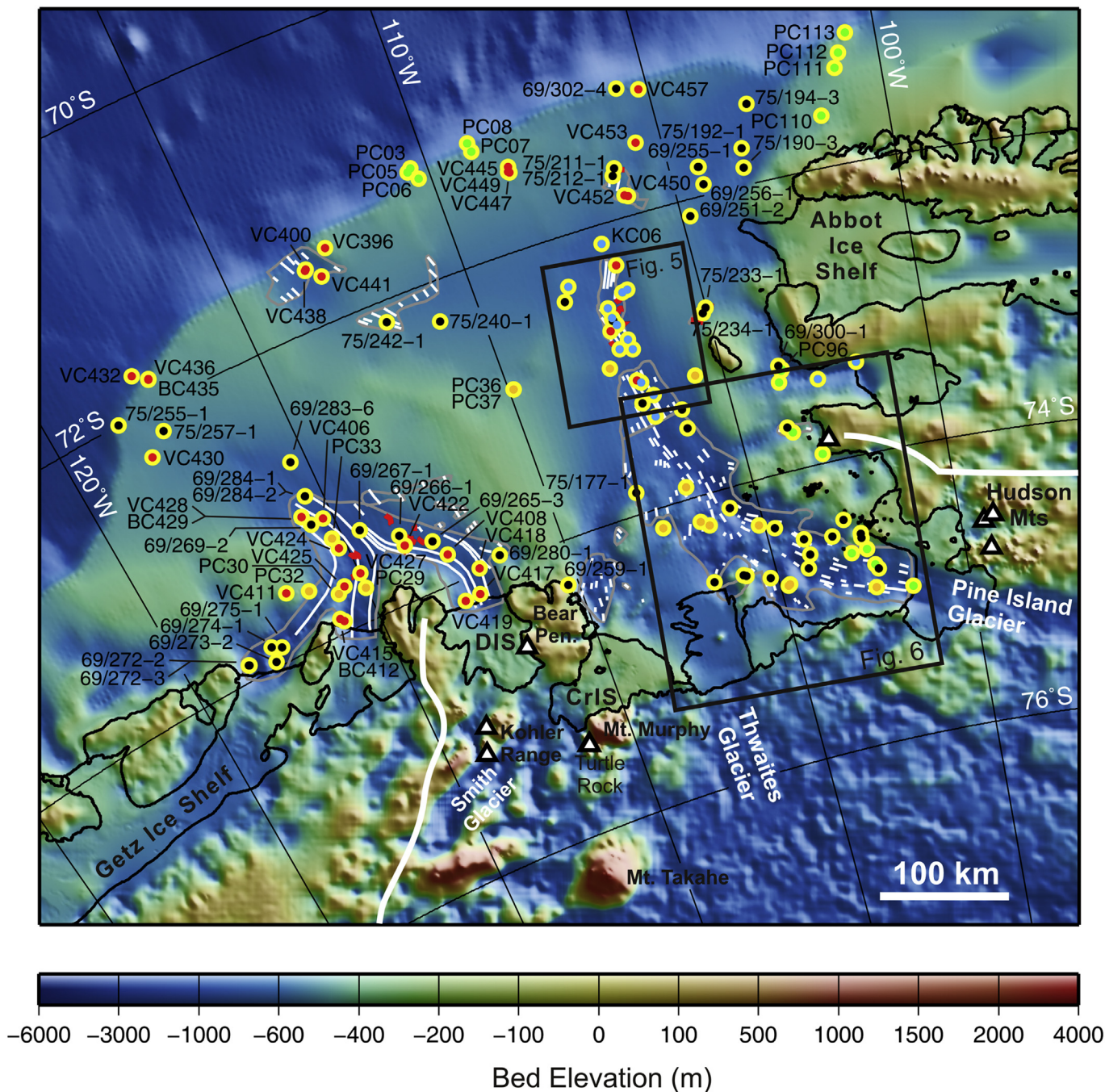


**Fig. 7.** Map of the Amundsen Sea Embayment showing continental shelf sediment core sites (yellow circles) and cosmogenic surface exposure age sample locations (white-filled triangles), overlaid on geomorphological features (see Fig. 3 for details) and Bedmap2 ice sheet bed and bathymetry (Fretwell et al., 2013), which is displayed with shaded-relief illumination from the upper right. Sediment core sites are shown for cores that recovered more than 1 m of sediment and for shorter cores from which AMS  $^{14}\text{C}$  dates have been obtained. Core site symbol fill colour indicates ship the core was collected on, as in Fig. 2. In most cases, where a box core or giant box core from which only a surface sample has been dated is co-located (within 50 m) with another core, only the other core is labelled (see co-ordinates in Supplementary Table 1 to identify co-located cores). Thick white lines mark major ice divides. Black rectangles outline area shown in greater detail in Figs. 5 and 6. Core sites outside the area shown in Figs. 5 and 6 are labelled with the core ID. CrIS – Crosson Ice Shelf; DIS – Dotson Ice Shelf.

“compact” diamicton, and sub-bottom profiles collected with a sparker system on the same cruise, that grounded ice had advanced to the continental shelf edge. Although no radiometric age constraints had been obtained from the cores, Kellogg and Kellogg (1987a) suggested that the last advance may have occurred during the LGM. Kellogg and Kellogg (1987b) observed that sediments in four cores recovered from inner PIB were almost barren of microfossils, and attributed this to deposition beneath a former extension of the floating terminus of PIG. They further suggested that ice shelf retreat from inner PIB occurred within the preceding century, and speculated that the “Thwaites Iceberg Tongue” (iceberg B-10), grounded north of the terminus of Thwaites Glacier at that time, might have originated from PIG. This latter hypothesis was assessed by Ferrigno et al. (1993) as being unlikely, on the basis that the crevassing pattern on the iceberg seen in Landsat images was a better match to that observed downstream of the grounding line on Thwaites Glacier than on PIG. This conclusion by Ferrigno et al. (1993) has subsequently been strengthened by the observation that a similar large iceberg calved from Thwaites Glacier in 2002 (iceberg B-22A) ran aground in the same position that iceberg B-10 had occupied for more than two decades before it drifted away in 1992 (Rabus et al., 2003).

Seabed surface sediments were collected from the outer shelf in the eastern ASE and from the outer and middle shelf in the western ASE during expedition ANT-XI/3 with RV *Polarstern* (Miller and Grobe, 1996). Results of various sedimentological, mineralogical, geochemical and micropalaeontological analyses on these samples were published as part of larger geographical compilations (Hillenbrand et al., 2003; Esper et al., 2010; Ehrmann et al., 2011; Hauck et al., 2012; Mackensen, 2012).

Piston cores were collected from inner and middle shelf areas during RVIB *Nathaniel B. Palmer* Cruise NBP9902 in 1999, and samples from these cores yielded the first radiocarbon dates from the region constraining ice retreat since the LGM (Anderson et al., 2002; Lowe and Anderson, 2002; Supplementary Table 2).

Lowe and Anderson (2002) used the ages and other data from the cores in the PIT region, such as the presence of subglacially deposited tills, together with multibeam swath bathymetry data and a single-channel seismic reflection profile collected on the same cruise (Anderson et al., 2001; Wellner et al., 2001; Lowe and Anderson, 2003), as the basis for a reconstruction of grounded ice extent at the LGM and the subsequent history of ice sheet retreat. They considered that the grounding line probably advanced to the shelf break during the LGM, but also defined a minimum LGM grounding line position near the boundary between the middle and outer parts of the continental shelf, at a latitude of about 72° 30'S. Lowe and Anderson (2002) interpreted subsequent retreat as having reached a mid-shelf position by about 16 ka BP (uncorrected  $^{14}\text{C}$  years), on the basis of an AMS  $^{14}\text{C}$  date on foraminifera from a core (PC39; Fig. 5) recovered to the west of Burke Island, at which point the grounding line retreat paused and a GZW started to develop. The precise age of these events remained quite uncertain because the 1-sigma uncertainty in the reported deglacial date from PC39 was  $\pm 3900$  yr, and the age we obtain from calibration is  $17,203 \pm 9430$  cal yr BP (Supplementary Table 2).

In their reconstruction of ice retreat, Lowe and Anderson (2002) interpreted grounding line unpinning from the mid-shelf GZW as having occurred between 16 and 12 ka BP (uncorrected  $^{14}\text{C}$  years, equivalent to 18.0 to 12.6 cal ka BP with the calibration parameters used in this paper), and suggested that subsequent retreat into PIB may have been rapid. A date of  $10,086 \pm 947$  cal yr BP (Supplementary Table 2) for foraminifera from glaciomarine sediment in a core (PC41; Fig. 6) recovered 250 km from the modern grounding line of PIG showed that ice had retreated at least as far as the outer part of PIB by early Holocene time.

Anderson et al. (2002) published additional AMS  $^{14}\text{C}$  dates on foraminifera from cores (TC22, TC/PC23, PC26) recovered farther west, in Wrigley Gulf (Fig. 2). The radiocarbon dates showed that ice had retreated to the inner shelf in WGT before the start of the Holocene (ages between  $15,610 \pm 651$  and  $14,321 \pm 536$  cal yr BP, Supplementary Table 2).

A core (PC46; Fig. 6) from the axis of one of the former subglacial channels in PIB recovered well-sorted sands and gravels at shallow depth below the sea floor (Lowe and Anderson, 2003). These well-sorted sediments were probably deposited from meltwater in either a subglacial or proglacial setting, but they suggest that subglacial meltwater flow was active in PIB during the last glacial period or deglaciation (Lowe and Anderson, 2003).

In contrast, sediment cores collected in 2006 on Cruise JR141, from the axes of channels located directly offshore from the Dotson and eastern Getz ice shelves, recovered sedimentary facies that do not support meltwater activity in those channels during the LGM or the last deglaciation (Smith et al., 2009). One of the cores collected from the axis of a channel offshore from the Getz Ice Shelf (VC415; Fig. 7) even recovered a sequence that typically records the retreat of a grounding line (i.e. subglacial till overlain by transitional sandy mud, overlain in turn by diatom-bearing mud deposited in seasonal open marine conditions similar to today), indicating that the channel floor was overridden by grounded ice since it was last active as a meltwater conduit (Smith et al., 2009).

A diatom ooze layer overlying glacial and deglacial transition sediments was recovered in several cores collected from inner shelf tributaries of DGT on JR141 and ANT-XXIII/4 (Fig. 7). AMS  $^{14}\text{C}$  dates on AIOM from samples of this layer yielded consistent AMS  $^{14}\text{C}$  ages which, when calibrated, are between  $14,312 \pm 510$  and  $11,881 \pm 455$  cal yr BP (Hillenbrand et al., 2010b; Supplementary Table 2). The low terrigenous sediment component of the ooze means that these ages are less likely to be affected by significant fossil organic carbon contamination. Constraints from relative palaeomagnetic intensity (RPI) records of cores penetrating the ooze layer, however, suggest that the oldest ages from the ooze must be affected by some contamination, and the ages considered to be most reliable from ooze samples range between 12,816 and 11,881 cal yr BP (Hillenbrand et al., 2010b; Smith et al., 2011). Radiocarbon dates obtained on two samples of acid-cleaned diatom tests from the ooze layer yielded ages that are significantly younger and inconsistent with constraints from RPI records (Hillenbrand et al., 2010b), probably due to adsorption of atmospheric  $\text{CO}_2$  on the highly reactive opal surfaces of the extracted diatom tests prior to sample graphitisation and combustion for AMS  $^{14}\text{C}$  dating (cf. Zheng et al., 2002). The dates obtained on the conventionally-treated ooze samples show that the ice margin had retreated from much of the inner shelf in the DGT before the start of the Holocene.

Smith et al. (2011) integrated the ages from the diatom ooze layer with a large dataset of radiocarbon ages obtained from glaciomarine sediments in cores retrieved along transects in DGT and its tributaries during JR141 and ANT-XXIII/4. The collated ages on both AIOM and, where present, foraminifera samples record rapid deglaciation across the middle and inner shelf from about 13,779 cal yr BP to within c.10–12 km of the present ice shelf front between 12,549 and 10,175 cal yr BP (Smith et al., 2011; calibrated ages from Supplementary Table 2). The distinction between glaciomarine and subglacial facies in the studied cores was based on a dataset comprising sedimentological parameters, physical properties and proxies for sediment provenance (Smith et al., 2011). Clay mineral changes between subglacial and postglacial sediments in cores retrieved from near-coastal sites in the ASE led Ehrmann et al. (2011) to the conclusion that the drainage basins of palaeo-ice streams discharging into the ASE have varied through time.



In 2010, sediment cores were also collected on both IB Oden (OSO0910) and RV *Polarstern* (ANT-XXVI/3): Kasten cores were collected from 27 sites during OSO0910, mostly in the mid-shelf part of PIT (Fig. 5; Kirshner et al., 2012), whereas 37 gravity cores, eight giant box cores and one multiple core were collected from various locations on the ASE shelf during ANT-XXVI/3 (Gohl, 2010; Hillenbrand et al., 2013; Klages et al., 2013).

Majewski (2013) analysed benthic foraminifera assemblages in the core tops of sediment cores collected on OSO0910, and Kirshner et al. (2012) carried out multi-proxy analyses on both the OSO0910 cores and cores collected previously on DF81 and NBP9902. The latter study included detailed identification and mapping of sedimentary facies and then established a chronostratigraphic framework constrained by previously published and 23 new AMS  $^{14}\text{C}$  dates. The authors also developed an updated reconstruction of ASE deglaciation, incorporating their new results. This reconstruction followed Graham et al. (2010) in interpreting the LGM limit of grounded ice in PITE as having been somewhere between the most seaward GZW and the continental shelf edge. An AMS  $^{14}\text{C}$  date on planktonic foraminifera from a core (DF81, PC07; Fig. 7) near the shelf edge farther west showed that glacial marine sediments began accumulating on the eastern ASE outer shelf before 16.4 cal ka BP (Supplementary Table 2), and this is therefore a minimum age for the start of grounding line retreat (Kirshner et al., 2012). A mud-dominated facies containing very little sand and devoid of pebbles, interpreted by Kirshner et al. (2012) as representing sub-ice shelf deposition, was recovered in cores from the inshore flank of the largest and most landward GZW in the mid-shelf part of PIT. AMS  $^{14}\text{C}$  dates on monospecific juvenile planktonic foraminifera from this unit indicate that it was deposited between 12.3 and 10.6 cal ka BP (Supplementary Table 2), which implies that the GZWs in the mid-shelf part of the trough all formed before 12.3 cal ka BP and that an ice shelf was present over the mid-shelf region for almost 2000 years (Kirshner et al., 2012). Kirshner et al. (2012) further suggested that during this interval the grounding line in PIT was likely to have been at the sedimentary to crystalline bedrock transition previously identified by Lowe and Anderson (2002). Sedimentological changes at the end of this interval (Kirshner et al., 2012) and geomorphological features (Jakobsson et al., 2012) have been interpreted as indicating that it was followed by ice shelf break-up and rapid grounding line retreat into inner PIB. Break-up of the ice shelf has been attributed to inflow of a warm water mass onto the shelf (Jakobsson et al., 2012; Kirshner et al., 2012). An abrupt change in sedimentation to a draping silt unit began between  $\sim 7.8$  and 7.0 cal ka BP. This terrigenous silt unit has been interpreted as a meltwater-derived facies (Kirshner et al., 2012).

Hillenbrand et al. (2013) presented a detailed facies analysis of three sediment cores collected from relatively shallow water sites in inner PIB on ANT-XXVI/3 (Fig. 5), and integrated this with 33 new radiocarbon dates to argue that the grounding line had retreated into inner PIB, to within 112 km of the modern PIB grounding line, before  $11,664 \pm 653$  cal yr BP. This age was obtained by calibration of an AMS  $^{14}\text{C}$  date of  $11,090 \pm 50$  yr BP (uncorrected  $^{14}\text{C}$  years) on mixed benthic and planktonic foraminifera from a facies consisting of mud alternating with layers and lenses of sand and/or gravelly sand in core PS75/214-1, the sandy layers being interpreted as turbidites. Hillenbrand et al. (2013) calibrated this date by following the same procedure as used in this paper, apart from assuming a different marine reservoir age ( $1100 \pm 200$  years, cf.  $1300 \pm 70$  years used in this paper). The age for the same sample in Supplementary Table 2 is  $11,157 \pm 248$  cal yr BP, highlighting the fact that, for some time intervals, small differences in the assumed reservoir age can propagate into larger differences in calibrated age. Although our calibrated age for this sample is more than 500 years

younger than that derived by Hillenbrand et al. (2013), the uncertainty range of the age still does not overlap with that of the date Kirshner et al. (2012) use to constrain the younger limit of the period of ice shelf cover over the mid-shelf area. If these two dates and the published interpretations of the dated facies are accepted, they imply that an ice shelf extending more than 200 km from the grounding line persisted after the grounding line retreated into inner PIB. Alternatively, one or other of the ages or facies interpretations must be misleading.

AMS  $^{14}\text{C}$  dates on carbonate samples from two other cores in inner PIB that support an interpretation of an early Holocene retreat of the grounding line to within c. 100 km of its present position were also presented by Hillenbrand et al. (2013). The oldest date from another core only c. 2 km from site PS75/214, yields an age of  $9015 \pm 251$  cal yr BP from the calibration in this paper, and the oldest date from a core only 93 km from the modern grounding line of Thwaites Glacier corresponds to an age of  $10,124 \pm 269$  cal yr BP (Supplementary Table 2). The oldest dates from two of the three inner PIB cores studied by Hillenbrand et al. (2013) are not from the dated samples deepest in the core (although the age of 10,124 cal yr BP is the deepest of 12 dated samples from the same core that are all in stratigraphic order, within the uncertainty of the calibrated ages), but these authors argue that regardless of subsequent redeposition from nearby, shallower shelf areas by gravitational downslope transport, the dated calcareous microfossils can only have lived near the core sites after the grounding line had retreated farther landward. Although it is theoretically possible that reworking of older foraminifera could have biased the oldest date (11,157 cal yr BP) determined from the inner PIB cores, contamination with 10% of very old (“radiocarbon dead”) foraminifera would be required to increase the measured age by 1000 years, and an age bias of this magnitude would require an even higher level of contamination with foraminifera that lived just before the LGM. Such extensive contamination would imply the existence of a significant ‘reservoir’ of pre-LGM microfossils somewhere in PIB, for which there is no evidence. If such a reservoir was shown to exist, this would reduce confidence in many other dates from sites in PIB and farther offshore.

Hillenbrand et al. (2013) also collated minimum ages of deglaciation from inner shelf cores collected in other parts of the Amundsen Sea that had previously been published by Anderson et al. (2002), Hillenbrand et al. (2010b) and Smith et al. (2011), and presented one new radiocarbon date on a carbonate sample from a core recovered from the inner shelf part of the small glacial trough offshore from the westernmost Getz Ice Shelf (PS75/129-1; Fig. 2; age  $12,825 \pm 236$  cal yr BP, Supplementary Table 2). The collated deglacial ages showed that WAIS retreat from the entire Amundsen Sea shelf was largely complete by the start of the Holocene.

Klages et al. (2013) presented six new AMS  $^{14}\text{C}$  dates on AIOM samples from the two sediment cores collected on a bank to the east of PIT and north of Burke Island on ANT-XXVI/3 (Fig. 7), and the ones they interpreted as minimum ages of deglaciation are  $19,146 \pm 269$  and  $17,805 \pm 578$  cal yr BP (Supplementary Table 2). These ages are older, but not incompatible with, the minimum age for the start of deglaciation of the outer shelf of 16.4 cal ka BP obtained by Kirshner et al. (2012), and suggest that deglaciation of the inter-ice stream ridge proceeded in parallel with retreat of the flanking ice streams.

### 3.2. Amundsen Sea region terrestrial studies

Before 2004, the subglacial topography of the ASE was only known from a few widely-spaced oversnow traverses and a handful

of airborne survey flights (e.g. Lythe et al., 2001). Radio echo sounding data density was greatly increased as a result of a collaborative US/UK airborne campaign that undertook a systematic geophysical survey during the austral summer of 2004/05 (Holt et al., 2006; Vaughan et al., 2006). In the PIG drainage basin these new data revealed that whereas there is a deep, inland sloping bed beneath the trunk of PIG, the lower basin of the glacier is surrounded by areas in which the bed is relatively shallow. After deglaciation and isostatic rebound, these shallow bed areas could rise above sea level and would impede ice-sheet collapse initiated near the grounding line (Vaughan et al., 2006). This contrasts with the survey results from the Thwaites Glacier drainage basin where, except for short-wavelength roughness, the bed slopes inland monotonically from the grounding line to the interior of the basin, continuing to the deepest part of the Byrd Subglacial Basin at 2300 m below sea level (Fig. 2; Holt et al., 2006).

The first constraints on changes in ice surface elevations in the ASE spanning thousands of years were published by Johnson et al. (2008), who obtained cosmogenic surface exposure ages on glacial erratic boulders collected from sites around PIB. From the resulting ages (Supplementary Table 3), these authors inferred average ice thinning rates of  $3.8 \pm 0.3 \text{ cm yr}^{-1}$  over the past 4.7 ka on Mount Manthe, in the Hudson Mountains near PIG, and  $2.3 \pm 0.2 \text{ cm yr}^{-1}$  over the past 14.5 ka on Turtle Rock, which lies between Smith and Pope glaciers near Mount Murphy (Figs. 3 and 7). An exposure age of  $2.2 \pm 0.2 \text{ ka}$  was obtained from an erratic boulder exposed at 8 m above sea level (m.a.s.l.) on an unnamed island near the tip of Canisteo Peninsula (Fig. 3), but it was not clear if this age represents retreat of the local ice margin or glacio-isostatic emergence (Johnson et al., 2008; Supplementary Table 3). Paired  $^{10}\text{Be}$  and  $^{26}\text{Al}$  cosmogenic surface exposure results on a sample of striated bedrock from 470 m.a.s.l. on Hunt Bluff, Bear Peninsula (on the southern coast of the ASE; Figs. 3 and 7) yielded ages in excess of 100 ka (Johnson et al., 2008; Supplementary Table 3). On a two-isotope diagram the results from this sample plot slightly below the “erosion island”, but as they are within error of one another they could plausibly represent continuous exposure throughout the last glacial period. However, as these are results from a single sample, we need to treat them with caution.

More extensive collections of glacial erratic samples from the Hudson Mountains (Figs. 3 and 7) obtained by a field party in the austral summer of 2007/08 and from sites accessed by helicopter during RV *Polarstern* expedition ANT-XXVI/3 in 2010 have provided surface exposure ages that indicate a more detailed history of surface elevation change. These ages suggest that there was a decrease in ice surface elevation in this area to near the modern level in the early Holocene (Bentley et al., 2011; Johnson et al., 2012).

Glacial erratic samples were also collected from sites in the Kohler Range that were accessed by helicopter during ANT-XXVI/3 (Figs. 3 and 7). From the cosmogenic surface exposure ages obtained from these samples, Lindow et al. (2011) inferred an average thinning rate of ca  $3 \text{ cm yr}^{-1}$  over the past 13 ka. This is similar to the thinning rate inferred by Johnson et al. (2008) for Turtle Rock, which lies about 70 km to the east (Figs. 3 and 7). However, each of these thinning rates is inferred from a very small sample set, so they must be treated with caution.

The Ford Ranges in western Marie Byrd Land straddle the ice divide between the Amundsen Sea and Ross Sea sectors (Fig. 2). Stone et al. (2003) published cosmogenic surface exposure ages from numerous nunataks in the Ford Ranges that indicated ice thinning rates in the inland part of the range of  $2.5\text{--}9 \text{ cm yr}^{-1}$  over the past 10.4 ka. Around the most seaward peaks, the surface exposure ages indicated gradual ice thinning up to 3.5 ka ago, then greatly increased thinning rates for about 1200 years. Stone et al.

(2003) interpreted these changes as resulting from retreat of the grounding line and consequent landward migration of a relatively steep ice surface gradient upstream of it (see also Anderson et al., 2014).

No surface exposure ages from the interior of the Amundsen Sea sector of the WAIS have yet been published, but in the Ross Sea sector about 70 km from the ice divide, important constraints on past ice surface elevations have been obtained from Mount Waesche (Fig. 2) by Ackert et al. (1999). These authors interpreted  $^3\text{He}$  and  $^{36}\text{Cl}$  surface exposure ages obtained from a lateral moraine on Mount Waesche, together with geomorphological observations, as indicating that the ice sheet was up to 45 m thicker in this area ca 10 ka ago. Furthermore, Ackert et al. (1999) suggested that the surface position 10 ka ago represents a highstand, and showed that increasing ice thickness in the area during the early stages of post-LGM Antarctic deglaciation can be simulated with a non-equilibrium ice sheet model (see also Anderson et al., 2014). Recently published results from a more sophisticated ice sheet modelling study are consistent with this scenario (Ackert et al., 2013).

Past ice surface elevations in the interior of the WAIS have also been estimated from total gas content, V, in the Byrd Station ice core (drilled at  $80^\circ 01' \text{ S}$ ,  $119^\circ 31' \text{ W}$  in the Ross Sea sector of the WAIS; Fig. 2), with variable results. A complicating factor for this ice core is that the site was not located near an ice divide, so the ice at depth in the core will have come from an upstream location that has a higher modern elevation. Using an early, sparse set of V measurements and without correcting for ice flow, Jenssen (1983) calculated ice surface elevations that were 400–500 m higher than present between 19 and 11 ka ago. However, Raynaud and Whillans (1982) presented new, more densely sampled V measurements, applied a correction for ice flow to them, and calculated that ice surface elevations were 200–250 m lower than present at the end of the LGM. Furthermore, Raynaud and Whillans (1982) inferred a thickening of the ice with time since the LGM, which they attributed to an increase in accumulation rate. Using the same V dataset, Lorius et al. (1984) revised the increase in surface elevation since the LGM down to 175–205 m as a result of using a new estimate of surface temperature increase since the LGM of  $10^\circ \text{ C}$  (cf.  $7^\circ \text{ C}$  used by Raynaud and Whillans, 1982). New estimates of past ice surface elevation in the interior of the WAIS may be expected soon from the WAIS Divide ice core (Fig. 2; <http://www.waisdivide.unh.edu/>; WAIS Divide Project Members, 2013).

Studies of the configuration of internal ice sheet layers detected in radio-echo sounding profiles have allowed conclusions about current and past migrations of the ice divides between the Amundsen Sea and Weddell Sea sectors (Ross et al., 2011) and the Amundsen Sea and Ross Sea sectors (Neumann et al., 2008; Conway and Rasmussen, 2009), respectively. Chronological constraints were inferred from modern rates of ice accumulation, compaction and flow velocity (Ross et al., 2011) or from correlation with dated ice cores (Neumann et al., 2008).

### 3.3. Bellingshausen Sea embayment marine studies

#### 3.3.1. Geophysical surveys and geomorphological studies

Although the southern Bellingshausen Sea continental shelf (Fig. 8) was the site of the first overwintering expedition in Antarctica, after the *Belgica* became beset by ice there in 1898 (Cook, 1909; Decleir, 1999), no extensive marine geoscientific investigations were carried out there for nearly a century. The region remains less intensively studied than the neighbouring ASE. A brief reconnaissance over the outer continental shelf between  $80^\circ$  and  $83^\circ \text{ W}$  was carried out during USNS *Eltanin* Cruise 42 in 1970, but only echo sounding data were collected on the shelf, whereas



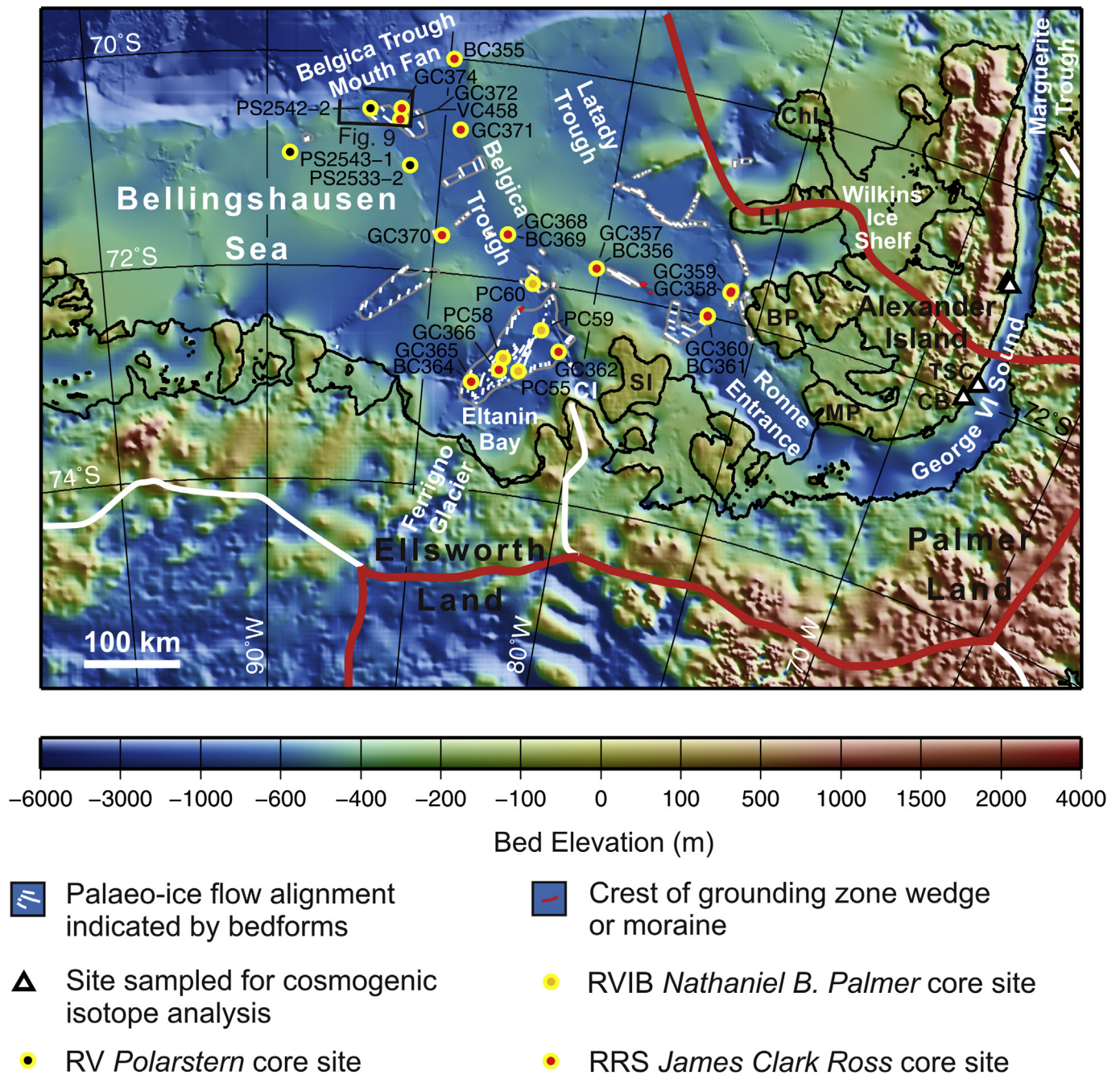


**Fig. 8.** Map of the Bellingshausen Sea region showing continental shelf sediment core sites (yellow circles), cosmogenic surface exposure age sample locations (white-filled triangles) and the main geomorphological features on the continental shelf, overlaid on Bedmap2 ice sheet bed and bathymetry (Fretwell et al., 2013), which is displayed with shaded-relief illumination from the upper right. Grey outlines mark areas in which bedforms indicative of past ice flow direction are observed in multibeam swath bathymetry data. Thin white lines indicate flow alignment. Thin red lines mark the crests of grounding zone wedges and moraines that represent past grounding line positions. Sediment core sites are shown and labelled with the core ID for cores that recovered more than 1 m of sediment and for shorter cores from which AMS  $^{14}\text{C}$  dates have been obtained. Core site symbol fill colour indicates ship the core was collected on, as in Fig. 2. Thick red line marks sector limit, along main modern ice divide between the Bellingshausen Sea and the Weddell Sea and an inferred palaeo-ice divide across Alexander Island. Thick white lines mark other major ice divides. In most cases, where a box core or giant box core from which only a surface sample has been dated is co-located (within 50 m) with another core, only the other core is labelled (see co-ordinates in Supplementary Table 1 to identify co-located cores). Black rectangle outlines area shown in greater detail in Fig. 9. BP – Beethoven Peninsula; CB – Citadel Bastion; CI – Carroll Inlet; ChI – Charcot Island; LI – Latady Island; MP – Monteverti Peninsula; SI – Smyley Island; TSC – Two Step Cliffs.

single-channel seismic profiles were collected across the slope and rise (Tucholke and Houtz, 1976).

In the austral summers of 1992/93 and 1993/94 the first research cruises of the modern era to investigate the continental shelf in this region were conducted on RRS *James Clark Ross* (JR04) and RV *Polarstern* (ANT-XI/3). Multichannel seismic profiles collected on these two cruises revealed an extensively prograded

outer continental shelf, an unusually deep shelf edge, and a low-gradient continental slope in the area now known to be the mouth of Belgica Trough (Cunningham et al., 1994, 2002; Nitsche et al., 1997, 2000). Acoustic sub-bottom profiles were also collected on both cruises, and some isolated swaths of multibeam bathymetry data were collected on ANT-XI/3 (Miller and Grobe, 1996).

Early in 1994, single beam echo sounding data were collected as RVIB *Nathaniel B. Palmer* Cruise NBP9402 traversed the southern Bellingshausen Sea continental shelf and reached the ice front in the Ronne Entrance. Further single-beam echo sounding surveys, with a particular focus on the Ronne Entrance and Carroll Inlet (Fig. 8), were carried out on HMS *Endurance* in 1996.

The first published multibeam swath bathymetry data from the region were collected early in 1999 on RVIB *Nathaniel B. Palmer* Cruise NBP9902, and revealed bedforms produced by glacial erosion in a deep trough in Eltanin Bay, separated by a drumlin field from mega-scale glacial lineations (MSGL) farther offshore (Wellner et al., 2001, 2006). Early in 2004, multibeam swath bathymetry data and sub-bottom profiler data were collected from several parts of the continental shelf and slope on RRS *James Clark Ross* Cruise JR104. Subglacial bedforms revealed by the multibeam and sub-bottom profiler data showed that past ice flow from the Ronne Entrance and Eltanin Bay had converged to form a large palaeo-ice stream in the Belgica Trough that advanced to, or close to, the shelf edge (Fig. 9; Ó Cofaigh et al., 2005b). Extensive multibeam swath bathymetry data collected over the part of the continental slope adjacent to the mouth of the Belgica Trough demonstrated the presence of a trough mouth fan (Dowdeswell et al., 2008). Systematic changes in the spatial density and size of upper slope gullies from the centreline of the trough to its margins were interpreted by Noormets et al. (2009) as indicating that the gullies were eroded by hyperpycnal flows initiated by sediment-laden subglacial meltwater discharges from a grounding line at the shelf edge. Further analysis of the fan geomorphology by Gales et al. (2013) supported this conclusion.

Graham et al. (2011) compiled all of the single beam and multibeam echo sounding data available at that time to produce a continuous gridded regional bathymetry map of the Bellingshausen Sea that provided the first accurate representation of the continental slope and major cross shelf troughs. Prior to this work the representation of the bathymetry of the region had been quite poor even in relatively recent circum-Antarctic bathymetry and

subglacial topography compilations (e.g. IOC, IHO and BODC, 2003; Le Brocq et al., 2010). Inclusion of some multibeam swath bathymetry datasets that have not been mentioned above helped improve definition of the continental shelf and slope. These included data collected on RRS *James Clark Ross* cruises JR141 and JR179, in early 2006 and early 2008, respectively. Other multibeam data that augmented coverage of inner shelf areas were collected early in 2007 on RRS *James Clark Ross* Cruise JR165.

### 3.3.2. Sediment core studies and geochronological data

The first sediment cores from the southern Bellingshausen Sea continental shelf were collected on RV *Polarstern* expedition ANT-XI/3 in the austral summer of 1993/94 (Miller and Grobe, 1996). Five giant box cores, three gravity cores and four multiple cores were collected from nine sites on the continental shelf, with additional gravity cores and multiple cores being collected from four sites on a transect across the adjacent continental slope (Hillenbrand et al., 2003, 2005, 2010a). Cores from both the shelf and the slope contain a similar succession of facies, with massive, homogenous diamictos overlain by terrigenous sandy muds, which are in turn overlain by bioturbated foraminifer-bearing muds. Although no radiocarbon dates were available on samples from the cores, Hillenbrand et al. (2005) inferred that the diamictos were of LGM age, interpreting the diamicton cored on the shelf as deformation till overlain by glacial marine diamicton, and the diamictos on the slope as glacial debris flow deposits. The sandy muds were interpreted as representing a deglaciation stage, and the bioturbated foraminifera-bearing muds as having been deposited in seasonally open water conditions like those that pertain today (Hillenbrand et al., 2005).

Piston cores collected on RV *Nathaniel B. Palmer* Cruise NBP9902 in 1999 from an area where MSGL were observed on the middle shelf recovered diamictos with moderate shear strength (<34 kPa), interpreted as tills, overlain by a thin cover of very soft diamicton with more abundant microfossils (Wellner et al., 2001).

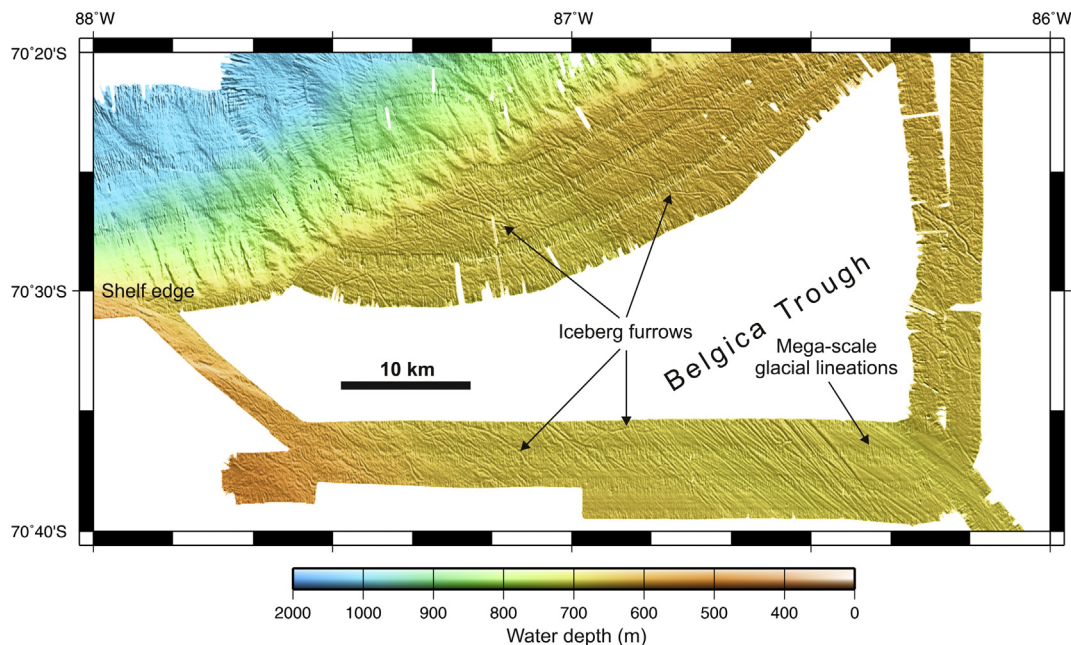


**Fig. 9.** Multibeam swath bathymetry data from the outer part of Belgica Trough showing mega-scale glacial lineations that extend to within 30 km of the continental shelf edge. Data shown were collected on RRS *James Clark Ross* cruises JR104 and JR141. The grid was generated using a near neighbour algorithm, has a cell size of 40 m and is displayed with shaded-relief illumination from 50°.



Early in 2004, gravity cores and box cores were collected from several parts of the continental shelf and slope on RRS *James Clark Ross* Cruise JR104. Samples from these extensively analysed cores yielded the only radiocarbon dates presently available from the region constraining ice retreat since the LGM (Hillenbrand et al., 2010a). Although planktonic foraminifera are present in sea-floor sediments (Hillenbrand et al., 2003, 2005) and radiocarbon dates were obtained from them (Hillenbrand et al., 2010a), their abundance decreases rapidly downcore and none of the earliest seasonally open-marine or deglacial sandy muds recovered in the JR104 cores contained enough foraminifera for AMS  $^{14}\text{C}$  dating. Therefore, minimum ages of grounding line retreat were obtained by AMS  $^{14}\text{C}$  dating of AIOM samples from the cores. Hillenbrand et al. (2005, 2009) analysed down-core changes of clay mineral assemblages, and Hillenbrand et al. (2010a) used this information to identify the deepest levels in the postglacial sediments at which the mineralogical provenance, and therefore the likely extent of fossil carbon contamination, were similar to those of recent seabed sediments. The calibrated ages suggest early ice retreat from the outermost part of Belgica Trough, starting before the global LGM (ages  $30,758 \pm 2262$  and  $29,585 \pm 1780$  cal yr BP, Supplementary Table 2), followed by a gradual retreat along the outer and middle shelf part of the trough, with the inner shelf tributaries in Eltanin Bay and the Ronne Entrance becoming free of grounded ice in the earliest and late Holocene, respectively (Hillenbrand et al., 2010a). While it is possible that a change in the amount of fossil carbon contamination independent of clay mineral provenance might be responsible for the surprisingly old ages from the outer shelf, it seems unlikely that such changes could account for the gradual retreat indicated by ages from the core transects.

The apparent continuation of gradual grounding line retreat towards the Ronne Entrance through the late Holocene contrasts not only with the retreat history indicated by data from Eltanin Bay, but also with those from neighbouring regions in the Amundsen Sea and southern Antarctic Peninsula, where the ice margin had retreated close to modern limits by early Holocene time (Heroy and Anderson, 2007; Smith et al., 2011; Hillenbrand et al., 2010a, 2013; Kilfeather et al., 2011; Bentley et al., 2011; Livingstone et al., 2012; Ó Cofaigh et al., in review). It is also difficult to reconcile with biological studies that have indicated the presence of a diversity hotspot in nematode fauna and microbial diversity in southern Alexander Island (Lawley et al., 2004; Maslen and Convey, 2006), implying that a glacial refuge has persisted somewhere in the area through several glacial cycles (Convey et al., 2008, 2009). The gradual retreat is, however, consistent with an ice history model that reconstructs an ice dome to the south of the Ronne Entrance persisting into the Holocene (Ivins and James, 2005).

Analyses of clay mineral assemblages in sediment cores recovered from the continental shelf and slope on ANT-XI/3 and JR104 provided evidence of past changes in sediment provenance (Hillenbrand et al., 2005, 2009). The geographical heterogeneity of clay mineral assemblages in sub- and pro-glacial diamictos and gravelly deposits recovered on the shelf was interpreted by Hillenbrand et al. (2009) as indicating that they were eroded from underlying sedimentary strata of different ages. Furthermore, Hillenbrand et al. (2009) interpreted the clay mineralogical heterogeneity of soft tills recovered on the shelf as evidence that the drainage area of the palaeo-ice stream flowing through Belgica Trough changed through time.

### 3.4. Bellingshausen Sea region terrestrial constraints

Subglacial topography in the part of West Antarctica to the south of the Bellingshausen Sea remains relatively poorly known, as there have been no systematic, regional airborne geophysical surveys like

those conducted in the Amundsen Sea region. A recent over-snow radio-echo sounding survey and data collected by the NASA Ice-bridge project have improved knowledge of subglacial topography in the drainage basin of the Ferrigno Ice Stream, which flows into Eltanin Bay (Fig. 8; Bingham et al., 2012). The new subglacial topography data, together with modelling of potential field data collected during earlier reconnaissance aerogeophysical surveys (Bingham et al., 2012), are consistent with a previous interpretation that the region contains Cenozoic basins formed by extension along a continuation of the West Antarctic Rift System that connected to a subduction zone along the Pacific margin of the Antarctic Peninsula (Eagles et al., 2009). The presence of these basins can be expected to influence the dynamic behaviour of this part of the WAIS, both through topographic effects on ice sheet stability and elevated heat flow (Bingham et al., 2012).

No surface exposure ages or ice core data have been published that constrain past surface elevations of the WAIS in the Bellingshausen Sea region. However, surface exposure ages have been published from several locations on Alexander Island, including some that lie just within the boundary of the sector under consideration, as defined in Fig. 1 (Bentley et al., 2006, 2011; Hodgson et al., 2009; Supplementary Table 3). These ages are on samples collected from sites close to the southern part of George VI Sound, at Two Step Cliffs and Citadel Bastion (Fig. 8). Ages on samples from a col below Citadel Bastion, at an elevation of 297 m, suggest that some ice thinning had occurred in that area by 13 ka ago, whereas ages of ca 10 ka on samples collected from the 465 m-high summit were interpreted by Hodgson et al. (2009) as representing the retreat of a plateau icefield. The recalculated ages in Supplementary Table 3 on samples from 370 to 380 m elevation at Two Step Cliffs, which are based on  $^{10}\text{Be}$  and  $^{26}\text{Al}$  concentrations reported by Bentley et al. (2006), range between 7.1 and 8.7 ka. The simplest interpretation of these ages would be that grounded ice was still present in southern George VI Sound until this time, even though there had been rapid ice thinning and retreat of the calving front along the northern part of George VI Sound by 9.6 ka ago (Bentley et al., 2005, 2011; Smith et al., 2007; Ó Cofaigh et al., in review). However, Bentley et al. (2011) point out that the Two Step Cliffs samples were collected from high, rather flat-topped ridges, and therefore the possibility that they represent retreat of another perched icefield cannot be ruled out. If this latter interpretation is correct it means that the grounding line could have retreated from the northern end of George VI Sound as far as Citadel Bastion in the early Holocene (Bentley et al., 2011).

### 4. Timeslice reconstructions

We have used the data sources summarized above as the basis for reconstructions of the Amundsen Sea and Bellingshausen Sea sector of the WAIS at 5 ka intervals since 25 ka ago (Figs. 10–15). The reconstructions described below have been made consistent with available data constraints, as far as this is possible. In instances where it is difficult or impossible to reconcile all of the available data, we explain the factors that were considered in deciding what is shown in the reconstruction for a particular time. It must be remembered that ages labelled next to core sites on Figs. 10–14 are *minimum* ages of deglaciation, and therefore when interpreting the position of the ice sheet limit, greatest weight has been placed on ages older than the time of the particular reconstruction. The reconstructions only show ice extent in the Amundsen Sea and Bellingshausen Sea sector, as reconstructions of neighbouring sectors are discussed in other papers in this volume (Anderson et al., 2014; Ó Cofaigh et al., in review; Hillenbrand et al., 2013).

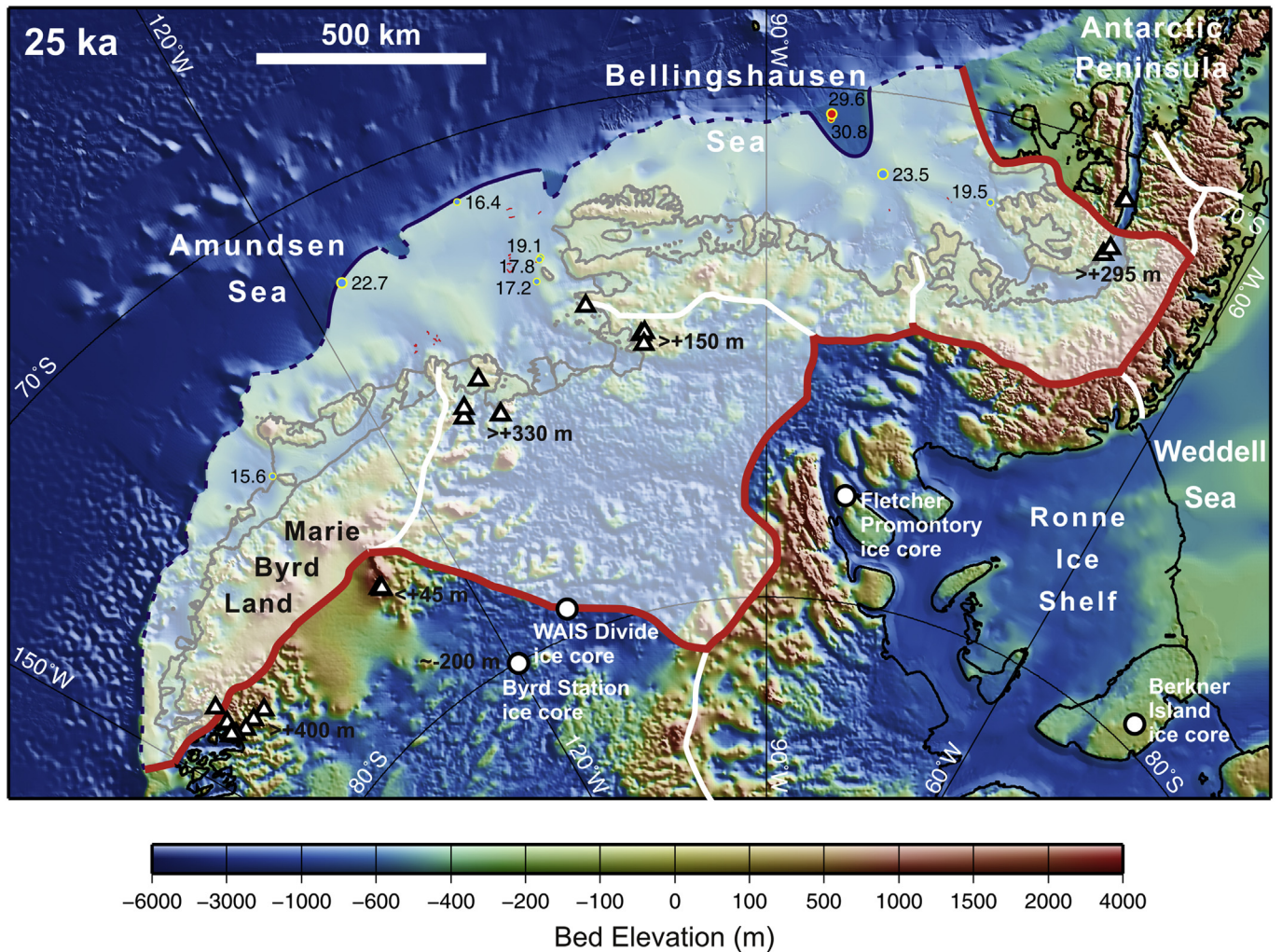


**Fig. 10.** Reconstruction for 25 ka overlaid on Bedmap2 ice sheet bed and bathymetry, which is displayed with shaded-relief illumination from the upper right. Extent of ice sheet indicated by semi-transparent white fill (only shown within Amundsen–Bellingshausen sector). Ice margin marked by dark blue line (dashed where less certain). Thick red line is the sector boundary, which follows the main ice drainage divides. Thick white lines mark other major ice divides. Core sites constraining reconstruction marked by yellow circles, with minimum ages of glaciation annotated (in cal ka BP) and indicated by size and fill colour (red fill – ages older than time of reconstruction; blue fill – younger ages; large circles – ages within  $\pm 5$  ka of time of reconstruction; small circles – ages within 5–10 ka). Cosmogenic surface exposure age sample locations marked by white-filled triangles, and deep ice core sites by white-filled circles, with surface elevation constraints they provide for time of reconstruction annotated. Thin red lines mark the crests of grounding zone wedge and moraines that represent past grounding line positions.

#### 4.1. 25 ka

Well-preserved subglacial bedforms in the outer part of several cross-shelf troughs (e.g. Figs. 4 and 9), in some cases supported by AMS  $^{14}\text{C}$  dates from thin glaciomarine sediments overlying the diamictites they are formed in, indicate that the grounding line advanced to, or at least close to, the continental shelf edge during the last glacial period (Fig. 10; Ó Cofaigh et al., 2005b; Evans et al., 2006; Graham et al., 2010; Smith et al., 2011; Kirshner et al., 2012). AMS  $^{14}\text{C}$  dates on AIOM samples from deglacial sediments in the outermost part of the Belgica Trough, however, suggest that the grounding line had already retreated from the shelf edge before 29 cal ka BP (ages  $30,758 \pm 2262$  and  $29,585 \pm 1780$  cal yr BP, Supplementary Table 2; Hillenbrand et al., 2010a).

Other AMS  $^{14}\text{C}$  dates on AIOM samples from soft tills in the outer and middle parts of Belgica Trough were interpreted by Hillenbrand et al. (2010a) as maximum ages for ice-sheet advance across the shelf. The ages we obtain from calibration of these dates are

$42,748 \pm 7165$  and  $39,481 \pm 7980$  cal yr BP (Supplementary Table 2).

Both in Belgica Trough and elsewhere, evidence of geomorphic features that might represent limits of LGM grounding line advance on the outer shelf is generally lacking. The only exceptions are the pair of asymmetric mounds in PITE that Graham et al. (2010) interpreted as GZWs (Fig. 3), but as yet there are no direct age constraints on these features. The simplest explanation of the fact that such features are generally lacking is that the grounding line advanced all the way to the shelf edge, that the grounded ice eroded features formed during advance, and that there were no significant pauses during subsequent grounding line retreat (e.g. Larter et al., 2009).

Ice surface elevations during the LGM were probably more than 150 m above the modern level in the Hudson Mountains (Bentley et al., 2011; Johnson et al., 2012), more than 400 m above the modern level in the landward parts of the Ford Ranges (Stone et al., 2003), but similar to, or even a little lower than, the modern level in the interior of WAIS (Raynaud and Whillans, 1982; Ackert et al., 1999).



Across most of the sector the detailed pattern and rate of ice retreat across the outer shelf is poorly constrained, as widespread ploughing of sea-floor sediments by iceberg keels makes undisturbed sedimentary records difficult to find (Lowe and Anderson,



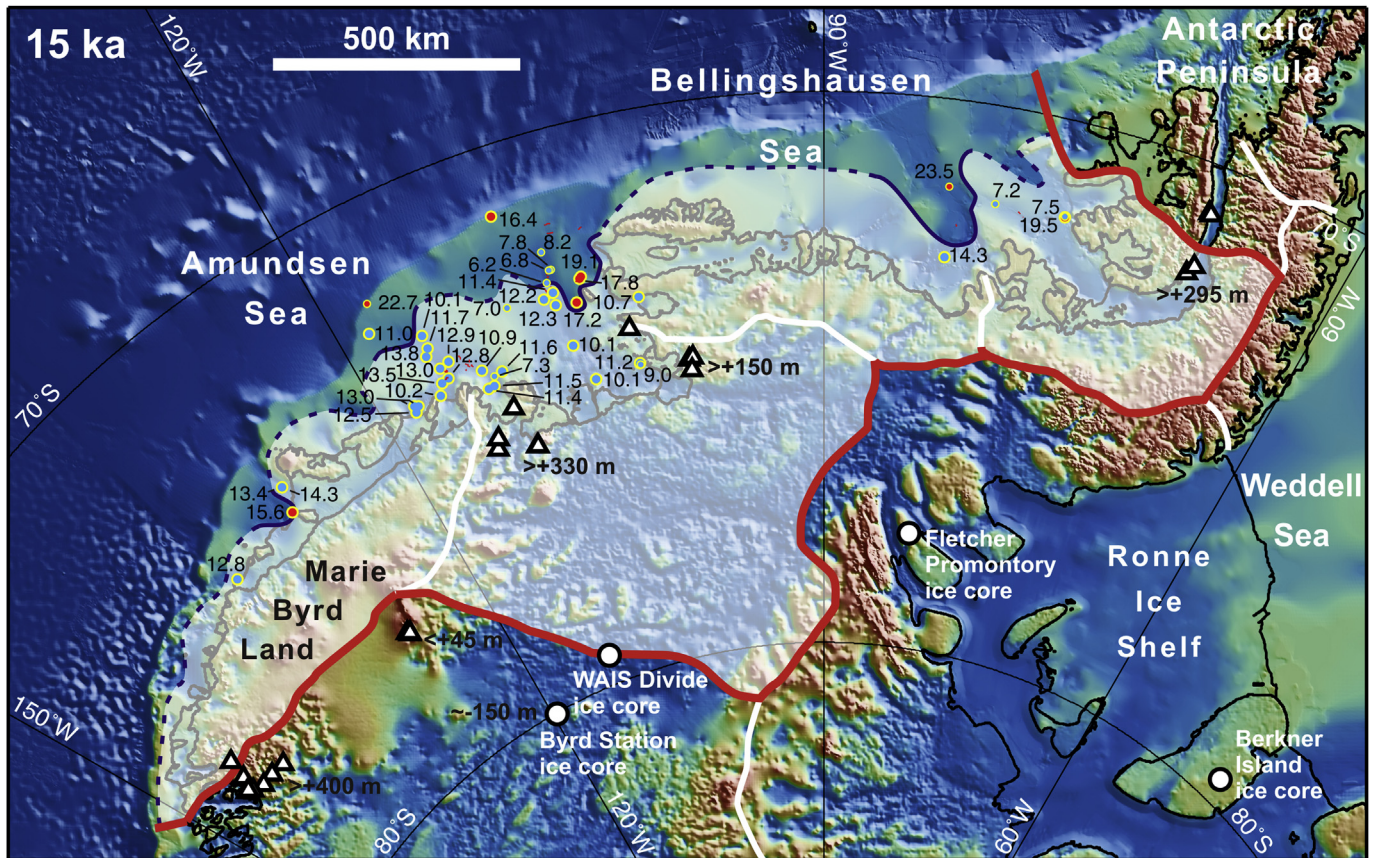


Fig. 12. Reconstruction for 15 ka. See Fig. 10 caption for explanation of symbols and annotations.

2002; Ó Cofaigh et al., 2005b; Dowdeswell and Bamber, 2007; Graham et al., 2010). At 15 cal ka BP, grounded ice still extended across the mid-shelf part of the ASE (Fig. 12; Smith et al., 2011; Kirshner et al., 2012), but it is not clear whether the grounding line retreated across the outer shelf gradually or in a stepwise manner. Graham et al. (2010) interpreted features observed in multibeam swath bathymetry and acoustic sub-bottom profiler data from the axis of PITE as GZWs, which suggests a stepwise retreat along this outer shelf trough.

Hillenbrand et al. (2010a) reported an AMS  $^{14}\text{C}$  date on AIOM from the base of seasonal open-marine muds in a core from Eltanin Bay (GC366; Fig. 8) of  $14,346 \pm 847$  cal yr BP (Supplementary Table 2). This indicates that grounding line retreat had reached the inner shelf along this tributary to Belgica Trough by around 15 cal ka BP (Fig. 12). In contrast, AMS  $^{14}\text{C}$  dates on a core (GC357; Fig. 8) from the area where the trough originating from Ronne Entrance narrows and shallows westward before merging with Belgica Trough indicate very limited retreat along that tributary before 15 cal ka BP (Hillenbrand et al., 2010a). In particular, a date on AIOM in gravelly-sandy mud from just below the transition to seasonally open-marine muds of only  $7180 \pm 561$  cal yr BP (Supplementary Table 2) suggests that ice remained pinned on the relatively shallow “saddle” in this trough until long after 15 cal ka BP (Fig. 12).

#### 4.4. 10 ka

Numerous AMS  $^{14}\text{C}$  dates record rapid grounding line retreat from the middle shelf to near modern limits across the entire Amundsen Sea between 15 and 10 ka ago (Fig. 13; Anderson et al., 2002; Lowe and Anderson, 2002; Smith et al., 2011; Kirshner et al.,

2012; Hillenbrand et al., 2013), and an ice shelf has been interpreted as having been present over the mid-shelf part of PIT from 12.3 to 10.6 cal ka BP (Kirshner et al., 2012). If this interpretation is accepted, and a date interpreted as indicating that the grounding line had already retreated into inner PIB by 11.2 cal ka BP is also accepted (Hillenbrand et al., 2013), then the implication is that a very extensive ice shelf was present for >600 years in the earliest Holocene.

The few available cosmogenic surface exposure age results suggest that gradual ice thinning took place in the part of the WAIS to the south of the ASE since 14.5 ka ago (Johnson et al., 2008; Lindow et al., 2011), and similar gradual thinning has occurred in the Ford Ranges since 10 ka ago (Stone et al., 2003). Ice thinning had also started in southern Alexander Island by 13 ka ago (Hodgson et al., 2009; Bentley et al., 2011). However, cosmogenic surface exposure age data from Mount Waesche have been interpreted as indicating a highstand of the ice surface in the interior of the WAIS around 10 ka ago at up to 45 m above the modern level (Ackert et al., 1999, 2013). In the Hudson Mountains, ice surface elevations remained more than 150 m above the modern level until after 10 ka ago (Johnson et al., 2008; Bentley et al., 2011; Johnson et al., 2012).

In the Ronne Entrance tributary of Belgica Trough, the date of  $7180 \pm 561$  cal yr BP mentioned in the section above indicates that ice retreat continued to be very slow until after 8 cal ka BP. There are no age data from Eltanin Bay that constrain the Holocene ice retreat along that tributary, but as noted above, retreat had already reached the inner shelf in that area by around 15 cal ka BP. Therefore, subsequent retreat to modern ice limits was probably relatively slow (Fig. 13).



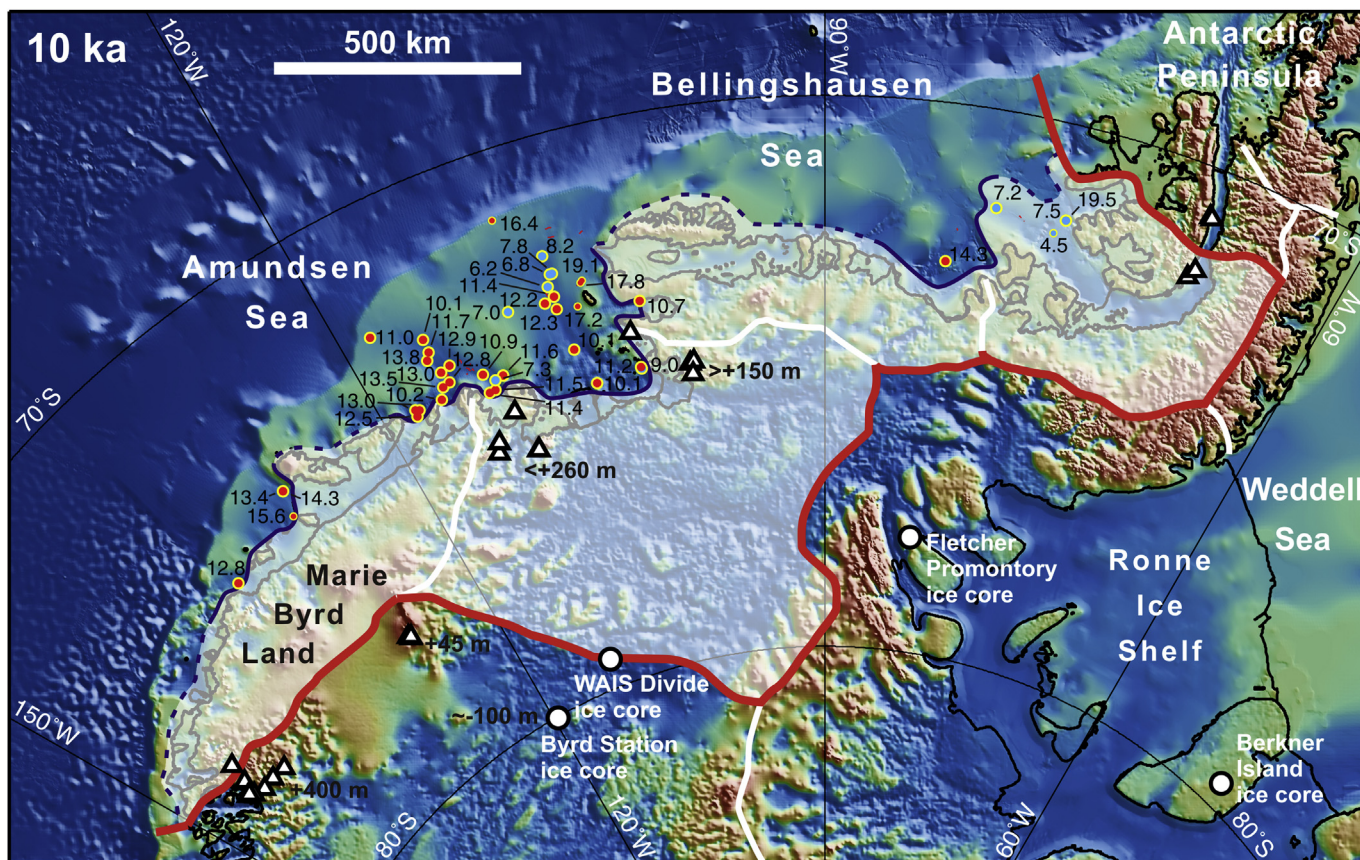


Fig. 13. Reconstruction for 10 ka. See Fig. 10 caption for explanation of symbols and annotations.

#### 4.5. 5 ka

In the Amundsen Sea and Eltanin Bay, the ice margin had already retreated close to modern limits before 10 cal ka BP (see above), and therefore there appears to have been little subsequent change in ice extent in these areas (Fig. 14), unless there was further retreat followed by readvance during the Holocene. So far, there is no evidence from this sector for such retreat and readvance, but neither can the possibility be dismissed. In the neighbouring Antarctic Peninsula sector, however, a rapid early Holocene ice retreat, accompanied by ice shelf collapse and followed by ice shelf reformation, has been documented in Marguerite Bay and George VI Sound (Bentley et al., 2005, 2011; Smith et al., 2007; Ó Cofaigh et al., in review).

The one part of the sector where the ice margin still appears to have been undergoing significant retreat 5 ka ago is in the Ronne Entrance (Fig. 14). This interpretation of continuing retreat is based on an AMS  $^{14}\text{C}$  date of  $4489 \pm 348$  cal yr BP (Supplementary Table 2) on AIOM from near the base of seasonally open-marine diatomaceous mud in a core (GC360; Fig. 8) located more than 170 km from the modern ice shelf front (Hillenbrand et al., 2010a). However, it is important to note that this date provides only a minimum age for grounding-line retreat.

In the interior of the WAIS, the cosmogenic surface exposure age results obtained by Ackert et al. (1999) from Mount Waesche (Fig. 2) imply ice thinning of no more than 45 m during the Holocene (i.e. an average rate of  $<0.5$  cm yr $^{-1}$ ). Surface exposure age data from the Ford Ranges in western Marie Byrd Land (Fig. 2) indicate gradual ice thinning at a faster rate of 2.5–9 cm yr $^{-1}$  through most of the Holocene (Stone et al., 2003). While an average

thinning rate within this range has also been estimated for the part of the WAIS to the south of the ASE, the sparse cosmogenic age data available from that area do not constrain the trajectory of thinning during the Holocene (Johnson et al., 2008; Lindow et al., 2011).

Palaeo-ice flow analysed using radio-echo sounding and global positioning system data acquired across the divide between the drainage basins of PIG and the Institute Ice Stream, which drains into the Weddell Sea, indicates that this ice divide has been stable for at least the last 7 ka, and possibly even the last 20 ka or longer (Ross et al., 2011). Neumann et al. (2008) tracked radar-detected layers from the Byrd ice core and a dated 105-m long ice core drilled near the western divide between the Amundsen Sea and the Ross Sea drainage basins in eastern Marie Byrd Land. The authors concluded from these data and modelling that the ice divide probably migrated within the last 8 ka. They infer that the divide is likely migrating toward the Ross Sea today but the direction of migration may have varied through the period studied.

#### 4.6. The modern ice sheet and observed recent changes

The modern configuration of the ice sheet in the sector is shown in Fig. 15. Over recent decades, the Amundsen–Bellingshausen sector of the WAIS has exhibited more rapid changes than any other part of Antarctica, with the possible exception of the Antarctic Peninsula (e.g. Cook et al., 2005). These changes have included thinning of ice shelves and thinning, flow velocity acceleration and grounding line retreat of ice streams feeding into them (Rignot, 1998; Rignot, 2008; Pritchard et al., 2009, 2012; Scott et al., 2009; Wingham et al., 2009; Joughin and Alley, 2011).



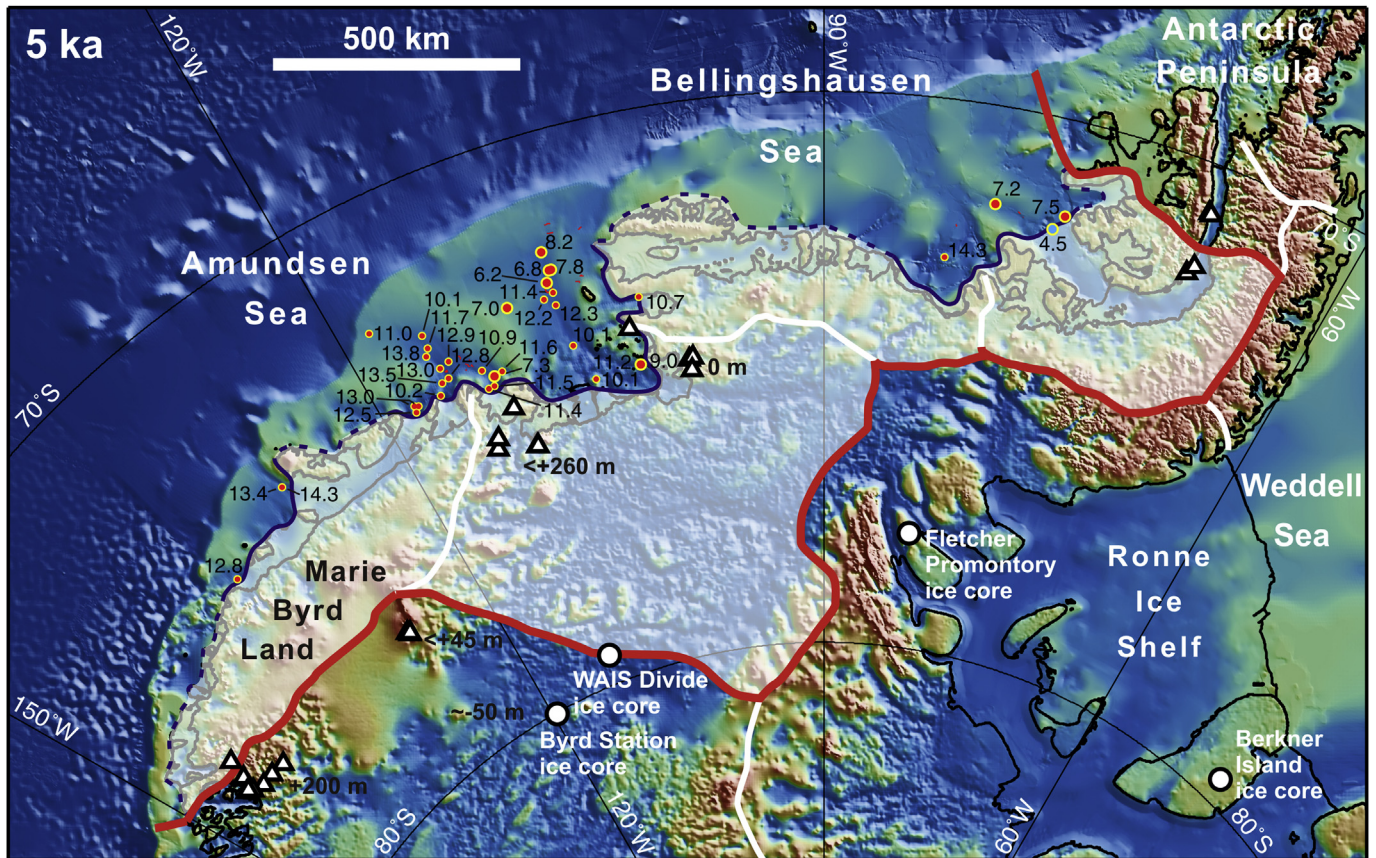


Fig. 14. Reconstruction for 5 ka. See Fig. 10 caption for explanation of symbols and annotations.

Analysis of ICESat laser altimetry data shows that ice shelves along the Amundsen and Bellingshausen Sea coasts thinned by up to  $6.8 \text{ m yr}^{-1}$  over the period 2003–2008 (Pritchard et al., 2012). Over approximately the same period (2003–2007), areas close to the grounding lines on Pine Island, Thwaites and Smith glaciers thinned by up to  $6 \text{ m yr}^{-1}$ ,  $\sim 4 \text{ m yr}^{-1}$ , and greater than  $9 \text{ m yr}^{-1}$ , respectively (Pritchard et al., 2009), and these rates are higher than those reported for the 2002–2004 period (Thomas et al., 2004). Similar recent thinning rates on PIG have been determined from ERS-2 and ENVISAT radar altimetry, and the longer time series of these data shows a progressive increase in thinning rate over the period 1995–2008 (Wingham et al., 2009). Ice flow velocities determined from interferometric Synthetic-Aperture Radar (InSAR) data collected with different satellites show that over the period 1996–2007 Pine Island and Smith glaciers sped up by 42% and 83%, respectively (Rignot, 2008). The flow velocity at the grounding line of PIG had accelerated to  $3500 \text{ m yr}^{-1}$  by 2006 and to  $4000 \text{ m yr}^{-1}$  by late 2008, with no further acceleration observed until early 2010 (Joughin et al., 2010). Whereas there was little or no acceleration along the centre line of Thwaites Glacier, the zone of fast flow widened over the same period (Rignot, 2008). An earlier increase in the flow velocity of Thwaites Glacier was calculated by tracking features in Landsat images, with average velocities 8% higher over 1984–1990 than over 1972–1984 (Ferrigno et al., 1993). Flow velocities on PIG determined from earlier InSAR data showed that the rate of acceleration increased with time, from  $0.8\% \text{ yr}^{-1}$  between 1974 and 1987 to  $3\% \text{ yr}^{-1}$  between 1996 and 2006 (Rignot, 2008). Ground based GPS measurements on PIG showed  $6.4\%$  acceleration  $55 \text{ km}$  upstream from the grounding line and  $4.1\%$  acceleration  $116 \text{ km}$  farther upstream over 2007 (Scott et al., 2009). PIG grounding line retreat of  $1.2 \pm 0.3 \text{ km yr}^{-1}$  between 1992 and 1996

was demonstrated using InSAR data by Rignot (1998). Further retreat by  $15 \pm 6 \text{ km}$  over the following 12 years has been estimated on the basis of changes in ice surface character observed in MODIS satellite images, and using the same approach up to  $8 \text{ km}$  retreat of the Smith Glacier grounding line has been depicted over the same 12-year period (Rignot, 2008). Joughin et al. (2010) inferred from Terra-SAR-X satellite data that sections of the PIG grounding-line had retreated by  $20 \text{ km}$  between 1996 and 2009.

Thwaites Glacier grounding line retreat of up to  $1 \text{ km yr}^{-1}$  between 1996 and 2009 was estimated by Tinto and Bell (2011) from comparing the 2009 grounding line position they calculated using airborne laser surface altimetry and radar ice thickness data with a 1996 position determined from a similar previous analysis by Rignot et al. (2004).

There is a growing consensus that these changes have resulted from increased inflow of relatively warm CDW across the continental shelf, which has increased basal melting of ice shelves (Jacobs et al., 1996, 2011; Shepherd et al., 2004; Arneborg et al., 2012; Pritchard et al., 2012). The CDW flows mainly along the bathymetric cross-shelf troughs (Walker et al., 2007; Wählin et al., 2010; Jacobs et al., 2011), and its upwelling is thought to be modulated by the westerly wind system over the Southern Ocean (Thoma et al., 2008). Siliceous microfossil assemblages from a sediment core on the Amundsen Sea continental rise have been interpreted as indicating that a climatic regime similar to the modern one, in which small perturbations in the westerly wind system may result in increased advection of CDW onto the continental shelf, became more common during interglacials after MIS 15 ( $621\text{--}563 \text{ ka ago}$ ; Konfirst et al., 2012). Over the past few decades, increased basal melting has caused thinning of ice shelves, reducing their buttressing effect and triggering a sequence of



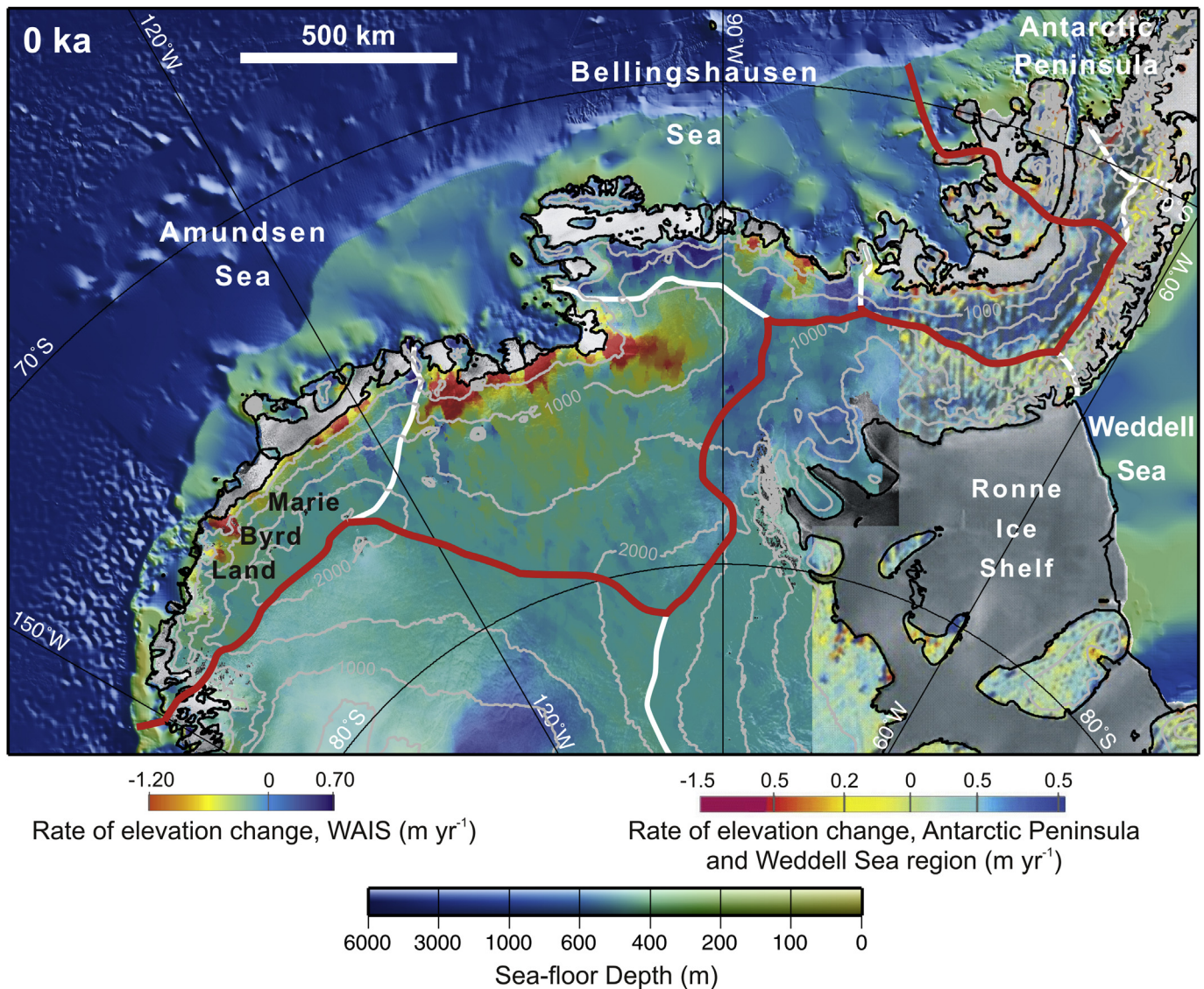


**Fig. 15.** Modern ice sheet configuration. Contours on the ice sheet (thin grey lines) show surface elevation at 500 m intervals from Bedmap2. Colours on ice sheet show rate of change of surface elevation over the period 2003–2007 from Pritchard et al. (2009); N.B. these data are displayed with slightly different colour scales over the WAIS compared to the Antarctic Peninsula and Weddell Sea region. Ice shelves and areas where elevation change data are lacking are shown with a grey or white fill. Colours offshore show bathymetry from Bedmap2, which is displayed with shaded-relief illumination from the upper right. Thick red line marks sector limit. Thick white lines mark other major ice divides.

changes in the ice streams commonly referred to as “dynamic thinning” (e.g. Pritchard et al., 2009). Through combined interpretation of sub-ice-shelf bathymetric data collected with an autonomous submersible vehicle and historical satellite imagery, Jenkins et al. (2010) showed that unpinning of the ice shelf from a submerged ridge about 30 years ago has probably been a major factor contributing to the observed dynamic thinning of PIG. On the basis of remote sensing data alone, Tinto and Bell (2011) suggested a similar scenario for Thwaites Glacier by arguing that about 55–150 years ago the ice stream may have uninned from the western part of a submarine ridge located 40 km seaward of its modern grounding line.

Most studies on recent and ongoing changes in the sector have focussed on the ASE, where the changes are conspicuous in a range of remote sensing datasets (Rignot, 1998, 2008; Chen et al., 2009; Pritchard et al., 2009, 2012; Wingham et al., 2009; Joughin et al., 2010; Lee et al., 2012). However, sub-ice shelf melting induced by upwelling of CDW has also been recorded in the Bellingshausen Sea

(Jenkins and Jacobs, 2008; Pritchard et al., 2012), while a negative mass balance has been calculated for drainage basins around it (Rignot et al., 2008; Pritchard et al., 2009). Furthermore, a recent study has shown that changes taking place in the Ferrigno Ice Stream, which flows into the Bellingshausen Sea, are comparable to those observed for the ASE ice streams (Bingham et al., 2012). A significant difference between the ASE and regions to its east and west is in the size of drainage basins. In contrast to the large drainage basins of Pine Island and Thwaites glaciers (combined area of 417,000 km<sup>2</sup>; Rignot et al., 2008), the drainage basin of Ferrigno Ice Stream, which is one of the largest around the Bellingshausen Sea, occupies an area of only 14,000 km<sup>2</sup> (Bingham et al., 2012).

Based on correlation of radar-layer data with the Byrd ice core and modelling, Neumann et al. (2008) showed that accumulation at the western divide between the Amundsen Sea and the Ross Sea drainage basins was approximately 30% higher than today from 5 ka BP to 3 ka BP. Conway and Rasmussen (2009) detected an



asymmetric pattern of thickness change across this ice divide and concluded that (i) the ice at the divide is currently thinning by  $0.08 \text{ m yr}^{-1}$ , and (ii) the divide is currently migrating towards the Ross Sea at a rate of  $10 \text{ m yr}^{-1}$ . The authors argued that the divide may have migrated towards the Siple Coast for at least the last 2000 years.

It has been argued that since the late 1950s atmospheric temperatures in the West Antarctic hinterland of the Amundsen-Bellingshausen Sea sector have risen faster than anywhere else in Antarctica (Steig et al., 2009), and that this area was even among the most rapidly warming regions on Earth (Bromwich et al., 2012). This warming, together with the increase of CDW upwelling onto the ASE shelf, has been linked to a teleconnection with atmospheric temperature increase in the tropical equatorial Pacific (Ding et al., 2011; Steig et al., 2012). Based on modelling results and climate data, Steig et al. (2012) concluded that a phase of significant warming in the central tropical Pacific around 1940 caused increased CDW upwelling onto the ASE shelf, which resulted in a partial ice-shelf collapse in inner PIB during that time. The authors argued that the ice-sheet changes observed in the ASE sector over the last two decades have their origin in this event and another episode of pronounced warming in the tropical Pacific that started around 1990 and intensified CDW advection onto the ASE shelf.

## 5. Discussion

### 5.1. Maximum ice extent and outer shelf ice dynamics

There is compelling evidence for the ice grounding line having advanced to, or at least close to, the continental shelf edge along several cross-shelf troughs during the last glacial period (Fig. 10). This evidence comes from a combination of streamlined bedforms observed in multibeam swath bathymetry images (e.g. Figs. 4 and 9), thin or absent acoustically-layered sediments overlying these bedforms, and radiocarbon dates from both the diamictos that host the bedforms and the overlying sediments (Lowe and Anderson, 2002; Ó Cofaigh et al., 2005b; Evans et al., 2006; Hillenbrand et al., 2010a; Graham et al., 2010; Smith et al., 2011; Kirshner et al., 2012).

Similar data from shallower parts of the outer shelf are more difficult to assess because most of these have been pervasively furrowed by iceberg keels, but it is unlikely that an advanced grounding line position could have been sustained in the troughs if ice was not also grounded on the intervening banks. As outlined in Section 4.2, AMS  $^{14}\text{C}$  dates on two foraminifera-bearing layers in a glaci-marine diamicton recovered from one of the outer shelf banks yielded LGM ages (Smith et al., 2011), which may hint at fluctuations of the LGM grounding line position. Such fluctuations might have occurred as a consequence of the inherent instability of ice sheet grounding lines on open, reverse gradient slopes (Weertmann, 1974; Schoof, 2007), which are typical on the outer shelf (Nitsche et al., 2007; Graham et al., 2011). Conversely, Alley et al. (2007) proposed that sensitivity to sea-level rise can be reduced by supply of sediment to the grounding line filling space beneath ice shelves. The presence of GZWs in the outer part of PITE suggests that sediment accumulation did temporarily retard grounding line retreat from the outer shelf during the last deglaciation, at least in that trough (Graham et al., 2010).

### 5.2. Ice dynamics and surface profile of the extended ice sheet

Although echo sounding data coverage over the continental shelf now accurately defines the positions of cross-shelf troughs across most of the sector, high-quality multibeam swath

bathymetry data still only covers a fraction of the area (Nitsche et al., 2007; Graham et al., 2011). Consequently, it is currently not possible to make a reliable assessment of how extensive streaming ice flow was on the continental shelf during the last glacial period, let alone the duration of such flow. This is important because the prevalence of streaming flow affects the average surface gradient near the margins of an ice sheet, and therefore such an assessment would be useful in estimating the volume of ice that covered the shelf during the LGM.

Margins of ice sheets where there are few ice streams have relatively steep surface gradients and the ice surface may rise by as much as 2 km within 150 km of the grounding line, e.g. in part of Wilkes Land in East Antarctica. In contrast, the average surface gradient is typically much lower on ice sheet margins with several closely-spaced ice streams, e.g. along the Siple Coast in the Ross Sea, where the average surface elevation 150 km upstream of the grounding line is  $< 300 \text{ m}$ . On this basis, the range of uncertainty in the thickness of ice over middle shelf areas in the Amundsen and Bellingshausen seas during the LGM is  $> 1700 \text{ m}$ , which also implies a large uncertainty in the mass of ice lost during deglaciation. However, the constraint that the maximum ice surface elevation at Mt Waesche, near the ice divide, during the last glacial cycle was only just above 2000 m implies lower elevations than this over the continental shelf. Moreover, as there were at least three major palaeo-ice streams in the ASE (in the DGT, PIT and Abbot Trough; Fig. 3; Nitsche et al., 2007), and two in the Bellingshausen Sea (in the Belgica and Latady Troughs; Fig. 8; Ó Cofaigh et al., 2005b; Graham et al., 2011) it seems likely that ice covering these broad shelf areas had a relatively low surface profile. As on the Siple Coast, extensive outcrop of sedimentary strata at the sea bed in the ASE and Bellingshausen Sea, which is documented in numerous seismic profiles (Nitsche et al., 1997, 2013; Wellner et al., 2001; Cunningham et al., 2002; Hillenbrand et al., 2009; Weigelt et al., 2009, 2012; Gohl et al., 2013b), probably facilitated development of a dilated basal sediment layer. Such a layer is widely considered to promote streaming flow (Alley et al., 1989; Tulaczyk et al., 1998; Kamb, 2001; Studinger et al., 2001; Wellner et al., 2001, 2006; Graham et al., 2009) and was recovered as a soft till in numerous cores from the study area (Lowe and Anderson, 2002; Hillenbrand et al., 2005, 2010a; Smith et al., 2011; Kirshner et al., 2012). In this context, it is also interesting to note that a diamicton with shear strength properties typical for soft till was recovered from the outer shelf to the west of Belgica Trough (site PS2543; Fig. 6; Hillenbrand et al., 2009, 2010a). This observation may suggest that at least at the end of the last glacial period ice streaming was not restricted to the trough, but occurred more widely on the outer shelf.

As noted in Section 3.2, cosmogenic surface exposure ages on a sample from 470 m above sea level on Bear Peninsula (on the southern coast of the ASE) could plausibly represent continuous exposure throughout the last glacial period (Johnson et al., 2008; Supplementary Table 3). As these are results from a single sample, we need to treat them with caution. However, if continuous exposure at this elevation on the southern coast of the ASE is confirmed by additional data, grounded ice on the shelf must have maintained a low surface profile throughout the LGM. This would suggest continuous, widespread streaming flow, rather than streaming starting at a late stage during the glacial period and triggering deglaciation (cf. Ó Cofaigh et al., 2005a; Mosola and Anderson, 2006). Moreover, confirmation of the result from Bear Peninsula by additional samples from high elevation coastal sites would provide an important constraint on the maximum ice volume on the ASE shelf and the dynamic behaviour of the LGM ice sheet. Therefore, collection of additional samples from such sites should be a priority for future research.

### 5.3. Spatially variable ice retreat histories

Perhaps the most surprising aspect of this reconstruction is the different ice retreat histories from the Amundsen and Bellingshausen Sea continental shelves (Figs. 10–15). In a wider context, the Amundsen Sea ice retreat to near present limits by early Holocene time, after relatively rapid retreat over the preceding few thousand years (Figs. 12 and 13; Smith et al., 2011; Kirshner et al., 2012; Hillenbrand et al., 2013), resembles the retreat history of the western Antarctic Peninsula (Heroy and Anderson, 2007; Bentley et al., 2011; Kilfeather et al., 2011). These retreat histories differ, however, from the progressive retreat in the western Ross Sea that had continued through most of the Holocene (e.g. Licht et al., 1996; Conway et al., 1999; Domack et al., 1999; Anderson et al., 2014). The gradual ice retreat along the outer and middle shelf parts of Belgica Trough and towards its Ronne Entrance tributary inferred by Hillenbrand et al. (2010a) is more similar to that recorded in the western Ross Sea, so available results suggest an alternation along the West Antarctic margin between zones in which gradual retreat continued during the Holocene with ones in which retreat close to modern limits was nearly complete by early Holocene time. Gradual Holocene ice retreat towards the Ronne Entrance (Figs. 13–15) is in marked contrast to the rapid early Holocene retreat and ice shelf collapse that occurred along the northern arm of George VI Sound (Bentley et al., 2005, 2011; Smith et al., 2007), but is consistent with an ice history model that reconstructs an ice dome to the south of the Ronne Entrance persisting into the Holocene (Ivins and James, 2005).

Although detailed records of oceanic, atmospheric and sea level forcing functions for the region remain sparse or lacking, there is presently no reason to suspect that they varied greatly across the sector. It is becoming increasingly clear that atmospheric warming and CDW inflow through cross-shelf troughs over the past few decades have affected the entire sector (Jenkins and Jacobs, 2008; Bromwich et al., 2012; Pritchard et al., 2012). If we presume that past forcings were similar across the sector and that the different retreat histories depicted in the reconstruction are correct, this implies that the differences are largely a consequence of how topographic and geological factors have affected ice flow, and of topographic influences on snow accumulation and warm water inflow. In this context, it may be significant that the mouth of the Belgica Trough is the deepest part of the shelf edge in this sector and, in contrast to the reverse gradient along most Antarctic palaeo-ice stream drainage paths, the sea floor dips slightly oceanward along the outer part of the trough (Fig. 8; Graham et al., 2011). Another factor that may have slowed retreat in Belgica Trough is the palaeo-ice drainage pattern, which is inferred to have been highly convergent on the inner and middle shelf (Ó Cofaigh et al., 2005b). In particular, available age data suggest that retreat paused for many thousands of years in the area where the trough originating from the Ronne Entrance narrows and shallows near its confluence with the main Belgica Trough (Hillenbrand et al., 2010a). Similarly, a “bottle neck” in PIT west of Burke Island may have been an important factor in causing the apparent pause in retreat and formation of GZWs in that area (Figs. 3 and 5; Lowe and Anderson, 2002; Graham et al., 2010; Jakobsson et al., 2012; Kirshner et al., 2012). The presence of GZWs in the DGT just to the north of where three tributary troughs merge (Larter et al., 2009; Gohl et al., 2013b) suggests a pause in retreat in that drainage system as well, although the timing of this pause is not well constrained by age data (Smith et al., 2011).

A priority for future ship-based work in the Bellingshausen Sea should be to search for additional core sites that are in shallower water but have escaped disturbance by iceberg keels, as such sites are more likely to preserve foraminifera of early deglacial age that

could be used to test the glacial retreat history proposed by Hillenbrand et al. (2010a).

### 5.4. Influence of reverse bed slopes on retreat

A long-standing and widely-held concern about ice-sheet grounding lines is that they are potentially unstable on submarine reverse slopes (bed slopes down towards continent) with the possibility of a runaway retreat (the “marine ice sheet instability hypothesis”; Weertman, 1974; Schoof, 2007; Katz and Worster, 2010). Although some recent modelling studies have simulated pauses in grounding line retreat (Jamieson et al., 2012) and even stable states (Gudmundsson et al., 2012) on such slopes in settings where there is convergent ice flow, ice grounded on reverse slopes is still thought to be vulnerable in most circumstances. This is a particular concern in relation to future retreat of the WAIS, as reverse slopes extend back from near the modern grounding line to deep basins beneath the centre of the ice sheet (Fig. 2). It has been estimated that loss of ice from the WAIS by unstable retreat along reverse bed slopes could contribute up to 3.4 m to global sea-level rise (Bamber et al., 2009b; Fretwell et al., 2013). The steepest reverse gradients on the broad ASE continental shelf occur on the seaward flanks of inner shelf basins that are up to 1600 m deep (Figs. 3, 6 and 7). In DGT, Smith et al. (2011) estimated that an average retreat rate of 18 m yr<sup>-1</sup> across the outer shelf accelerated to > 40 m yr<sup>-1</sup> as the grounding line approached the deep basins. The deglacial age data presented by Smith et al. (2011) allow the possibility that retreat across the deep basins and back into the tributary troughs was much faster, but the short distances between cores sites and uncertainties associated with the ages mean the level of confidence in such rates is low. In PIT, the grounding line retreated from the middle shelf by 12.3 cal ka BP (Kirshner et al., 2012) and had already retreated across the deepest inner shelf basins to reach inner PIB by 11.2 cal ka BP (Hillenbrand et al., 2013; recalibrated age from Supplementary Table 2). These dates imply a retreat by about 200 km in ~1100 years, which equates to a retreat rate of c. 180 m yr<sup>-1</sup> (between 110 and 370 m yr<sup>-1</sup>, allowing for the uncertainty ranges of the calibrated ages). Therefore, available deglacial ages from shelf sediment cores suggest relatively rapid retreat across these deep basins, which is consistent with the marine ice sheet instability hypothesis. However, in both cases the inner shelf basins also lie landward of the point where the narrowest “bottle neck” in the trough occurs, so these observations are also consistent with the hypothesis that flow convergence may have contributed to a previous pause or slowdown in retreat. Our calculated grounding-line retreat rate for the PIT palaeo-ice stream around the start of the Holocene is almost an order of magnitude lower than fast retreat recorded for PIG over the last 30 years (Joughin et al., 2010), but it should be noted that the palaeo-retreat rate is averaged over more than a millennium.

A range of factors could have contributed to the slow-down in retreat rates when the PIG grounding line approached its modern position, e.g. high basal shear stress over the rugged bedrock that characterises the inner shelf (Wellner et al., 2001, 2006; Lowe and Anderson, 2002; Nitsche et al., 2013), the transverse ridge under the modern Pine Island ice shelf acting as a pinning point (Jenkins et al., 2010), and the fact that inner PIB is another “bottle neck” constricting the flow of the trunk of PIG.

Slow grounding-line retreat from the outer to middle shelf in Belgica Trough (Hillenbrand et al., 2010a) may be explained by the seaward sloping bed of the outer continental shelf in the trough (Fig. 8; Graham et al., 2011). The slow-down and subsequent acceleration of palaeo-ice stream retreat from the middle to the inner shelf along the Ronne Entrance tributary of Belgica



Trough was attributed to bed-slope control associated with the existence of a bathymetric saddle in this area (Hillenbrand et al., 2010a).

Modelling studies may provide further insight into how shelf topography and drainage pattern have affected ice retreat rates (e.g. Gudmundsson et al., 2012; Jamieson et al., 2012). The lack/scarcity of LGM to recent records of oceanic, atmospheric and relative sea-level forcing from within the sector, however, presents a substantial obstacle to realistic modelling of long-term ice sheet changes. The most relevant records of atmospheric change come from the Byrd Station ice core (Blunier and Brook, 2001), which was drilled in the neighbouring Ross Sea sector, and the WAIS Divide ice core (Fig. 2; WAIS Divide Project Members, 2013). A record from a deep ice core drilled on Fletcher Promontory in the Weddell Sea sector, which will be the nearest to the Bellingshausen Sea region, should also become available soon (Fig. 10; R. Mulvaney, pers. comm.). No records of relative sea-level change or changes in continental shelf water masses are available from the sector. Moreover, despite investigations of possible shelf water mass proxies (e.g. Carter et al., 2012; Majewski, 2013), a reliable and practical one has yet to be established. Obtaining LGM to recent records of forcing functions applicable to this critical sector of the WAIS should be a priority for future research.

#### 5.5. The role of subglacial meltwater

There is evidence of extensive bedrock erosion by subglacial meltwater in PIB and in front of the eastern Getz Ice Shelf, but the timing of meltwater discharges is poorly constrained and therefore it remains unclear whether or not they played a significant role in deglaciation (Lowe and Anderson, 2002, 2003; Larter et al., 2009; Smith et al., 2009; Nitsche et al., 2013). Comparison of the size of some of the channels with modelled melt production rates suggests that water must have been stored subglacially and released episodically in order to achieve the flow velocities that would be required to erode bedrock (Nitsche et al., 2013). Furthermore, in view of the dimensions of some of the channels and the fact that they have been carved into bedrock, it seems likely that they formed incrementally over many glacial cycles (Smith et al., 2009; Nitsche et al., 2013). Well-sorted sands and gravels recovered at shallow depth below the seabed in a sediment core from one channel in PIB suggest that this channel was active during deglaciation, although there are no direct age constraints (Lowe and Anderson, 2003). Furthermore, in PIT a mud drape has been interpreted as a meltwater outflow deposit (Kirshner et al., 2012). In contrast, the sequence of facies recovered in three sediment cores from subglacial meltwater-eroded channels in the western ASE is very different, with that recovered from a site north of the eastern Getz Ice Shelf giving evidence that the channel there was overridden by grounded ice since it was last active (Smith et al., 2009).

#### 5.6. Ice surface elevation changes

The few available palaeo-ice surface elevation constraints from the sector suggest that interior elevations have changed little since the LGM (Raynaud and Whillans, 1982; Lorus et al., 1984; Ackert et al., 1999) whereas, in general, a gradual decrease in surface elevations has been detected near the ice sheet margins by 2.5–9 cm yr<sup>-1</sup> since up to 14.5 ka ago (Stone et al., 2003; Bentley et al., 2006, 2011; Johnson et al., 2008; Hodgson et al., 2009; Lindow et al., 2011). Such thinning may have started earlier, but if so ice either covered all nunataks in coastal areas or ones that record the earliest stages of thinning have not yet been sampled. Greater thinning rates that have occurred over short intervals in some coastal areas

may be associated with retreat of steeper ice surface gradients near the grounding line (e.g. Stone et al., 2003).

#### 5.7. Long-term context of recent changes

The rates of thinning and grounding line retreat observed on ice shelves and glaciers around the ASE over the past two decades are significantly faster than any that can be reliably established in deglacial records from the sector. With the available data, however, we cannot insist that such rapid changes are unprecedented since the LGM. Taking into account the evidence for highly episodic grounding-line retreat from the outer and middle shelf parts of PIT during the early stages of the last deglaciation (e.g. Graham et al., 2010; Jakobsson et al., 2012), the grounding line may well have retreated from one GZW position to the next landward GZW position at a rate comparable to that of modern retreat. Although the net retreat of the PIG grounding line has been no more than 112 km over the past 11.2 ka (an average rate of 10 m yr<sup>-1</sup>), we cannot presently discount the possibility that this could have been achieved by up to four periods of retreat lasting no more than 30 years, each at rates similar to those observed over recent decades, with the grounding line remaining steady between those periods (Hillenbrand et al., 2013). Neither can we dismiss the possibility that the grounding line may have retreated beyond its present position at some stage during the Holocene and subsequently re-advanced prior to the period of historical observations. Although there is presently no clear evidence for such a scenario, it is one possible interpretation of recently-reported observations from beneath the PIG ice shelf (Graham et al., 2013). Similarly, if there were past, short-lived phases of ice thinning at rates similar to those observed in the recent past (i.e. several m yr<sup>-1</sup>), the sparse cosmogenic surface exposure age sample sets presently available from the sector are not yet adequate to resolve such abrupt changes.

### 6. Summary and conclusions

Over the past decade airborne and marine surveys in this sector have greatly improved knowledge of bed topography beneath the ice sheet (Fretwell et al., 2013) and of continental shelf bathymetry (Nitsche et al., 2007, 2013; Graham et al., 2011), providing a much more accurate basal boundary for ice sheet and palaeo-ice sheet models. Further airborne geophysical surveys are needed, however, to improve knowledge of ice bed topography around the Bellingshausen Sea and coastal areas of Marie Byrd Land, and further multibeam swath bathymetry surveys are needed to constrain the dynamics of ice that covered continental shelf areas.

Over the same period there has been a several-fold increase in the number of radiocarbon and cosmogenic surface exposure dates constraining the progress of the last deglaciation. Despite this increase, data points remain sparse and unevenly distributed, and in many cases the uncertainty range of ages is too large to determine reliable rates of change. Cosmogenic surface exposure age data remain particularly sparse, and are completely lacking for the region to the south of the Bellingshausen Sea. Although there are few nunataks in this region, collecting samples from them for cosmogenic isotope dating should be a priority for future research. Radiocarbon dates constraining ice retreat are almost exclusively from cross-shelf troughs because, in general, shallower parts of the continental shelf have been pervasively furrowed by icebergs, making it difficult to find undisturbed records extending back to the time of grounding line retreat. However, renewed efforts need to be made to locate sites between cross-shelf troughs that have been protected from iceberg furrowing (e.g. small depressions surrounded by closed contours), particularly as carbonate material

is more likely to be preserved at shallower water sites (Hillenbrand et al., 2003, 2013; Hauck et al., 2012). The radiocarbon dates presently constraining ice retreat in the Bellingshausen Sea are all on AIOM, so it is particularly important to search for carbonate material of early deglacial age from that region in order to refine the history of retreat.

Although there are several shortcomings and large gaps in the available data, we are able to draw the following conclusions:

1. The ice grounding line advanced to, or close to, the continental shelf edge across most of the Amundsen-Bellingshausen sector during the last glacial period, although in at least one area (Belgica Trough) the maximum advance seems to have occurred before the global LGM (23–19 cal ka BP).
2. In the extended ice sheet at least three major ice streams flowed across the continental shelf in the ASE and at least two flowed across the Bellingshausen Sea shelf. We cannot be certain that these were all active throughout the last glacial period, but if they were, then it is likely that ice covering these broad shelf areas had a relatively low surface profile.
3. The middle and outer continental shelf in the ASE and at least the outer shelf in the Bellingshausen Sea are underlain by thick sedimentary strata, which would have made widespread streaming flow more likely by facilitating the formation of a dilated sediment layer at the bed of overriding ice.
4. The few cosmogenic surface exposure ages and ice core data available from the interior of West Antarctica indicate that ice surface elevations there have changed little since the LGM.
5. Ice in the Amundsen Sea had retreated close to its modern limits by early Holocene time, after relatively rapid retreat from the middle shelf during the preceding few thousand years. In contrast, gradual ice retreat occurred from the outer to middle-shelf along Belgica Trough in the Bellingshausen Sea. The inner shelf of its Eltanin Bay tributary had also become free of grounded ice by the early Holocene, but retreat into its Ronne Entrance tributary continued through most of the Holocene. The retreat trajectory in the ASE resembles that on the continental shelf west of the Antarctic Peninsula, whereas the trajectory along the Ronne Entrance tributary of Belgica Trough resembles the progressive retreat recorded in the Ross Sea. Therefore, there seems to be an alternation along the West Antarctic margin between zones in which gradual retreat continued during the Holocene and ones in which retreat close to modern limits was nearly complete by early Holocene time.
6. Grounding line retreat paused for several thousand years and GZWs formed in an area where there is a “bottle neck” in Pine Island Trough, west of Burke Island. Available age data from the Bellingshausen Sea suggest a similar pause in retreat where the trough originating from the Ronne Entrance narrows and shallows near its confluence with the main Belgica Trough.
7. The highest ice retreat rates are found where the grounding line retreated across deep basins on the inner shelf parts of the Pine Island and Dotson-Getz troughs, which is consistent with the marine ice sheet instability hypothesis.
8. Although there is evidence of extensive bedrock erosion by subglacial meltwater on parts of the inner continental shelf in the ASE, the timing of meltwater discharges is poorly constrained and therefore it remains unclear whether or not they played a significant role in deglaciation.
9. In most areas near the margin of the ice sheet from which cosmogenic surface exposure data are available there appears to have been a gradual decrease in surface elevations by 2.5–9 cm yr<sup>-1</sup> since up to 14.5 ka ago. However, in most areas average rates have been derived from small sample sets that would not resolve short periods of more rapid change.
10. The rates of thinning and grounding line retreat observed on ice shelves and glaciers around the ASE over the past two decades are significantly faster than any that can be reliably established in deglacial records from the sector. With existing data, however, we cannot insist that they are unprecedented during the Holocene.

## Acknowledgements

This paper draws on results obtained from many research cruises and field parties. We thank all of the captains, officers, crews, pilots, field support staff, technicians and fellow scientists who contributed to collection of the data used. The Scientific Committee for Antarctic Research Past Antarctic Ice Sheet Dynamics Programme (SCAR-PAIS) and the earlier Antarctic Climate Evolution Programme (SCAR-ACE) have supported the Community Antarctic Ice Sheet Reconstruction Project to which this work contributes. The paper was improved by constructive comments from two anonymous referees.

## Appendix A. Supplementary data

Supplementary data related to this article can be found at <http://dx.doi.org/10.1016/j.quascirev.2013.10.016>.

## References

- Ackert, R.P., Barclay, D.J., Borns, H.W., Calkin, P.E., Kurz, M.D., Fastook, J.L., Steig, E.J., 1999. Measurements of past ice sheet elevations in interior West Antarctica. *Science* 286, 276–280.
- Ackert, R.P., Putnam, A.E., Mukhopadhyay, S., Pollard, D., DeConto, R.M., Kurz, M.D., Borns, H.W., 2013. Controls on interior West Antarctic ice sheet elevations: inferences from geologic constraints and ice sheet modelling. *Quat. Sci. Rev.* 65, 26–38.
- Alley, R.B., Blankenship, D.D., Bentley, C.R., Rooney, S.T., 1987. Till beneath Ice Stream B. 3. Till deformation: evidence and implications. *J. Geophys. Res.* 92, 8921–8929.
- Alley, R.B., Blankenship, D.D., Rooney, S.T., Bentley, C.R., 1989. Sedimentation beneath ice shelves: the view from Ice Stream B. *Mar. Geol.* 85, 101–120.
- Alley, R.B., Anandakrishnan, S., Dupont, T.K., Parizek, B.R., Pollard, D., 2007. Effect of sedimentation on ice-sheet grounding-line stability. *Science* 315, 1838–1841.
- Anderson, J.B., Myers, N.C., 1981. USCGC *Glacier* Deep Freeze 81 expedition to the Amundsen sea and Bransfield Strait. *Antarct. J. U. S.* 16 (5), 118–119.
- Anderson, J.B., Wellner, J.S., Lowe, A.L., Mosola, A.B., Shipp, S.S., 2001. Footprint of the expanded West Antarctic Ice Sheet: ice stream history and behavior. *GSA Today* 11 (10), 4–9.
- Anderson, J.B., Shipp, S.S., Lowe, A.L., Wellner, J.S., Mosola, A.B., 2002. The Antarctic Ice Sheet during the Last Glacial Maximum and its subsequent retreat history: a review. *Quat. Sci. Rev.* 21, 49–70.
- Anderson, J.B., Conway, H., Bart, P.J., Witus, A.E., Greenwood, S.L., McKay, R.M., Hall, B.L., Ackert, R.P., Licht, K., Jakobsson, M., Stone, J.O., 2014. Ross Sea paleo-ice sheet drainage and deglacial history during and since the LGM. *Quat. Sci. Rev.* 100, 31–54. <http://dx.doi.org/10.1016/j.quascirev.2013.08.020>.
- Andrews, J.T., Domack, E.W., Cunningham, W.L., Leverter, A., Licht, K.J., Jull, A.J.T., DeMaster, D.J., Jennings, A.E., 1999. Problems and possible solutions concerning radiocarbon dating of surface marine sediments, Ross Sea, Antarctica. *Quat. Res.* 52, 206–216.
- Arneborg, L., Wählin, A.K., Björk, G., Liljebladh, B., Orsi, A.H., 2012. Persistent inflow of warm water onto the central Amundsen shelf. *Nat. Geosci.* 5, 876–880.
- Arthern, R.J., Winebrenner, D.P., Vaughan, D.G., 2006. Antarctic snow accumulation mapped using polarization of 4.3-cm wavelength microwave emission. *J. Geophys. Res.* 111, D06107. <http://dx.doi.org/10.1029/2004JD005667>.
- Balco, G., Stone, J.O., Lifton, N.A., Dunai, T.J., 2008. A complete and easily accessible means of calculating surface exposure ages or erosion rates from <sup>10</sup>Be and <sup>26</sup>Al measurements. *Quat. Geochronol.* 3, 174–195.
- Bamber, J.L., Alley, R.B., Joughin, I., 2007. Rapid response of modern day ice sheets to external forcing. *Earth Planet. Sci. Lett.* 257, 1–13.



- Bamber, J.L., Gomez-Dans, J.L., Griggs, J.A., 2009a. A new 1 km digital elevation model of the Antarctic derived from combined satellite radar and laser data – Part 1: data and methods. *The Cryosphere* 3, 101–111. <http://dx.doi.org/10.5194/tc-3-113-2009>.
- Bamber, J.L., Riva, R.E.M., Vermeersen, B.L.A., LeBrocq, A.M., 2009b. Reassessment of the potential sea-level rise from a collapse of the West Antarctic Ice Sheet. *Science* 324, 901–903.
- Bentley, M.J., 2010. The Antarctic palaeo record and its role in improving predictions of future Antarctic Ice Sheet change. *J. Quat. Sci.* 25, 5–18.
- Bentley, M.J., Hodgson, D.A., Sugden, D.E., Roberts, S.J., Smith, J.A., Leng, M.J., Bryant, C., 2005. Early Holocene retreat of the George VI ice shelf, Antarctic Peninsula. *Geology* 33, 173–176.
- Bentley, M.J., Fogwill, C.J., Kubik, P.W., Sugden, D.E., 2006. Geomorphological evidence and cosmogenic  $^{10}\text{Be}/^{26}\text{Al}$  exposure ages for the Last Glacial Maximum and deglaciation of the Antarctic Peninsula Ice Sheet. *Geol. Soc. America* 118, 1149–1159.
- Bentley, M.J., Johnson, J.S., Hodgson, D.A., Dunai, T., Freeman, S.P.H.T., Ó Cofaigh, C., 2011. Rapid deglaciation of Marguerite Bay, western Antarctic Peninsula in the early Holocene. *Quat. Sci. Rev.* 30, 3338–3349.
- Bentley, M.J., Johnson, J.S., Fogwill, C.J., 2011. Deglacial history of Hudson Mountains, Amundsen Sea embayment. In: 11th International Symposium on Antarctic Earth Sciences, p. 245. Program and Abstracts (John McIntyre Conference Centre, Edinburgh, Scotland, 11–15 July 2011), Abstract PS19.10.
- Berkman, P.A., Forman, S.L., 1996. Pre-bomb radiocarbon and the reservoir correction for calcareous marine species in the Southern Ocean. *Geophys. Res. Lett.* 23, 363–366.
- Bindschadler, R., 1998. Future of the west Antarctic ice sheet. *Science* 282, 428–429.
- Bingham, R.G., Ferraccioli, F., King, E.C., Larter, R.D., Pritchard, H.D., Smith, A.M., Vaughan, D.G., 2012. Inland thinning of West Antarctic Ice Sheet steered along subglacial rifts. *Nature* 487, 468–471.
- Blunier, T., Brook, E.J., 2001. Timing of millennial-scale climate change in Antarctica and Greenland during the last glacial period. *Science* 291, 109–112.
- Bromwich, D.H., Nicolas, J.P., Monaghan, A.J., Lazzara, M.A., Keller, L.M., Weidner, G.A., Wilson, A.B., 2012. Central west Antarctica among the most rapidly warming regions on Earth. *Nat. Geosci.* 6, 139–145.
- Cande, S.C., Stock, J.M., Müller, R.D., Ishihara, T., 2000. Cenozoic motion between East and West Antarctica. *Nature* 404, 145–150.
- Carter, P., Vance, D., Hillenbrand, C.-D., Smith, J.A., Shoosmith, D.R., 2012. The neodymium isotopic composition of waters masses in the eastern Pacific sector of the Southern Ocean. *Geochim. Cosmochim. Acta* 79, 41–59.
- Chen, J.L., Wilson, C.R., Blankenship, D., Tapley, B.D., 2009. Accelerated Antarctic ice loss from satellite gravity measurements. *Nat. Geosci.* 2, 859–862.
- Convey, P., Gibson, J.A.E., Hillenbrand, C.-D., Hodgson, D.A., Pugh, P.J.A., Smellie, J.L., Stevens, M.I., 2008. Antarctic terrestrial life – challenging the history of the frozen continent? *Biol. Rev.* 83, 103–117.
- Convey, P., Stevens, M.I., Gibson, J.A.E., Hodgson, D.A., Smellie, J.L., Hillenbrand, C.-D., Barnes, D.K.A., Clarke, A., Pugh, P.J.A., Linse, K., Cary, S.C., 2009. Exploring biological constraints on the glacial history of Antarctica. *Quat. Sci. Rev.* 28, 3035–3048.
- Conway, H., Rasmussen, L.A., 2009. Recent thinning and migration of the western divide, central West Antarctica. *Geophys. Res. Lett.* 36, L12502. <http://dx.doi.org/10.1029/2009GL038072>.
- Conway, H., Hall, B.L., Denton, G.H., Gades, A.M., Waddington, E.D., 1999. Past and future grounding-line retreat of the West Antarctic Ice Sheet. *Science* 286, 280–283.
- Cook, F.A., 1909. Through the First Antarctic Night 1898–1899: a Narrative of the Voyage of the “Belgica” Among Newly Discovered Lands and over an Unknown Sea about the South Pole. Doubleday, Page and Co, New York, p. 478. <http://archive.org/details/throughfirstanta00cookrich>.
- Cook, A.J., Fox, A.J., Vaughan, D.G., Ferrigno, J.G., 2005. Retreating glacier fronts on the Antarctic Peninsula over the past half-century. *Science* 308, 541–544.
- Corr, H.F.J., Vaughan, D.G., 2008. A recent volcanic eruption beneath the West Antarctic ice sheet. *Nat. Geosci.* 1, 122–125.
- Cunningham, A.P., Larter, R.D., Barker, P.F., 1994. Glacially prograded sequences on the Bellingshausen Sea continental margin near 90°W. *Terra Antarctica* 1, 267–268.
- Cunningham, A.P., Larter, R.D., Barker, P.F., Gohl, K., Nitsche, F.O., 2002. Tectonic evolution of the Pacific margin of Antarctica 2. Structure of Late Cretaceous–early Tertiary plate boundaries in the Bellingshausen Sea from seismic reflection and gravity data. *J. Geophys. Res.* 107, 2346. <http://dx.doi.org/10.1029/2002JB001897>.
- Danesi, S., Morelli, A., 2000. Group velocity of Rayleigh waves in the Antarctic region. *Phys. Earth Planet. Interiors* 122, 55–66.
- Deleir, H. (Ed.), 1999. Roald Amundsen's Belgica Diary: the First Scientific Expedition to the Antarctic, p. 208. Bluntisham, Huntingdon (U.K.).
- Desilets, D., Zreda, M., Prabu, T., 2006. Extended scaling factors for in situ cosmogenic nuclides: new measurements at low latitude. *Earth Planet. Sci. Lett.* 246, 265–276.
- Ding, Q., Steig, E.J., Battisti, D.S., Küttel, M., 2011. Winter warming in West Antarctica caused by central tropical Pacific warming. *Nat. Geosci.* 4, 398–403.
- Domack, E.W., Jacobson, E.A., Shipp, S., Anderson, J.B., 1999. Late Pleistocene–Holocene retreat of the west Antarctic ice-sheet system in the Ross sea: Part 2. Sedimentologic and stratigraphic signature. *Geol. Soc. America Bull.* 111, 1517–1536.
- Domack, E.W., Leventer, A., Dunbar, R., Taylor, F., Brachfeld, S., Sjunneskog, C., ODP Leg 178 Scientific Party, 2001. Chronology of the Palmer Deep site, Antarctic Peninsula: a Holocene paleoenvironmental reference for the circum-Antarctic. *Holocene* 11, 1–9.
- Domack, E., Duran, D., Leventer, A., Ishman, S., Doane, S., McCallum, S., Ambblas, D., Ring, J., Gilbert, R., Prentice, M., 2005. Stability of the Larsen B ice shelf on the Antarctic Peninsula during the Holocene epoch. *Nature* 436, 681–685.
- Dowdeswell, J.A., Bamber, J., 2007. Keel depths of modern Antarctic icebergs and implications for sea-floor scouring in the geological record. *Mar. Geol.* 243, 120–131.
- Dowdeswell, J.A., Ó Cofaigh, C., Pudsey, C.J., 2004. Thickness and extent of the subglacial till layer beneath an Antarctic paleo-ice stream. *Geology* 32, 13–16.
- Dowdeswell, J.A., Evans, J., Ó Cofaigh, C., Anderson, J.B., 2006. Morphology and sedimentary processes on the continental slope off Pine Island Bay, Amundsen Sea, West Antarctica. *Geol. Soc. America Bull.* 118, 606–619.
- Dowdeswell, J.A., Ó Cofaigh, C., Noormets, R., Larter, R.D., Hillenbrand, C.-D., Benetti, S., Evans, J., Pudsey, C.J., 2008. A major trough-mouth fan on the continental margin of the Bellingshausen Sea, West Antarctica: the Belgica Fan. *Mar. Geol.* 252, 129–140.
- Dunai, T., 2001. Influence of secular variation of the magnetic field on production rates of in situ produced cosmogenic nuclides. *Earth Planet. Sci. Lett.* 193, 197–212.
- Eagles, G., Larter, R.D., Gohl, K., Vaughan, A.P.M., 2009. West Antarctic rift system in the Antarctic Peninsula. *Geophys. Res. Lett.* 36, L21305. <http://dx.doi.org/10.1029/2009GL040721>.
- Ehrmann, W., Hillenbrand, C.-D., Smith, J.A., Graham, A.G.C., Kuhn, G., Larter, R.D., 2011. Provenance changes between recent and glacial-time sediments in the Amundsen Sea embayment, West Antarctica: clay mineral assemblage evidence. *Antarc. Sci.* 23, 471–486.
- Esper, O., Gersonde, R., Kadagies, N., 2010. Diatom distribution in southeastern Pacific surface sediments and their relationship to modern environmental variables. *Palaeogeogr. Palaeoclimatol. Palaeoecol.* 287, 1–27.
- Evans, J., Dowdeswell, J.A., Ó Cofaigh, C., Benham, T.J., Anderson, J.B., 2006. Extent and dynamics of the West Antarctic Ice Sheet on the outer continental shelf of Pine Island Bay during the last glaciation. *Mar. Geol.* 230, 53–72.
- Ferrigno, J.G., Lucchitta, B.K., Mullins, K.F., Allison, A.L., Allen, R.J., Gould, W.G., 1993. Velocity measurements and changes in position of Thwaites glacier/iceberg tongue from aerial photography, Landsat images and NOAA AVHRR data. *Ann. Glaciol.* 17, 239–244.
- Finn, C.A., Müller, R.D., Panter, K.S., 2005. A Cenozoic diffuse alkaline magmatic province (DAMP) in the southwest Pacific without rift or plume origin. *Geochim. Geophys. Geosyst.* 6, Q02005. <http://dx.doi.org/10.1029/2004GC000723>.
- Fretwell, P., Pritchard, H.D., Vaughan, D.G., 57 others, 2013. Bedmap2: improved ice bed, surface and thickness datasets for Antarctica. *Cryosphere* 7, 375–393. <http://dx.doi.org/10.5194/tc-7-375-2013>.
- Gales, J.A., Larter, R.D., Mitchell, N.C., Dowdeswell, J.A., 2013. Geomorphic signature of Antarctic submarine gullies: implications for continental slope processes. *Mar. Geol.* 337, 112–124.
- Gohl, K. (Ed.), 2007. The Expedition ANTARKTIS-XXIII/4 of the Research Vessel “Polarstern” in 2006. Berichte zur Polar- und Meeresforschung, vol. 557. Alfred-Wegener-Institut für Polar- und Meeresforschung, Bremerhaven (Germany), p. 166. <http://hdl.handle.net/10013/epic.27102>.
- Gohl, K. (Ed.), 2010. The Expedition of the Research Vessel “Polarstern” to the Amundsen Sea, Antarctica, in 2010 (ANT-xxvi/3). Berichte zur Polar- und Meeresforschung, vol. 617. Alfred-Wegener-Institut für Polar- und Meeresforschung, Bremerhaven (Germany), p. 168. <http://hdl.handle.net/10013/epic.35668>.
- Gohl, K., 2012. Basement control on past ice sheet dynamics in the Amundsen Sea Embayment, West Antarctica. *Palaeogeogr. Palaeoclimatol. Palaeoecol.* 335–336, 35–41.
- Gohl, K., Teterin, D., Eagles, G., Netzeband, G., Grobys, J.W.G., Parsiegl, N., Schlüter, P., Leinweber, V., Larter, R.D., Uenzelmann-Neben, G., Udintsev, G.B., 2007. Geophysical Survey Reveals Tectonic Structures in the Amundsen Sea Embayment, West Antarctica. U.S. Geological Survey and The National Academies. USGS OF-2007-1047, Short Research Paper 047 <http://dx.doi.org/10.3133/of2007-1047.srp047>.
- Gohl, K., Denk, A., Wobbe, F., Eagles, G., 2013a. Deciphering tectonic phases of the Amundsen Sea Embayment shelf, West Antarctica, from a magnetic anomaly grid. *Tectonophysics* 585, 113–123.
- Gohl, K., Uenzelmann-Neben, G., Larter, R.D., Hillenbrand, C.-D., Hochmuth, K., Kalberg, T., Weigelt, E., Davy, B., Kuhn, G., Nitsche, F.O., 2013b. Seismic stratigraphic record of the Amundsen Sea Embayment shelf from pre-glacial to recent times: evidence for a dynamic West Antarctic ice sheet. *Mar. Geo.* 344, 115–131.
- Graham, A.G.C., Larter, R.D., Gohl, K., Hillenbrand, C.-D., Smith, J.A., Kuhn, G., 2009. Bedform signature of a West Antarctic palaeo-ice stream reveals a multi-temporal record of flow and substrate control. *Quat. Sci. Rev.* 28, 2774–2793.
- Graham, A.G.C., Larter, R.D., Gohl, K., Dowdeswell, J.A., Hillenbrand, C.-D., Smith, J.A., Evans, J., Kuhn, G., 2010. Flow and retreat of the Late Quaternary Pine Island–Thwaites palaeo-ice stream, West Antarctica. *J. Geophys. Res.* 115, F03025. <http://dx.doi.org/10.1029/2009JF001482>.
- Graham, A.G.C., Nitsche, F.O., Larter, R.D., 2011. An improved bathymetry compilation for the Bellingshausen Sea, Antarctica, to inform ice-sheet and ocean models. *Cryosphere* 5, 95–106. <http://dx.doi.org/10.5194/tc-5-95-2011>.

- Graham, A.G.C., Dutrieux, P., Vaughan, D.G., Nitsche, F.O., Gyllencreutz, R., Greenwood, S.L., Larter, R.D., Jenkins, A., 2013. Sea-bed corrugations beneath an Antarctic ice shelf revealed by autonomous underwater vehicle survey: origin and implications for the history of Pine Island Glacier. *J. Geophys. Res.* 118. <http://dx.doi.org/10.1002/jgrf.20087>.
- Granot, R., Cande, S.C., Stock, J.M., Davey, F.J., Clayton, R.W., 2010. Postspredding rifting in the Adare Basin, Antarctica: regional tectonic consequences. *Geochim. Geophys. Geosyst.* 11, Q08005. <http://dx.doi.org/10.1029/2010GC003105>.
- Gudmundsson, G.H., Krug, J., Durand, G., Favier, L., Gagliardini, O., 2012. The stability of grounding lines on retrograde slopes. *Cryosphere* 6, 1497–1505. <http://dx.doi.org/10.5194/tc-6-1497-2012>.
- Harden, S.L., DeMaster, D.J., Nittrouer, C.A., 1992. Developing sediment geochronologies for high-latitude continental shelf deposits: a radiochemical approach. *Mar. Geol.* 103, 69–97.
- Hauck, J., Gerdes, D., Hillenbrand, C.-D., Hoppema, M., Kuhn, G., Nehrke, G., Völker, C., Wolf-Gladrow, D.A., 2012. Distribution and mineralogy of carbonate sediments on Antarctic shelves. *J. Mar. Syst.* 90, 77–87.
- Heroy, D.C., Anderson, J.B., 2007. Radiocarbon constraints on Antarctic Peninsula ice sheet retreat following the last glacial maximum (LGM). *Quat. Sci. Rev.* 26, 3286–3297.
- Hillenbrand, C.-D., Grobe, H., Diekmann, B., Kuhn, G., Fütterer, D.K., 2003. Distribution of clay minerals and proxies for productivity in surface sediments of the Bellingshausen and Amundsen seas (West Antarctica) – relation to modern environmental conditions. *Mar. Geol.* 193, 253–271.
- Hillenbrand, C.-D., Baesler, A., Grobe, H., 2005. The sedimentary record of the last glaciation in the western Bellingshausen Sea (West Antarctica): implications for the interpretation of diamictites in a polar-marine setting. *Mar. Geol.* 216, 191–204.
- Hillenbrand, C.-D., Ehrmann, W., Larter, R.D., Benetti, S., Dowdeswell, J.A., Ó Cofaigh, C., Graham, A.G.C., Grobe, H., 2009. Clay mineral provenance of sediments in the southern Bellingshausen Sea reveals drainage changes of the West Antarctic Ice Sheet during the Late Quaternary. *Mar. Geol.* 265, 1–18.
- Hillenbrand, C.-D., Larter, R.D., Dowdeswell, J.A., Ehrmann, W., Ó Cofaigh, C., Benetti, S., Graham, A.G.C., Grobe, H., 2010a. The sedimentary legacy of a palaeo-ice stream on the shelf of the southern Bellingshausen Sea: clues to West Antarctic glacial history during the Late Quaternary. *Quat. Sci. Rev.* 29, 2741–2763.
- Hillenbrand, C.-D., Smith, J.A., Kuhn, G., Esper, O., Gersonde, R., Larter, R.D., Maher, B., Moreton, S.G., Shimmield, T.M., Korte, M., 2010b. Age assignment of diatomaceous ooze deposited in the western Amundsen Sea Embayment after the Last Glacial Maximum. *J. Quat. Sci.* 25, 280–295. <http://dx.doi.org/10.1002/jqs.1308>.
- Hillenbrand, C.-D., Kuhn, G., Smith, J.A., Gohl, K., Graham, A.G.C., Larter, R.D., Klages, J.P., Downey, R., Moreton, S.G., Forwick, M., Vaughan, D.G., 2013. Grounding-line retreat of the west Antarctic ice sheet from inner Pine island Bay. *Geology* 41, 35–38.
- Hillenbrand, C.-D., Bentley, M.J., Stollendorf, T.D., Hein, A.S., Kuhn, G., Graham, A.G.C., Fogwill, C.J., Kristoffersen, Y., Smith, J.A., Anderson, J.A., Larter, R.D., Melles, M., Hodgson, D.A., Mulvaney, R., Sugden, D.E., 2013. Reconstruction of changes in the Weddell Sea sector of the Antarctic Ice Sheet since the Last Glacial Maximum. *Quat. Sci. Rev.* <http://dx.doi.org/10.1016/j.quascirev.2013.07.020>.
- Hochmuth, K., Gohl, K., 2013. Glacio-marine sedimentation dynamics of the Abbot glacial trough of the Amundsen Sea Embayment shelf, West Antarctica. In: Hambrey Barker, M., P.F., Barrett, P.J., Bowman, V., Davies, B., Smellie, J.L., Tranter, M. (Eds.), *Antarctic Palaeoenvironments and Earth-surface Processes*, Geological Society Special Publications, vol. 381. Geological Society, London (U.K.). <http://dx.doi.org/10.1144/SP381.21>.
- Hodgson, D.A., Roberts, S.J., Bentley, M.J., Smith, J.A., Johnson, J.S., Verleyen, E., Vyverman, W., Hodson, A.J., Leng, M.J., Czfierszky, A., Fox, A.J., Sanderson, D.C.W., 2009. Exploring former subglacial Hodgson lake, Antarctica Paper I: site description, geomorphology and limnology. *Quat. Sci. Rev.* 28, 2295–2309.
- Hole, M.J., LeMasurier, W., 1994. Tectonic controls on the geochemical composition of Cenozoic, mafic alkaline volcanic rocks from West Antarctica. *Contrib. Mineral. Petrol.* 117, 187–202.
- Holt, J.W., Blankenship, D.D., Morse, D.L., Young, D.W., Peters, M.E., Kempf, S.D., Richter, T.G., Vaughan, D.G., Corr, H.F.J., 2006. New boundary conditions for the West Antarctic Ice Sheet: subglacial topography of the Thwaites and Smith glacier catchments. *Geophys. Res. Lett.* 33, L09502. <http://dx.doi.org/10.1029/2005GL025561>.
- Hughes, T.J., 1981. The weak underbelly of the West Antarctic ice sheet. *J. Glaciol.* 27, 518–525.
- IOC, IHO and BODC, 2003. Centenary Edition of the GEBCO Digital Atlas. Published on CD-ROM on behalf of the Intergovernmental Oceanographic Commission and the International Hydrographic Organization as part of the General Bathymetric Chart of the Oceans. British Oceanographic Data Centre, Liverpool (U.K.).
- Ivins, E.R., James, T.S., 2005. Antarctic glacial isostatic adjustment: a new assessment. *Antarc. Sci.* 17, 541–553.
- Jacobs, S.S., Hellmer, H.H., Jenkins, A., 1996. Antarctic ice sheet melting in the Southeast Pacific. *Geophys. Res. Lett.* 23, 957–960.
- Jacobs, S.S., Jenkins, A., Giulivi, C.F., Dutrieux, P., 2011. Stronger ocean circulation and increased melting under Pine Island Glacier ice shelf. *Nat. Geosci.* 4, 519–523.
- Jakobsson, M., Anderson, J.B., Nitsche, F., Dowdeswell, J.A., Gyllencreutz, R., Kirchner, N., Mohammad, R., O'Regan, M., Alley, R.B., Anandakrishnan, S., Eriksson, B., Kirchner, A., Fernandez, R., Stollendorf, T., Minzoni, R., Majewski, W., 2011. Geological record of ice shelf break-up and grounding line retreat, Pine Island Bay, West Antarctica. *Geology* 39, 691–694.
- Jakobsson, M., Anderson, J.B., Nitsche, F., Gyllencreutz, R., Kirchner, N., O'Regan, M., Mohammad, R., Eriksson, B., 2012. Ice sheet retreat dynamics inferred from glacial morphology of the central Pine Island Bay Trough, West Antarctica. *Quat. Sci. Rev.* 38, 1–10.
- Jamieson, S.S.R., Vieli, A., Livingstone, S.J., Ó Cofaigh, C., Stokes, C., Hillenbrand, C.-D., Dowdeswell, J.A., 2012. Ice-stream stability on a reverse bed slope. *Nat. Geosci.* 5, 799–802.
- Jenkins, A., Jacobs, S., 2008. Circulation and melting beneath George VI ice shelf, Antarctica. *J. Geophys. Res.* 113, C04013. <http://dx.doi.org/10.1029/2007JC004449>.
- Jenkins, A., Dutrieux, P., Jacobs, S.S., McPhail, S.D., Perrett, J.R., Webb, A.T., White, D., 2010. Observations beneath Pine island glacier in west Antarctica and implications for its retreat. *Nat. Geosci.* 3, 468–472.
- Jenssen, D., 1983. Elevation and climatic changes from total gas content and stable isotopic measurements. In: Robin de, G.Q. (Ed.), *The Climatic Record in Polar Ice Sheets*. Cambridge University Press, London (U.K.), pp. 138–144.
- Johnson, J.S., Bentley, M.J., Gohl, K., 2008. First exposure ages from the Amundsen sea embayment, west Antarctica: the Late Quaternary context for recent thinning of Pine Island, Smith, and Pope Glaciers. *Geology* 36, 223–226.
- Johnson, J.S., Schaefer, J.M., Bentley, M.J., Fogwill, C.J., Smith, J.A., Schimmelpennig, I., Gohl, K., 2012. Rapid early- to mid-Holocene thinning of Pine Island Glacier detected using cosmogenic exposure dating (abstract). *Mineraol. Mag.* 76 (6), 1903.
- Jordan, T.A., Ferraccioli, F., Vaughan, D.G., Holt, J.W., Corr, H., Blankenship, D.D., Diehl, T.M., 2010. Aerogravity evidence for major crustal thinning under the Pine Island Glacier region (West Antarctica). *Geol. Soc. America Bull.* 122, 714–726.
- Joughin, I., Alley, R.B., 2011. Stability of the West Antarctic ice sheet in a warming world. *Nat. Geosci.* 4, 506–513.
- Joughin, I., Smith, B.E., Holland, D.M., 2010. Sensitivity of 21st century sea level to ocean-induced thinning of Pine Island Glacier, Antarctica. *Geophys. Res. Lett.* 37, L20502. <http://dx.doi.org/10.1029/2010GL044819>.
- Kamb, B., 2001. Basal zone of the West Antarctic ice streams and its role in lubrication of their rapid motion. In: Alley, R.B., Bindschadler, R.A. (Eds.), *The West Antarctic Ice Sheet: Behavior and Environment*, Antarctic Research Series, vol. 77. AGU, Washington, D. C., pp. 157–199.
- Katz, R.F., Worster, M.G., 2010. Stability of ice-sheet grounding lines. *Proc. R. Soc. A* 466, 1597–1620.
- Kellogg, T.B., Kellogg, D.E., 1987a. Late Quaternary deglaciation of the Amundsen Sea: implications for ice sheet modelling. In: Waddington, E.D., Walder, J.S. (Eds.), *The Physical Basis of Ice Sheet Modelling*. International Association of Hydrological Sciences Publication No. 170. IAHS Press, Wallingford (U.K.), pp. 349–357.
- Kellogg, T.B., Kellogg, D.E., 1987b. Recent glacial history and rapid ice retreat in the Amundsen Sea. *J. Geophys. Res.* 92, 8859–8864.
- Kilfeather, A.A., Ó Cofaigh, C., Lloyd, J.M., Dowdeswell, J.A., Xu, S., Moreton, S.G., 2011. Ice-stream retreat and ice-shelf history in Marguerite Trough, Antarctic Peninsula: sedimentological and foraminiferal signatures. *Geol. Soc. America Bull.* 123, 997–1015.
- King, M.A., Bingham, R.J., Moore, P., Whitehouse, P.L., Bentley, M.J., Milne, G.A., 2012. Lower satellite-gravimetry estimates of Antarctic sea-level contribution. *Nature* 491, 586–589.
- Kirchner, A., Anderson, J.B., Jakobsson, M., O'Regan, M., Majewski, W., Nitsche, F., 2012. Post-LGM deglaciation in Pine island Bay, west Antarctica. *Quat. Sci. Rev.* 38, 11–26.
- Klages, J.P., Kuhn, G., Hillenbrand, C.-D., Graham, A.G.C., Smith, J.A., Larter, R.D., Gohl, K., 2013. First geomorphological record and glacial history of an inter-ice stream ridge on the West Antarctic continental shelf. *Quat. Sci. Rev.* 61, 47–61.
- Konfirst, M.A., Scherer, R.P., Hillenbrand, C.-D., Kuhn, G., 2012. A marine diatom record from the Amundsen Sea — Insights into oceanographic and climatic response to the Mid-Pleistocene Transition in the West Antarctic sector of the Southern Ocean. *Mar. Micropaleontol.* 92–93, 40–51.
- Lal, D., 1991. Cosmic ray labeling of erosion surfaces: in situ nuclide production rates and erosion models. *Earth Planet. Sci. Lett.* 104, 424–439.
- Larter, R.D., Gohl, K., Hillenbrand, C.-D., Kuhn, G., Deen, T.J., Dietrich, R., Eagles, G., Johnson, J.S., Livermore, R.A., Nitsche, F.O., Pudsey, C.J., Schenke, H.-W., Smith, J.A., Udintsev, G., Uenzelmann-Neben, G., 2007. West Antarctic ice sheet change since the last glacial period. *Eos, Transactions. Am. Geophys. Union* 88, 189–190. <http://dx.doi.org/10.1029/2007EO170001>.
- Larter, R.D., Graham, A.G.C., Gohl, K., Kuhn, G., Hillenbrand, C.-D., Smith, J.A., Deen, T.J., Livermore, R.A., Schenke, H.-W., 2009. Subglacial bedforms reveal complex basal regime in a zone of paleo-ice stream convergence, Amundsen Sea Embayment, West Antarctica. *Geology* 37, 411–414.
- Lawley, B., Ripley, S., Bridge, P., Convey, P., 2004. Molecular analysis of geographic patterns of eukaryotic diversity in Antarctic soils. *Appl. Environ. Microbiol.* 70, 5963–5972.
- Le Brocq, A.M., Payne, A.J., Vieli, A., 2010. An improved Antarctic dataset for high resolution numerical ice sheet models (ALBMAP v1). *Earth Syst. Sci. Data* 2, 247–260. <http://dx.doi.org/10.5194/essd-2-247-2010>.
- Lee, H., Shum, C.K., Howat, I.M., Monaghan, A., Ahn, Y., Duan, J., Guo, J.-Y., Kuo, C.-Y., Wang, L., 2012. Continuously accelerating ice loss over Amundsen Sea catchment, West Antarctica, revealed by integrating altimetry and GRACE data. *Earth Planet. Sci. Lett.* 321–322, 74–80.



- LeMasurier, W., Kawachi, Y., Rex, D., Wade, F., 1990. Marie Byrd Land. In: LeMasurier, W., Thomson, J., Baker, P., Kyle, P., Rowley, P., Smellie, J., Verwoerd, W. (Eds.), 1990. Volcanoes of the Antarctic Plate and Southern Oceans, Antarctic Research Series, vol. 48. AGU, Washington, D. C., p. 487.
- Licht, K.J., Andrews, J.T., 2002. The  $^{14}\text{C}$  record of Late Pleistocene ice advance and retreat in the central Ross Sea, Antarctica. *Arctic, Antarct. Alpine Res.* 34, 324–333.
- Licht, K.J., Jennings, A.E., Andrews, J.T., Williams, K.M., 1996. Chronology of late Wisconsin ice retreat from the western Ross Sea, Antarctica. *Geology* 24, 223–226.
- Licht, K.J., Cunningham, W.L., Andrews, J.T., Domack, E.W., Jennings, A.E., 1998. Establishing chronologies from acid-insoluble organic  $^{14}\text{C}$  dates on Antarctic (Ross Sea) and Arctic (North Atlantic) marine sediments. *Polar Res.* 17, 203–216.
- Lifton, N.A., Bieber, J.W., Clem, J.M., Duldig, M.L., Evenson, P., Humber, J.E., Pyle, R., 2005. Addressing solar modulation and long-term uncertainties in scaling secondary cosmic rays for in situ cosmogenic nuclide applications. *Earth Planet. Sci. Lett.* 239, 140–161.
- Lindow, J., Spiegel, C., Johnson, J., Castex, M., Lisker, F., Gohl, K., 2011. Glacial retreat since the Last Glacial Maximum – New constraints from the Walgreen Coast, West Antarctica. In: 11th International Symposium on Antarctic Earth Sciences, p. 513. Program and Abstracts (John McIntyre Conference Centre, Edinburgh, Scotland, 11–15 July 2011), Abstract PO19.4.
- Livingstone, S.J., Ó Cofaigh, C., Stokes, C.R., Hillenbrand, C.-D., Vieli, A., Jamieson, S.S.R., 2012. Antarctic palaeo-ice streams. *Earth-Science Rev.* 111, 90–128.
- Lorius, C., Raynaud, D., Petit, J.-R., Jouzel, J., Merlivat, L., 1984. Late-glacial maximum–Holocene atmospheric and ice-thickness changes from Antarctic ice-core studies. *Ann. Glaciol.* 5, 88–94.
- Lowe, A.L., Anderson, J.B., 2002. Reconstruction of the West Antarctic ice sheet in Pine Island Bay during the Last Glacial maximum and its subsequent retreat history. *Quat. Sci. Rev.* 21, 1879–1897.
- Lowe, A.L., Anderson, J.B., 2003. Evidence for abundant subglacial meltwater beneath the paleo-ice sheet in Pine Island Bay, Antarctica. *J. Glaciol.* 49, 125–138.
- Lythe, M., Vaughan, D.G., the BEDMAP Consortium, 2001. BEDMAP: a new ice thickness and subglacial topographic model of Antarctica. *J. Geophys. Res.* 106, 11,335–11,352.
- Mackensen, A., 2012. Strong thermodynamic imprint on recent bottom-water and epibenthic  $\delta^{13}\text{C}$  in the Weddell Sea revealed: Implications for glacial Southern Ocean ventilation. *Earth Planet. Sci. Lett.* 317–318, 20–26.
- Majewski, W., 2013. Benthic foraminifera from Pine island and Ferrero bays, Amundsen sea. *Polish Polar Res.* 34, 169–200.
- Martinerie, P., Raynaud, D., Etheridge, D.M., Barnola, J.-M., Mazaudier, D., 1992. Physical and climatic parameters which influence the air content in polar ice. *Earth Planet. Sci. Lett.* 112, 1–13.
- Maslen, N.R., Convey, P., 2006. Nematode diversity and distribution in the southern maritime Antarctic – clues to history? *Soil Biol. Biochem.* 38, 3141–3151.
- Mercer, J.H., 1978. West Antarctic ice sheet and  $\text{CO}_2$  greenhouse effect: a threat of disaster. *Nature* 271, 321–325.
- Miller, H., Grobe, H. (Eds.), 1996. The Expedition ANTARKTIS-XI/3 with RV Polarstern in 1994. Reports on Polar Research, 188. Alfred-Wegener-Institut für Polar- und Meeresforschung, Bremerhaven (Germany), p. 115. <http://hdl.handle.net/10013/epic.10189>.
- Mosola, A.B., Anderson, J.B., 2006. Expansion and rapid retreat of the West Antarctic Ice Sheet in eastern Ross Sea: possible consequence of over-extended ice streams? *Quat. Sci. Rev.* 25, 2177–2196.
- Muto, A., Anandakrishnan, S., Alley, R.B., 2013. Subglacial bathymetry and sediment layer distribution beneath the Pine Island Glacier ice shelf, West Antarctica, modelled using aerogravity and autonomous underwater vehicle data. *Ann. Glaciol.* 54. <http://dx.doi.org/10.3189/2013AoG64A110>.
- Neumann, T.A., Conway, H., Price, S.F., Waddington, E.D., Catania, G.A., Morse, D.L., 2008. Holocene accumulation and ice sheet dynamics in central West Antarctica. *J. Geophys. Res.* 113, F02018. <http://dx.doi.org/10.1029/2007JF000764>.
- Nishiizumi, K., Kohl, C.P., Arnold, J.R., Winterer, E.L., Lal, D., Klein, J., Middleton, R., 1989. Cosmic ray production rates of  $^{26}\text{Al}$  and  $^{10}\text{Be}$  in quartz from glacially polished rocks. *J. Geophys. Res.* 94, 17907–17915.
- Nitsche, F.-O., 1998. Bellingshausen Sea and Amundsen Sea: Development of a Sedimentation Model. *Berichte zur Polarforschung*, vol. 258. Alfred-Wegener-Institut für Polar- und Meeresforschung, Bremerhaven (Germany), p. 144. <http://hdl.handle.net/10013/epic.10261>.
- Nitsche, F.O., Gohl, K., Vanneste, K., Miller, H., 1997. Seismic expression of glacially deposited sequences in the Bellingshausen and Amundsen Seas, West Antarctica. In: Barker, P.F., Cooper, A.K. (Eds.), *Geology and Seismic Stratigraphy of the Antarctic Margin*, Part 2. Antarctic Research Series vol. 71. AGU, Washington, D.C., pp. 95–108.
- Nitsche, F.O., Cunningham, A.P., Larter, R.D., Gohl, K., 2000. Geometry and development of glacial continental margin depositional systems in the Bellingshausen Sea. *Mar. Geol.* 162, 277–302.
- Nitsche, F.O., Jacobs, S.S., Larter, R.D., Gohl, K., 2007. Bathymetry of the Amundsen Sea continental shelf: implications for geology, oceanography, and glaciology. *Geochim. Geophys. Geosyst.* 8, Q10009. <http://dx.doi.org/10.1029/2007GC001694>.
- Nitsche, F.O., Gohl, K., Larter, R.D., Hillenbrand, C.-D., Kuhn, G., Smith, J.A., Jacobs, S., Anderson, J.B., Jakobsson, M., 2013. Paleo ice flow and subglacial meltwater dynamics in Pine Island Bay, West Antarctica. *Cryosphere* 7, 249–262. <http://dx.doi.org/10.5194/tc-7-249-2013>.
- Noormets, R., Dowdeswell, J.A., Larter, R.D., Ó Cofaigh, C., Evans, J., 2009. Morphology of the upper continental slope in the Bellingshausen and Amundsen Seas – implications for sedimentary processes at the shelf edge of West Antarctica. *Mar. Geol.* 258, 100–114.
- Ó Cofaigh, C., Dowdeswell, J.A., Allen, C.S., Hiemstra, J.F., Pudsey, C.J., Evans, J., Evans, D.J.A., 2005a. Flow dynamics and till genesis associated with a marine-based Antarctic palaeo-ice stream. *Quat. Sci. Rev.* 24, 709–740.
- Ó Cofaigh, C., Larter, R.D., Dowdeswell, J.A., Hillenbrand, C.-D., Pudsey, C.J., Evans, J., Morris, P., 2005b. Flow of the West Antarctic Ice Sheet on the continental margin of the Bellingshausen Sea at the Last Glacial Maximum. *J. Geophys. Res.* 110, B11103. <http://dx.doi.org/10.1029/2005JB003619>.
- Ó Cofaigh, C., Evans, J., Dowdeswell, J.A., Larter, R.D., 2007. Till characteristics, genesis and transport beneath Antarctic paleo-ice streams. *J. Geophys. Res.* 112, F03006. <http://dx.doi.org/10.1029/2006JF000606>.
- Ó Cofaigh, C., Davies, B.J., Livingstone, S.J., Smith, J.A., Johnson, J.S., Hocking, E.P., Hodgson, D.A., Anderson, J.B., Bentley, M.J., Canals, M., Domack, E., Dowdeswell, J.A., Evans, J., Glasser, N.F., Hillenbrand, C.-D., Larter, R.D., Roberts, S.J., Simms, A.R., Reconstruction of ice-sheet changes in the Antarctic Peninsula since the Last Glacial Maximum. *Quat. Sci. Rev.* (in review).
- Oppenheimer, M., 1998. Global warming and the stability of the West Antarctic Ice Sheet. *Nature* 393, 325–332.
- Powell, R.D., 1984. Glacimarine processes and inductive lithofacies modelling of ice shelf and tidewater glacier sediments based on Quaternary examples. *Mar. Geology* 57, 1–52.
- Pritchard, H.D., Arthern, R.J., Vaughan, D.G., Edwards, L.A., 2009. Extensive dynamic thinning on the margins of the Greenland and Antarctic ice sheets. *Nature* 461, 971–975.
- Pritchard, H.D., Ligtenberg, S.R.M., Fricker, H.A., Vaughan, D.G., van den Broeke, M.R., Padman, L., 2012. Antarctic ice-sheet loss driven by basal melting of ice shelves. *Nature* 484, 502–505.
- Pudsey, C.J., Murray, J.W., Appleby, P., Evans, J., 2006. Ice shelf history from petrographic and foraminiferal evidence, Northeast Antarctic Peninsula. *Quat. Sci. Rev.* 25, 2357–2379.
- Rabus, B.T., Lang, O., Adolphs, U., 2003. Interannual velocity variations and recent calving of Thwaites Glacier Tongue, West Antarctica. *Ann. Glaciol.* 36, 215–224.
- Raynaud, D., Lebel, B., 1979. Total gas content and surface elevation of polar ice sheets. *Nature* 281, 289–291.
- Raynaud, D., Whillans, I.M., 1982. Air content of the Byrd core and past changes in the West Antarctic Ice Sheet. *Ann. Glaciol.* 3, 269–273.
- Reimer, P.J., et al., 2009. IntCal09 and Marine09 radiocarbon age calibration curves, 0–50,000 years cal BP. *Radiocarbon* 51, 1111–1150.
- Rignot, E.J., 1998. Fast recession of a west Antarctic glacier. *Science* 281, 549–551.
- Rignot, E., 2008. Changes in West Antarctic ice stream dynamics observed with ALOS PALSAR data. *Geophys. Res. Lett.* 35, L12505. <http://dx.doi.org/10.1029/2008GL033365>.
- Rignot, E., Vaughan, D.G., Schmeltz, M., Dupont, T., MacAyeal, D., 2002. Acceleration of Pine island and Thwaites glaciers, west Antarctica. *Ann. Glaciol.* 34, 189–194.
- Rignot, E., Thomas, R.H., Kanagaratnam, P., Casassa, G., Frederick, E., Gogineni, S., Krabill, W., Rivera, A., Russell, R., Sonntag, J., Swift, R., Yungel, J., 2004. Improved estimation of the mass balance of glaciers draining into the Amundsen Sea sector of West Antarctica from the CECS/NASA 2002 campaign. *Ann. Glaciol.* 39, 231–237.
- Rignot, E., Bamber, J.L., van den Broeke, M.R., Davis, C., Li, Y., van de Berg, W.J., van Meijgaard, E., 2008. Recent Antarctic ice mass loss from radar interferometry and regional climate modelling. *Nat. Geosci.* 1, 106–110.
- Rignot, E., Mouginot, J., Scheuchl, B., 2011. Ice flow of the Antarctic ice sheet. *Science* 333, 1427–1430.
- Rosenheim, B.E., Day, M.B., Domack, E., Schrum, H., Benthien, A., Hays, J.M., 2008. Antarctic sediment chronology by programmed-temperature pyrolysis: methodology and data treatment. *Geochim. Geophys. Geosyst.* 9, Q04005. <http://dx.doi.org/10.1029/2007GC001816>.
- Ross, N., Siegert, M.J., Woodward, J., Smith, A.M., Corr, H.F.J., Bentley, M.J., Hindmarsh, R.C.A., King, E.C., Rivera, A., 2011. Holocene stability of the Amundsen-Weddell ice divide, West Antarctica. *Geology* 39, 935–938.
- Schoof, C., 2007. Ice sheet grounding line dynamics: steady states, stability, and hysteresis. *J. Geophys. Res.* 112, F03S28. <http://dx.doi.org/10.1029/2006JF000664>.
- Scott, J.B.T., Gudmundsson, G.H., Smith, A.M., Bingham, R.G., Pritchard, H.D., Vaughan, D.G., 2009. Increased rate of acceleration on Pine Island Glacier strongly coupled to changes in gravitational driving stress. *Cryosphere* 3, 125–131. <http://www.the-cryosphere.net/3/125/2009/>.
- Shapiro, N.M., Ritzwoller, M.H., 2004. Inferring surface heat flux distributions guided by a global seismic model: particular application to Antarctica. *Earth Planet. Sci. Lett.* 223, 213–224.
- Shepherd, A., Wingham, D., Rignot, E., 2004. Warm ocean is eroding west Antarctic ice sheet. *Geophys. Res. Lett.* 31, L23402. <http://dx.doi.org/10.1029/2004GL021106>.
- Shepherd, A., Ivins, E.R., 45 others, 2012. A reconciled estimate of ice-sheet mass balance. *Science* 338, 1183–1189.
- Siddoway, C.S., Sass, L.C., Esser, R.P., 2005. Kinematic history of western Marie Byrd Land, west Antarctica: direct evidence from Cretaceous mafic dykes. In: Vaughan, A.P.M., Leat, P.T., Pankhurst, R.J. (Eds.), *Terrane Processes at the*

- Margins of Gondwana, Geological Society Special Publications, vol. 246. Geological Society, London (U.K.), pp. 417–438.
- Smith, A.M., Murray, T., 2009. Bedform topography and basal conditions beneath a fast-flowing West Antarctic ice stream. *Quat. Sci. Rev.* 28, 584–596.
- Smith, J.A., Bentley, M.J., Hodgson, D.A., Roberts, S.J., Leng, M.J., Lloyd, J.M., Barrett, M.S., Bryant, C., Sugden, D.E., 2007. Oceanic and atmospheric forcing of early Holocene ice shelf retreat, George VI Ice Shelf, Antarctica Peninsula. *Quat. Sci. Rev.* 26, 500–516.
- Smith, J.A., Hillenbrand, C.-D., Larter, R.D., Graham, A.G.C., Kuhn, G., 2009. The sediment infill of subglacial meltwater channels on the West Antarctic continental shelf. *Quat. Res.* 71, 190–200.
- Smith, J.A., Hillenbrand, C.-D., Kuhn, G., Larter, R.D., Graham, A.G.C., Ehrmann, W., Moreton, S.G., Forwick, M., 2011. Deglacial history of the west Antarctic ice sheet in the western Amundsen sea embayment. *Quat. Sci. Rev.* 30, 488–505.
- Smith, A.M., Jordan, T.A., Ferraccioli, F., Bingham, R.G., 2013. Influence of subglacial conditions on ice stream dynamics: seismic and potential field data from Pine Island Glacier, West Antarctica. *J. Geophys. Res.* 118, 1471–1482. <http://dx.doi.org/10.1029/2012JB009582>.
- Solomon, S., Qin, D., Manning, M., Chen, Z., Marquis, M., Averyt, K.B., Tignor, M., Miller, H.L. (Eds.), 2007. Contribution of Working Group I to the Fourth Assessment Report of the Intergovernmental Panel on Climate Change, 2007. Cambridge University Press, Cambridge, UK and New York, NY, USA, p. 1056. [http://www.ipcc.ch/publications\\_and\\_data/ar4/wg1/en/contents.html](http://www.ipcc.ch/publications_and_data/ar4/wg1/en/contents.html).
- S.P.R.I.T.E., Group, Boyer, C.G., 1992. The southern rim of the Pacific ocean: preliminary geologic report of the Amundsen Sea–Bellingshausen sea cruise of the *Polar Sea*, 12 February–21 March 1992. *Antarc. J. U. S.* 27 (1), 11–14.
- Steig, E.J., Schneider, D.P., Rutherford, S.D., Mann, M.E., Comiso, J.C., Shindell, D.T., 2009. Warming of the Antarctic ice-sheet surface since the 1957 International Geophysical Year. *Nature* 457, 459–462.
- Steig, E.J., Ding, Q., Battisti, D.S., Jenkins, A., 2012. Tropical forcing of Circumpolar deep water inflow and outlet glacier thinning in the Amundsen sea embayment, west Antarctica. *Ann. Glaciol.* 53 (60), 19–28.
- Stone, J.O., 2000. Air pressure and cosmogenic isotope productions. *J. Geophys. Res.* 105, 23753–23759.
- Stone, J.O., Balco, G.A., Sugden, D.E., Caffee, M.W., Sass, L.C., Cowdery, S.G., Siddoway, C., 2003. Holocene deglaciation of Marie Byrd Land, west Antarctica. *Science* 299, 99–102.
- Studinger, M., Bell, R.E., Blankenship, D.D., Finn, C.A., Arko, R.A., Morse, D.L., Joughin, I., 2001. Subglacial sediments: a regional geological template for ice flow in West Antarctica. *Geophys. Res. Lett.* 28, 3493–3496.
- Studinger, M., Allen, C., Blake, W., Shi, L., Elieff, S., Krabill, W.B., Sonntag, J.G., Martin, S., Dutrieux, P., Jenkins, A., Bell, R.E., 2010. Mapping Pine Island Glacier's Sub-ice Cavity with Airborne Gravimetry. Abstract C11A-0528, Fall Meeting. AGU.
- Thoma, M., Jenkins, A., Holland, D., Jacobs, S., 2008. Modelling circumpolar deep water intrusions on the Amundsen sea continental shelf, Antarctica. *Geophys. Res. Lett.* 35, L18602. <http://dx.doi.org/10.1029/2008GL034939>.
- Thomas, R., Rignot, E., Casassa, G., Kanagaratnam, P., Acuña, C., Akins, T., Brecher, H., Frederick, E., Gogineni, P., Krabill, W., Manizade, S., Ramamoorthy, H., Rivera, A., Russell, R., Sonntag, J., Swift, R., Yungel, J., Zwally, J., 2004. Accelerated sea-level rise from West Antarctica. *Science* 306, 255–258.
- Tinto, K.J., Bell, R.E., 2011. Progressive unpinning of Thwaites glacier from newly identified offshore ridge: constraints from aerogravity. *Geophys. Res. Lett.* 38, L20503. <http://dx.doi.org/10.1029/2011GL049026>.
- Tucholke, B.E., Houtz, R.E., 1976. Sedimentary framework of the Bellingshausen Basin from seismic profiler data. In: Hollister, C.D., Craddock, C., et al. (Eds.), Initial Reports of the Deep Sea Drilling Project, vol. 35. U.S. Government Printing Office, Washington, D.C., pp. 197–228.
- Tulaczyk, S., Kamb, B., Scherer, R.P., Engelhardt, H.F., 1998. Sedimentary processes at the base of a West Antarctic ice stream; constraints from textural and compositional properties of subglacial debris. *J. Sediment. Res.* 68, 487–496.
- Uenzelmann-Neben, G., Gohl, K., Larter, R.D., Schlüter, P., 2007. Differences in Ice Retreat across Pine Island Bay, West Antarctica, since the Last Glacial Maximum: Indications from Multichannel Seismic Reflection Data. U.S. Geological Survey and The National Academies. USGS OF-2007-1047, Short Research Paper 084 <http://dx.doi.org/10.3133/of2007-1047.srp084>.
- Vaughan, D.G., 2008. West Antarctic Ice Sheet collapse – the fall and rise of a paradigm. *Clim. Change* 91, 65–79.
- Vaughan, D.G., Corr, H.F.J., Ferraccioli, F., Frearson, N., O'Hare, A., Mach, D., Holt, J.W., Blankenship, D.D., Morse, D.L., Young, D.A., 2006. New boundary conditions for the West Antarctic ice sheet: subglacial topography beneath Pine Island Glacier. *Geophys. Res. Lett.* 33, L09501. <http://dx.doi.org/10.1029/2005GL025588>.
- Wählin, A.K., Yuan, X., Björk, G., Nohr, C., 2010. Inflow of warm Circumpolar Deep Water in the central Amundsen shelf. *J. Phys. Oceanogr.* 40, 1427–1434.
- WAIS Divide Project Members, 2013. Onset of deglacial warming in West Antarctica driven by local orbital forcing. *Nature*. <http://dx.doi.org/10.1038/nature12376>.
- Walker, D.P., Brandon, M.A., Jenkins, A., Allen, J.T., Dowdeswell, J.A., Evans, J., 2007. Oceanic heat transport onto the Amundsen Sea shelf through a submarine glacial trough. *Geophys. Res. Lett.* 34, L02602. <http://dx.doi.org/10.1029/2006GL028154>.
- Weertman, J., 1974. Stability of the junction of an ice sheet and an ice shelf. *J. Glaciol.* 13, 3–11.
- Weigelt, E., Gohl, K., Uenzelmann-Neben, G., Larter, R.D., 2009. Late Cenozoic ice sheet cyclicity in the western Amundsen Sea Embayment – evidence from seismic records. *Glob. Planet. Change* 69, 162–169.
- Weigelt, E., Uenzelmann-Neben, G., Gohl, K., Larter, R.D., 2012. Did massive glacial dewatering modify sedimentary structures on the Amundsen Sea Embayment shelf, West Antarctica? *Global Planet. Change* 92–93, 8–16.
- Wellner, J.S., Lowe, A.L., Shipp, S.S., Anderson, J.B., 2001. Distribution of glacial geomorphic features on the Antarctic continental shelf and correlation with substrate: implications for ice behavior. *J. Glaciol.* 47, 397–411.
- Wellner, J.S., Heroy, D.C., Anderson, J.B., 2006. The death mask of the Antarctic ice sheet: comparison of glacial geomorphic features across the continental shelf. *Geomorphology* 75, 157–171.
- Whitehouse, P.L., Bentley, M.J., Milne, G.A., King, M.A., Thomas, I.D., 2012. A new glacial isostatic adjustment model for Antarctica: calibrated and tested using observations of relative sea-level change and present-day uplift rates. *Geophys. J. Int.* 190, 1464–1482.
- Wilch, T.I., McIntosh, W.C., Dunbar, N.W., 1999. Late Quaternary volcanic activity in Marie Byrd Land: potential  $^{40}\text{Ar}/^{39}\text{Ar}$ -dated time horizons in West Antarctic ice and marine cores. *Geol. Soc. America Bull.* 111, 1563–1580.
- Wingham, D.J., Wallis, D.W., Shepherd, A., 2009. Spatial and temporal evolution of Pine Island Glacier thinning, 1995–2006. *Geophys. Res. Lett.* 36, L17501. <http://dx.doi.org/10.1029/2009GL039126>.
- Zheng, Y., Anderson, R.F., Froelich, P.N., Beck, W., McNichol, A.P., Guilderson, T., 2002. Challenges in radiocarbon dating organic carbon in opal rich marine sediments. *Radiocarbon* 44, 123–136.